Carles Pérez Cervera

Ground thermal modelling and analysis of energy pile foundations

Abstract

Geothermal resources represent a great potential of directly usable and renewable energy for heating and cooling buildings. Energy piles are deep foundations that combine the structural function as a foundation with a heat exchanger serving the thermal needs of the buildings. These systems represent one of the most suitable systems for heating maximizing economic and environmental benefits.

The purpose of this thesis is to evaluate ground thermal response to energy pile foundations using numerical models and methods because they are nowadays a powerful tool for engineering used in many areas of geotechnical design. Because of this, two different study cases were evaluated carrying out both 2D and 3D numerical models.

The first case was a preliminary study that evaluates ground thermal response to energy piles foundations in a long term transient analysis for a new building in Kupittaa, Turku. The main objectives of this case were to study ground seasonal heat storage capacity keeping the ground thermal balance during seasonal operations and also the study of a vertical insulation barrier surrounding the pile foundation. The results showed that it was needed to balance the heat extraction from the ground in long term analysis. The effect of the insulation barrier was negligible at ten meters from it but presents good thermal results in points located close to the vertical barrier.

The second case evaluated the melting process of the frozen soil below Myllypuro ice rink running several numerical models and studying the thawing settlement produced. The numerical models carried out showed that the time needed to melt the frozen ground was around 800 days. Otherwise, the estimated thaw settlement was around 1.8m until 6.6m of frost penetration.

Preface

At this point I would like to thank all the personnel and colleagues of the Laboratory of Soil Mechanics and Foundation Engineering at Aalto University for sharing with me the journey to the completion of this thesis. Especially thank to Professor Leena Korkiala-Tanttu and University Teacher Henry Gustavsson for teaching, guidance, advice and the opportunity to work in this project. I also would like to thank Jarmo Vihervuori, Matti Lojander and Matti Ristimäki for helping me in the laboratory tests and for their patience and loyal support.

I would like to thank all the people who made this thesis possible. I am extremely grateful to everybody who have supported me in my work and who have always made me feel very comfortable and treated me so warmly at the department.

I also would like to thank the company Ruukki OY for all the information and material that they have provided me; it was very helpful in the development of this thesis.

In addition I would like to thank my supervisor in Spain, Professor Joaquín Celma Giménez for his support, advice and always interesting and helpful discussions.

Finally, I wish to thank my family and friends for their support and encouragement during my study time, without them none of this would never have been possible.

Espoo 20.11.2013

Carles Pérez Cervera

Carles Pérez Cervera

Contents

List of symbols

Q	[J]	Quantity of heat
q	[J/m^{2}s]	Heat flux through an area
m	[kg]	Mass
c	[J/kgK]	Mass heat capacity
C	[J/m^{3}K]	Volumetric heat capacity
T	[K]	Temperature
A	[m^2]	Area
t	[s]	Time
L	[kJ/m^3]	Latent heat
L_o	[kJ/m^3]	Latent vaporisation heat
λ	[W/mK]	Thermal conductivity
α	[mm^2/s]	Thermal diffusivity
ρ	[kg/m^3]	Bulk density
ρ_d	[kg/m^3]	Dry density
ρ_w	[kg/m^3]	Water density
ρ_s	[kg/m^3]	Specific gravity
ω	[%]	Volumetric water content
S_r	[%]	Degree of saturation
n	[%]	Porosity
e_o		Initial void ratio
γ	[kN/m^3]	Natural unit weight
SP_0	[mm^2/Kh]	Segregation potential
x_i	[%]	Volumetric fraction of ground components
ς	[kPa]	Effective stress
ε	[mm]	Deformations

Abbreviations

GHP	Geothermal heat pump
GSHP	Ground source heat pump
EGH	Enhanced geothermal systems
HDR	Hot dry rock
UTES	Underground thermal energy storage
SPF	Seasonal performance factor
COP	Coefficient of performance
COP_C	Coefficient of performance (Cooling)
COP_H	Coefficient of performance (Heating)
BC	Boundary condition
SP	Segregation potential

1 Introduction

Nowadays, the global aim to reduce greenhouse-gas emission to avoid the energy dependence on fossil fuels and the new building energy requirements have urged to seek for new environmentally friendly energy sources worldwide. In this regard, geothermal energy represents a powerful source of renewable energy that can be found almost everywhere. Shallow geothermal energy sources combined with deep foundations are a great solution for indoor heating and cooling, which represents a big percentage of the total energy consumption of the buildings. This combination of thermo active foundations helps to reduce the energy consumption and maximize economic and environmental benefits. This thesis focused on the energy pile foundations. There are also other thermo-active foundations such as energy tunnels, anchors, basement walls or heating systems for road pavements; however they are not studied here.

Most of the previous studies on energy pile foundations have focused on the thermal behaviour of the piles but Kupittaa case in Turku focuses mainly on the ground thermal response. This case evaluated ground thermal response to energy pile foundations in a long-term transient analysis. The main objectives of this case were to keep the ground thermal balance during seasonal operations and evaluate the efficiency of an insulation barrier. Energy pile systems maximize their efficiency when they operate seasonally. The study of the ground thermal response to a non-balance seasonal operation is necessary in order to keep the ground thermal balance, especially in Nordic countries where heating needs are higher than cooling. For this, simplified 2D and 3D numerical modelling has been carried out with geotechnical software specialized in heat transfer in order to evaluate and analyse the ground thermal behaviour in a long-term. The efficiency of a vertical insulation barrier surrounding the pile foundation was also evaluated and reported.

Furthermore, this study also evaluated the ground thermal response of the frozen soil below the Myllypuro ice rink in Eastern Helsinki. A new foundation system with energy piles was built to ensure the superstructure affected by frost heaving. By using these piles as energy piles it is also possible to melt the frozen clay formed under the rink during 30 years of continuous operation of the facility. Several 2D and 3D models were performed for the evaluation of the thermal behaviour of the frozen clay. The primary objective of this study was to analyse the time-dependent melting process and determine the required constant temperature pumped by the piles that prevents the ground from freezing again.

In situ sampling was done at the Myllypuro site. Thermal properties of the ground and other parameters were obtained from laboratory tests on collected samples. A series of six frost cell tests were carried out at the Soil Mechanics and Foundation Engineering laboratory at Aalto University. These tests were focused specially on the thawing settlement due to the freezing-thawing processes. The main objective was to get an estimation of the thawing settlement after the melting process of the frozen clay. Other parameters such as frost heave rate, temperature gradient and segregation potential were also calculated during the frost heave test.

2 Literature Review

2.1 Basics of Geothermal Energy

2.1.1 Introduction

Geothermal energy is the thermal energy generated and stored in the Earth crust and also in its internal fluids or gases. The fluids are mostly water in liquid phase with different amounts of salts and dissolved gases or sometimes heated steam vapour phase but not include other earth resources such as (Clauser, 2006; 2009):

- Fossil fuels in the subsurface
- Solar energy
- Hydropower in rivers and seas
- Wind energy

Resources of geothermal energy range from the shallow ground to a few kilometres beneath the surface of the Earth where hot water and hot rock can be found, and down even deeper to the extremely high temperatures of molten rock called magma (Wendell et al., 2003). The geothermal gradient is the temperature difference between the core of the planet and its surface, drives a continuous conduction of thermal energy in the form of heat from the core to the surface (Figure 2-1). The average value of geothermal gradient is between 25-30 $^{\circ}$C/km (in the lithosphere) depending on the regions (Banks, 2008).
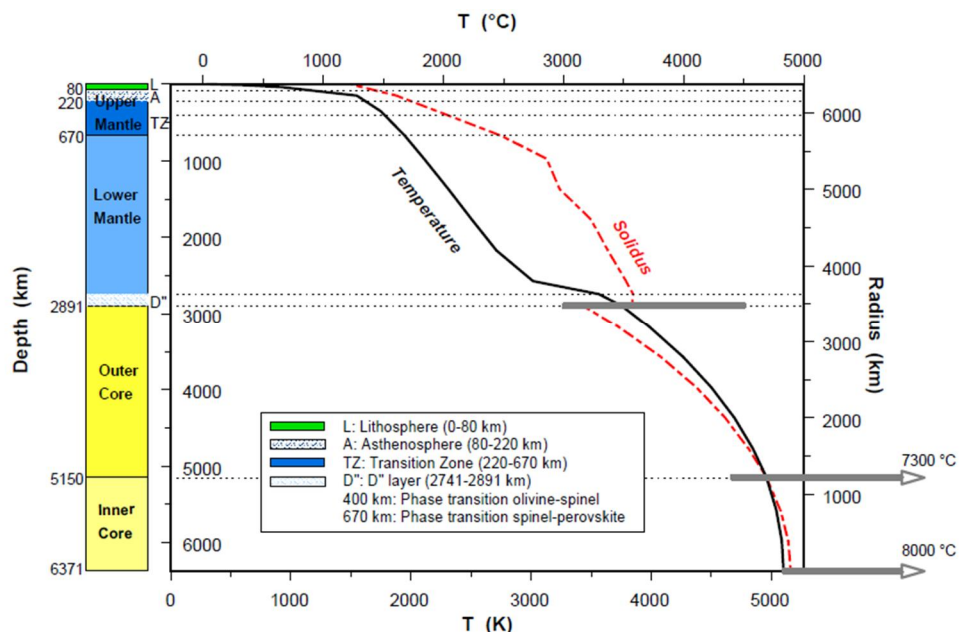
Figure 2-1. The variation of the Earth's temperature with depth (Clauser, 2006)

The energy in the form of heat stored in the Earth comes from internal and external heat sources. The most important external heat source is the solar radiation that provides a solar energy of 1.5×10^{22} J in one day, which is sufficient to meet the global energy demand for 30 years (Clauser, 2006). Another external energy source is electromagnetism from gravitational energy due to the sun, moon and earth rotation

which produce tidal forces. These tidal forces in the form of kinetic energy are converted into heat due to the friction and energy dissipation.

In case of internal sources, the most important source is the decay of radiogenic isotopes in the rocks of crust of the Earth which produces more than $8.6x10^{18}$ J of energy per year (Clauser, 2006). Other internal heat sources are:

- Original heat of the Earth when the planet was created, which was higher than the temperature at present.
- Frictional heat due to the energy released in earthquakes and tectonic movements.
- Potential energy produced by the formation of new crust and iron in the core of the Earth.

All these heat sources produce a global terrestrial heat flow rate of around 1.400 EJ/year (Goldstein et al., 2011) and a geothermal heat flux of 88 mW/m^2 (Wendell et al., 2003). However, not all this energy is profitable and only a small amount of geothermal energy storage in the Earth can be used or converted into other forms of energy, which can be stored. In addition, it is important to take into account the economic aspects to know which of the geothermal sources are useful and accessible (Clauser, 2006). For this reason, geothermal resources are divided into:

- Accessible resource base: Amount of heat which can be produced theoretically.
- Resources: Fraction of the accessible resource base which is expected to become economical within 40-50 years.
- Reserves: Fraction of the accessible resource base which is expected to become economical within 10-20 years.

Geothermal energy is classified as a renewable, clean, efficient and environmentally friendly energy resource. It contributes to reduce the emissions of greenhouse gases and represents nowadays a great potential resource in energy production. Currently, the demand of green and renewable energy and lower energy consumption are increasing interest of ground thermal energy. The geothermal resources of the Earth are theoretically more than adequate to supply global energy needs, but only a very small fraction may be profitably exploited (Johnsston et al., 2011).

2.1.2 Geothermal Resources

Geothermal resources are usually classified and distinguished by the way that heat is stored because it defines how it can be used. Table 1 and Figure 2-2 show the main types of geothermal resources, uses and range of temperatures.
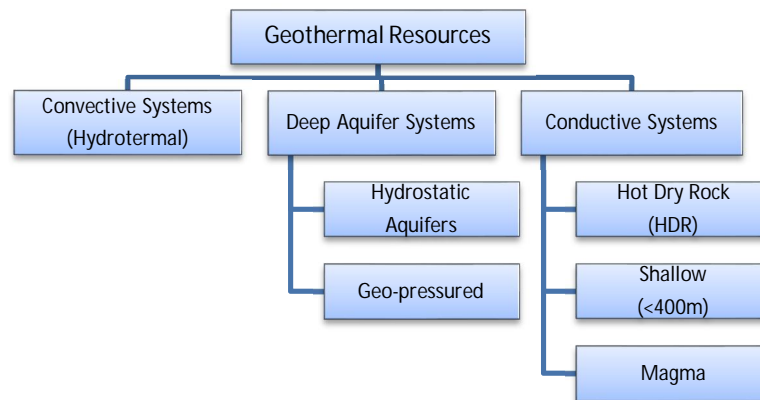
Figure 2-2. Classification of Geothermal resources (Goldstein et al., 2011)

Table 1. Classification of geothermal resources by temperature and utilization (Modified from Goldstein et al., 2011)

Type	Subtype	Temperature	Utilization
Convective Systems	-	High	Power Generation
Conductive Systems	Shallow	Low	Direct Use
	Hot rock (EGS)	High	Direct Use & Power generation
Deep Aquifer Systems	Hydrostatic Aquifers	High & Low	Direct Use
	Geo-pressured	High & Low	Direct Use

Temperature range: Low: from Ambient to +100^{0}C ; High: >180^{0}C

2.1.3 Types of Geothermal Energy Use

Underground resources and geothermal energy have many varieties of possible applications such as heat storage mediums or heat resources. These geothermal resources can be used for power generation for industrial and residential purposes, and also for direct heating purposes such as efficient home heating and cooling through geothermal heat pumps (Wendell et al., 2003). There are two main types of geothermal energy sources, namely, deep and shallow, and two different uses: one is power generation and the other is direct use for heating and air-conditioning or other nonelectrical applications (Johnsston et al., 2011). Deep geothermal resources are usually related to power generation meanwhile shallow geothermal energy is commonly used as direct thermal energy (Figure 2-3).
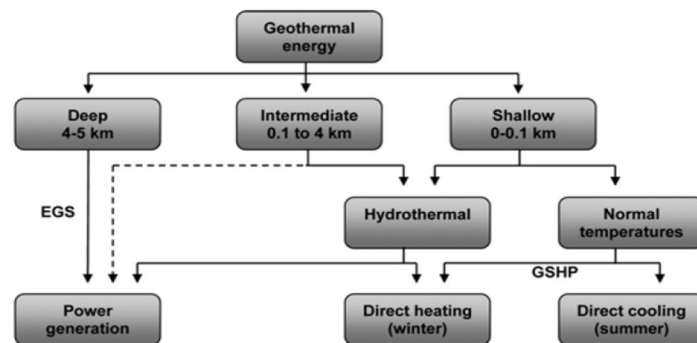

Figure 2-3.Geothermal energy technologies and uses. Enhanced Geothermal Systems (EGS) & Ground Source Heat Pumps (GSHP) (Johnsston et al., 2011)

Direct Use

Direct geothermal heat can be used almost everywhere because the temperature and soil property requirements are lower than in power generation (Goldstein et al., 2011). In addition, direct use of geothermal energy resources is more efficient because it does not require any conversion into another energy source. Otherwise, heat cannot be transported and transmitted over long distances without losses and reduction of the efficiency.

As the heat is not converted into another energy source, the direct use of heat is more appropriate for cold and moderate climates (Clauser 2006). The geothermal energy is increasingly used in developed countries, especially for heating and cooling purposes (Figure 2-4).
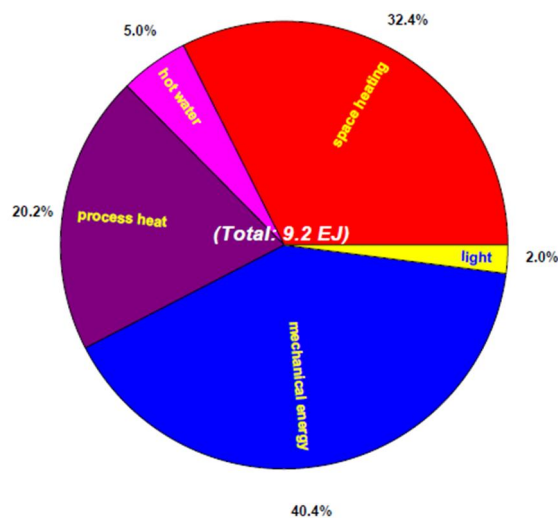
Figure 2-4. Energy consumption distribution in Germany in 2002 (Clauser, 2006)

There are two main types for extracting the heat storage from the soil for direct use, namely, Ground Source Heat Pumps (GSHP) and Hydrothermal Aquifers (Goldstein et al., 2011).

- There are many different types of GSHP systems and in all of them the conduction is the main mechanism of heat extraction (Llopis & Rodrigo, 2010). Some of GSHP systems are listed below:

  - Horizontal ground heat exchangers
  - Energy Piles or Heat exchanger piles
  - Shallow/Deep borehole heat exchangers
  - Others thermo-active foundations: Energy tunnels, energy basement walls, energy anchors.

- Hydrothermal Aquifers: most of the systems are installed with two different boreholes, one for production and another one for injection. The production borehole extracts hot water from the aquifer and fed it into another secondary distribution circuit in the building. The water is cooled in the surface and then is pumped again into the reservoir via the injection borehole.

Power Generation

Heat storage in the Earth can also be used for power generation but requirements for power generation are higher than for the direct use of geothermal energy (Goldstein et al., 2011). Geothermal power generation is limited by the temperature of the resource, because it needs vapour to drive the turbines. The steam for driving the turbines can be found in natural reservoirs (Hot Sedimentary Aquifers) or it can be produced by injecting water into hot rocks (HDR and EGS systems). These heat sources of geothermal energy can be used at depths between 1-5 km, where the temperature is around +200°C (lower temperatures are less efficient).

The temperature and depth of the resource and other geological and economic factors cause that the requirements for power generation higher than for direct use. Worldwide geothermal power plants are mainly concentrated in few countries such as USA, Philippines, Iceland and Mexico (LLopis & Rodrigo, 2010). In general, geothermal power generation is increasing every year because it is a renewable energy source and also contributes to reduce the global greenhouse-gas emission while replaces the use of fossil-fuels.

2.2 Shallow Geothermal Resources

Shallow geothermal resources use thermal energy stored in the Earth at depths lower than 400m. Rocks and soils are good insulators and at a few meters below the surface (15-20m) ground temperature remains constant during the whole year. At this depth, ground temperature fluctuations caused by the daily variations are small, allowing the ground temperature to stay within a range of +5 to +10°C depending on the regions (Brandl, 2006). These constant temperature conditions of the ground can be used for cooling and heating of buildings in addition with Geothermal Heat Pumps system.

The ground can be used as a heat source in the winter and also as storage for the heat that is wasted during the summer, providing a balanced combination for cooling and heating (Figure 2-5). In the summer, heat pump is designed to circulate cold fluid around the building, extracting the heat from the building and transferring it to the ground. During the winter the direction of the heat pump is reversed, extracting heat from the ground and transferring it to the building. In this way, the ground works as an Underground Thermal Energy Storage (UTES) (Sanner, 2005).
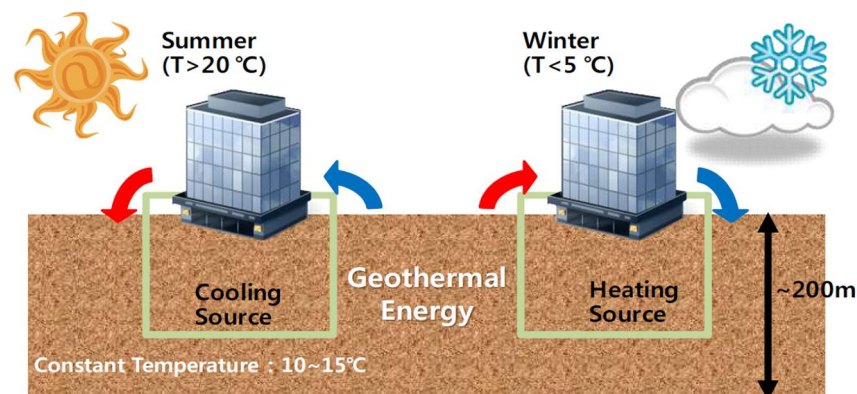

Figure 2-5. Shallow geothermal systems operation (Lee, 2009)

Direct geothermal systems for heating and cooling buildings that use the heat storage in the ground at shallow depths are divided into three main parts (Figure 2-6; Sanner, 2005):

1. Primary circuit: Depending on the system the primary circuit could be built in piles, boreholes, ground loops in trenches or other building foundations. Inside the primary circuit, the fluid circulates through pipes and exchanges the heat with the ground depending on the seasonal operation.

2. Heat Pump: The heat pump connects primary and secondary circuit transferring the heat. Heating and cooling of buildings require higher temperature values than can be found in the ground. The heat pump uses ground thermal energy with a small amount of electrical or mechanical energy to reach temperature that is required for indoor heating.

3. Secondary circuit: This part of the system circulates the heat through pipes installed inside the building and also returns the hot or cold liquid to the heat pump to restart the cycle. Secondary circuit can be divided into two different systems for cooling and heating.
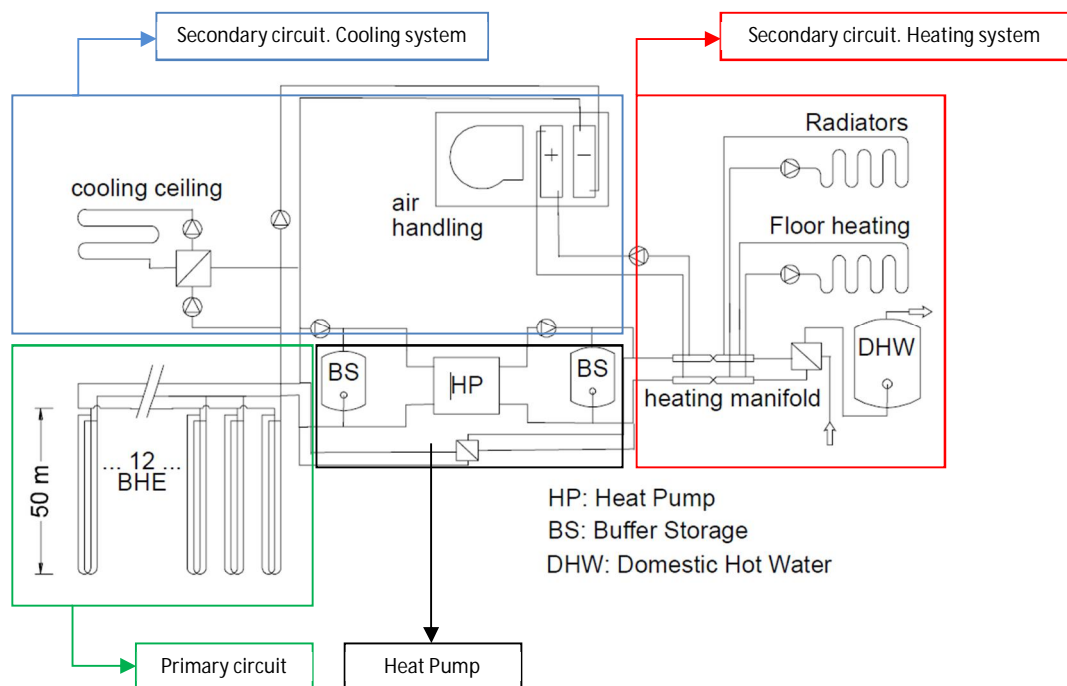
Figure 2-6. Main parts of shallow geothermal systems (Sanner, 2005)

In GSHP systems, the cycle starts exchanging the heat between the ground and the primary circuit. The hot or cold fluid circulates through pipes from the primary circuit to the heat pump, which transfers the heat to the secondary circuit. The heat pump extracts the heat from the liquid and uses it for heating and cooling the building depending on the seasonal operation. To conclude the cycle, the hot or cold liquid return to the pipes of the primary circuit buried in the ground and the cycle starts again (Figure 2-6).

2.2.1 Types of Direct Geothermal Systems for Heating

Direct geothermal systems are typically classified into two major groups (Figure 2- 7), namely, open-loop and closed-loop (Johnsston et al., 2011). In closed loop systems, the heat transfer fluid circulates through pipes embedded in the ground; meanwhile the open loop systems use directly the groundwater as the heat transfer fluid. Consequently, closed loop systems where the heat transfer occurs via the materials surrounding the absorber pipes are less efficient than open loop (Lee, 2009).

Closed loop systems that usually consist one or more U-tubes (absorber pipes) inserted in the ground or other foundations have more advantages and more potential applications than open loop systems (Figure 2-7 & Table 2). In closed-loop systems, the heat transfer fluid never contacts with the ground and it can be used almost everywhere because it does not require specific hydrogeological conditions (Johnsston et al., 2011).
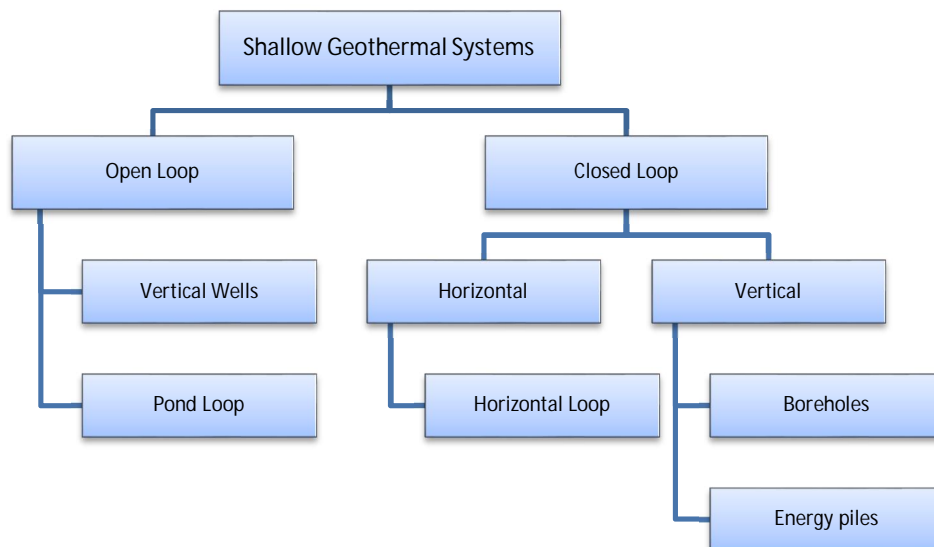
Figure 2-7. Main types of shallow geothermal systems (LLopis & Rodrigo, 2010)

Table 2. Types of shallow geothermal systems (Modified from Lee, 2009)

Type	Subtype	Efficiency	Installation cost	Ground Conditions
Open Loop	Vertical Wells Pond Loop	High	High Medium	Difficult Difficult
Closed Loop	Horizontal Loop	Low	Low	Simple
	Boreholes Energy Piles	High	High Medium	Simple

At the beginning when the closed loop systems were introduced, they were installed in vertical boreholes and pipe lines in horizontal trenches. The vertical borehole systems need deep drills to install the pipes that would increase installation cost. Horizontal pipe system needs, on the other hand, large surface areas that are not available in the urban areas. Nowadays, the absorber pipes for the heat exchangers can be built

embedded in subsurface structural elements like piles, tunnels, basement walls and slabs (Brandl, 2006) (Figure 2-8).

Figure 2-8. Different heat exchanger systems for shallow geothermal energy sources (Loveridge, 2012)

Thermo-active foundations are foundations that also work as heat exchangers. The principle advantage of energy foundations (energy piles, energy tunnels, energy wells or basement walls) is that the ground heat exchanger is already required for structural purposes (Brandl, 2006). They use the contact between th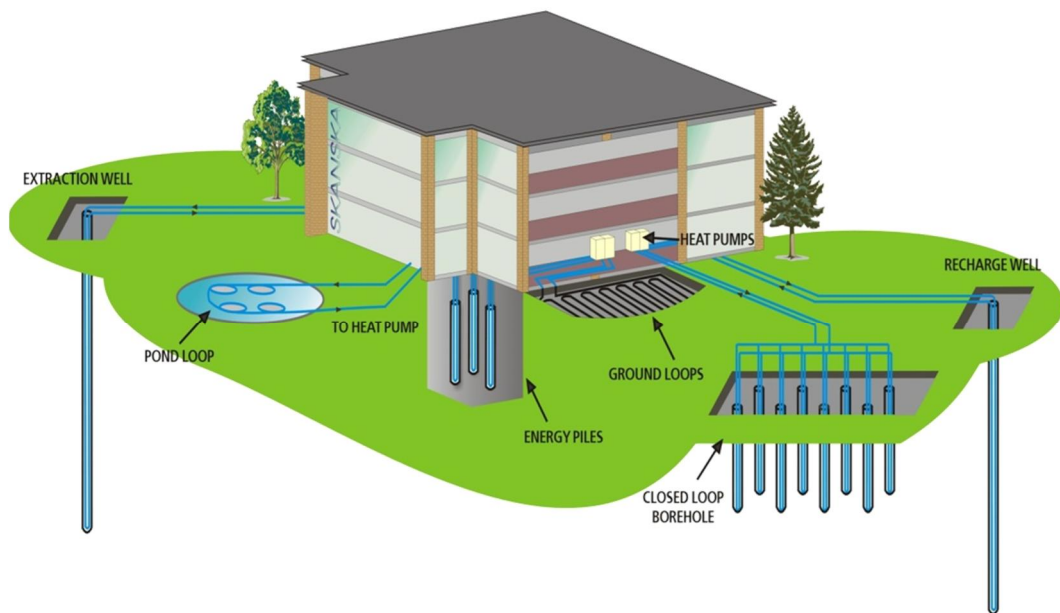e structural elements (with closed circuit pipes embedded) and the ground for the exchange of heat. With the new thermo-active foundations, the installation costs can be reduced because the absorber pipes are already embedded inside the foundation and therefore no additional costs related to making a separate structure. Otherwise, this innovative method uses clean and renewable energy and is therefore more environmentally friendly than other conventional space heating systems.

2.2.2 Economic Benefits

Worldwide, more than half a million of geothermal heat pumps are in operation and produce over 7000 MW (Wendell et al., 2003). The use of geothermal heat pumps is increasing rapidly because ground energy systems offer a number of benefits over traditional heating and cooling systems (Figure 2-9). Some of the benefits are:

- Small size of heat pumps.
- Energy supply does not depend on weather conditions.
- Helps to reduce the peak demand of electric power generation plants by supplying extra energy whenever needed.
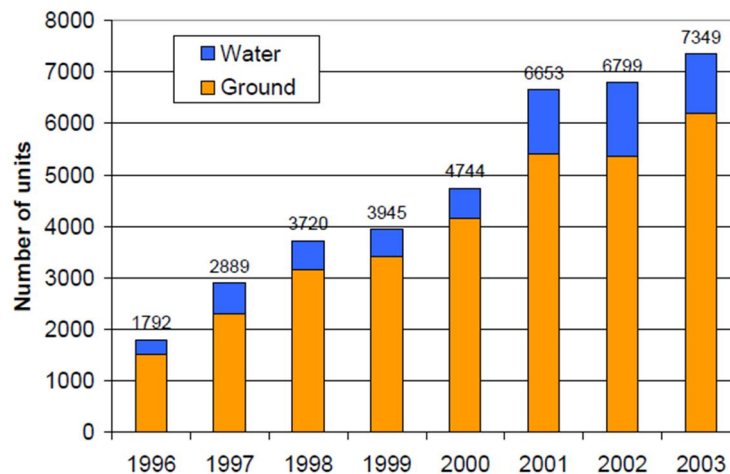
Figure 2-9. Number of Heat Pumps sold in Germany between 1996-2003 (Sanner, 2005)

The initial costs for the installation of a GSHP are bigger than other heating-cooling systems (Johnsston et al., 2011). The extra cost comes principally from the excavation works needed to install the heat exchanger and for the installation costs of all the equipment. The additional costs depend on the ground energy system and the soil conditions. In the beginning, the payback time for ground energy systems were too long to be economic. Now, the ratio is decreasing and the extra expense can be amortized between 4-10 years depending on the system (Loveridge, 2012 and Johnsston et al., 2011).

Ground energy systems use only 25% of the energy required for an equivalent conventional heating and cooling systems (Loveridge, 2012). The ground energy systems provide significant energy savings, more than 75% compared to the electric heating systems and between 30-60% in relation to other heating systems (Wendell et al., 2003). The benefit comes from reduced operating costs, which depend on the price of the electricity and reduced maintenance costs. It is also important to take into account that the efficiency of the GHP is higher when seasonal heating and cooling need is in balance (Brandl, 2006), because it allows to improve the coefficient of performance (COP) of the heat pump.

Other factors that improve the efficiency and the payback periods of GSHPs are:

- The improvement of the performance of the systems.
- Reduction of the installation cost when the contractors become more experienced with the installation techniques.
- New regulations and taxation policy for renewable energies.
- Increase in the price of electricity and fossil fuels.

2.2.3 Energy Piles

Energy piles are an integration of heat exchanger pipes with structural pile foundations. The use of energy foundations, combining pile foundations and heat exchangers as a part of the ground energy system can save a significant amount of energy for building projects especially when the ground is used as an energy storage

system. The heat exchange system consists of absorbing and transporting ground thermal energy to buildings via fluid that circulates in pipes embedded in piles. The heat exchanger pipes are connected to a heat pump in order to produce thermal energy required for buildings to satisfy the need for heat in winter and to expel excess heat resulting from air conditioning in summer.

The use of geothermal energy, especially the use of energy piles, is increasing rapidly due to its economic and environmental benefits (Figure 2-10). The energy savings and the new energy requirements for buildings make energy piles in connection with heat pumps a good solution for heating and cooling of the buildings.

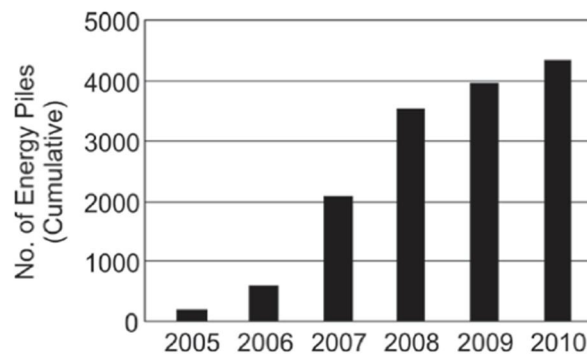Figure 2-10. Number of energy piles installed in the United Kingdom (Loveridge, 2012)

The main difference of an energy pile system compared with other shallow geothermal systems is that the primary circuit has also a structural function as building foundation. Figure 2-11 shows the main components of an energy pile system that are explained below.
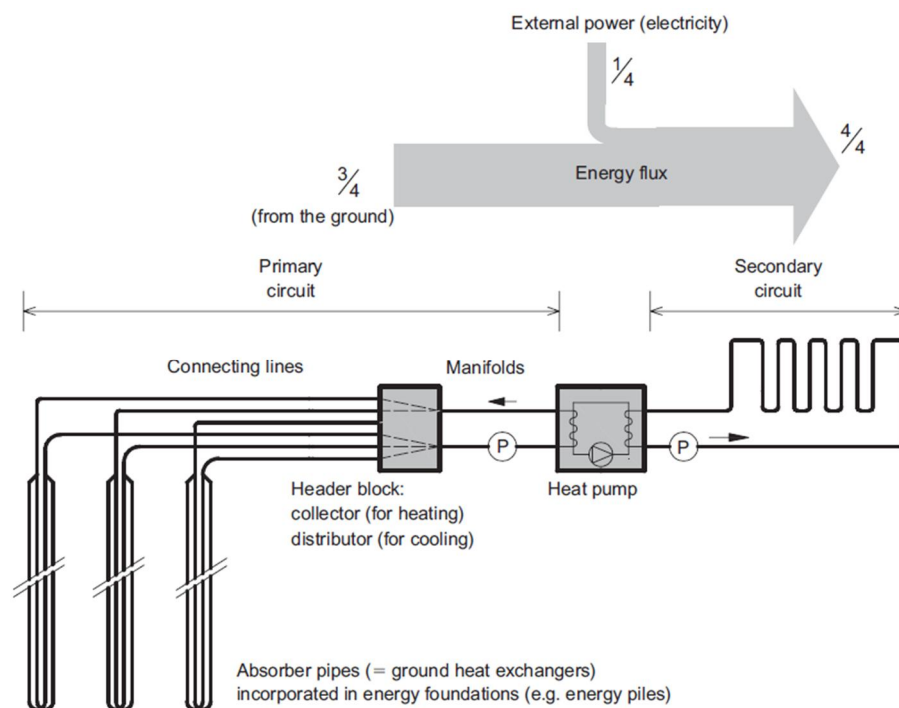

Figure 2-11. Scheme of a geothermal system with energy piles (Brandl, 2006)

a. Primary Circuit

The primary circuit of a GSHP is the part of the system that exchanges the heat with the surrounding ground. Piles working as a heat exchanger are a good solution for the primary circuit. The pile is filled with pipes and concrete. Concrete has a good thermal conductivity and thermal storage capacity and its properties make it a good medium for heat exchange. The closed loop circuit for the heat exchange is attached to the reinforcement of the pile and it circulates the heat carrier fluid through the entire pile.

Heat Transfer in Energy Piles

The temperature difference between ground and the heat carrier fluid circulating inside the pile produces the heat transfer in an energy pile system. The mechanisms of heat transfer involved in an energy pile system are (Figure 2-12):
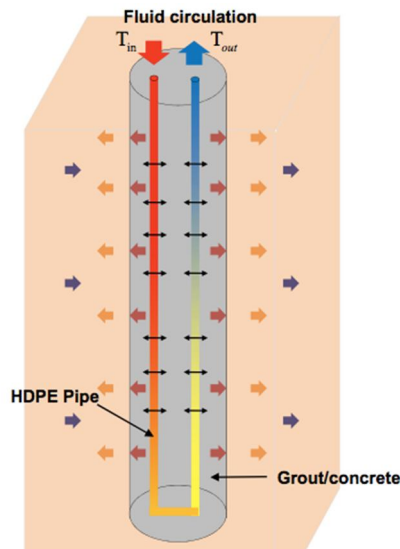
1. Conductive heat flow in the concrete/grout or steel
2. Conductive heat flow in the ground
3. Convective heat flow between the liquid and the pipe
4. Convective heat flow in the ground (If ground water flow exists)

Figure 2-12. Scheme of the heat transfer mechanism in energy piles (Lee, 2009)

The total usable heat extracted by the system is [2.1] (Lee, 2009):

$$Q_{tot} = Q_{in} - Q_{out} = m\, c_{fluid}(T_{in} - T_{out}) \qquad [2.1]$$

Where:

– m: Mass flux density of circulation fluid [kg]

– c_{fluid}: Heat capacity of circulation fluid $\left[\frac{J}{kg \cdot K}\right]$

– Q: Total heat extracted [J]

– T_{in}: Inlet temperature [K]

– T_{out}: Outlet temperature [K]

The most important factors that affect the performance of the energy pile systems are (Brandl, 2006):

- – Heterogeneous ground conditions
- – Seasonal ground water table
- – Ground water flow
- – Ground thermal properties

Steel Piles

Energy piles are commonly built with concrete but steel piles filled with concrete are also a good solution. On one hand, thermal conductivity of steel is higher than concrete and it reduces the thermal resistance of the energy pile. It is easier to put the heat exchanger pipes inside the steel piles because they have a hollow structure (Uotinen et al., 2012). This is an advantage especially in small piles with outer diameter between 100-300mm. Another benefit of steel piles is the installation mechanism, because they can be drilled or driven.

Heat Exchanger Pipes

The pipes embedded inside the piles are commonly made of high-density polyethene. The diameter of the absorber pipes vary between 20-25mm (Brandl, 2006). The heat transfer fluid used inside the pipes is a mixture of water and ethanol, but saline solutions are also used. There are many different configurations for the installation of the pipes inside the energy piles. Some of the most common loop configurations are shown in figure 2-13:
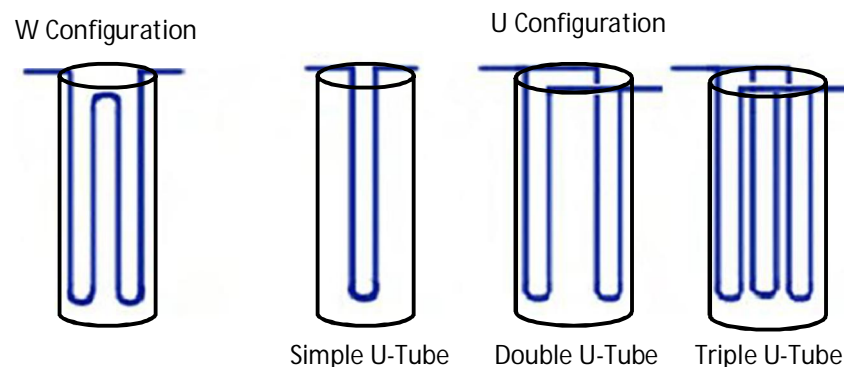
Figure 2-13. Different types of pipe configurations inside energy piles

There are limits for the temperature of the fluid circulating through the pipes embedded in the energy piles. For summer operation, when the heat is pumped in the ground, fluid temperature must be kept below +40 °C (SIA, 2005). For winter operation, when the heat is extracted from the ground, the temperature should not fall below 0°C (Brandl, 2006). However, this is a conservative approach and fluid temperature could be negative without producing negative temperatures in the ground surrounding the pile (Loveridge, 2012).

b. Geothermal Heat Pumps (GHP)

Shallow geothermal sources use heat storage in the ground at low temperatures. The temperatures of the ground are not enough to satisfy the human requirements for space heating but Geothermal Heat Pumps (GHP) help to overcome these limitations.

The application of GHP is typically for space heating and domestic hot water in commercial and residential buildings (Brandl, 2006). The requirements for the installation of these systems are lower than for other geothermal energy systems (LLopis & Rodrigo, 2010) and some of the reasons are:

- Low installation costs
- Large range of GHP types and power
- Easy installation
- Low maintenance costs

In addition, the efficiency of GHP is better than conventional heat pumps (LLopis & Rodrigo, 2010). Meanwhile conventional heat pumps use atmosphere temperatures (high variation) for heat exchange, GHP systems use ground temperature for heat exchange. The temperature of the ground remains nearly constant throughout the year and it allow the GHP to provide better results and improve the efficiency.

The use of GSHPs is increasing in the developed countries for the direct use of geothermal resources (Clauser, 2006). Table 3 shows the number of GHPs installed in different countries to date. As it can be seen from Table 3, Sweden has installed the largest number of GHP per inhabitant. This is because the thermal energy required for space heating in cold countries is higher and it is also a proof of the efficiency of GHPs.

Table 3. Principal countries with geothermal heat pumps installed (Modified from Clauser, 2006)

Country	Population (x10^6)	N° of GHP's	Annual Production (TJ)	Total Power installed (MW)
Sweden	9	200.000	28.800	2.000
EEUU	294	500.000	13.392	3.720
Germany	82	51.000	4.212	780
Canada	32	36.000	1.080	435
Switzerland	7	27.000	2.268	420
Austria	8	23.000	1.332	275
TOTAL	432	837.000	51.084	7.630

Efficiency of the Heat Pump

The heat pump connects the primary and the secondary circuits increasing the temperature level of the primary circuit (ranges between +10 to +15°C) to the required temperature in the secondary circuit (ranges between +25 to +35°C) (Brandl, 2006). To generate this temperature increment, external energy is needed, usually electricity or mechanical energy. The coefficient of performance (COP) measures the ratio between the external energy consumed and the energy that comes from the ground. It is defined as:

$$COP = \frac{Energy\ output\ after\ heat\ pump\ [kW]}{Energy\ imput\ for\ operation [kW]}$$
[2.2]

For economic reasons, the required value of COP should be ≥4 (Brandl, 2006 & 2013). That means that at least 75% of the usable energy is coming from the ground. The COP can be different for winter and summer operations. For winter operations, the COP heating (COP_H) ranges between 3-5 meanwhile during summer, the COP cooling (COP_C) ranges between 2.5-3.5 (LLopis & Rodrigo, 2010).

The seasonal performance factor (SPF) of the ground energy systems is defined as the ratio between the usable energy output of the system and all the required energy inputs for the system. It includes the heat pump and also all the other elements of the system that need energy. Currently the range of SPF values is between 3.8-4.3 (Brandl, 2013).

$$SPF = \frac{Usable\ energy\ output\ of\ the\ energy\ system\ [kW]}{Energy\ input\ of\ the\ energy\ system\ [kW]} \qquad [2.3]$$

Heat Pump Cycle

Heat pumps follow the Boyle's Law, producing heat transfer due to changes in pressure, volume, phase or temperature, but the heat transfer due to phase change is higher (Johnsston et al., 2011). Heat pumps take profit of the fluid's properties in order to achieve an efficient heat transfer. The schematic of the operation cycle of a heat pump is shown in Figure 2-14.
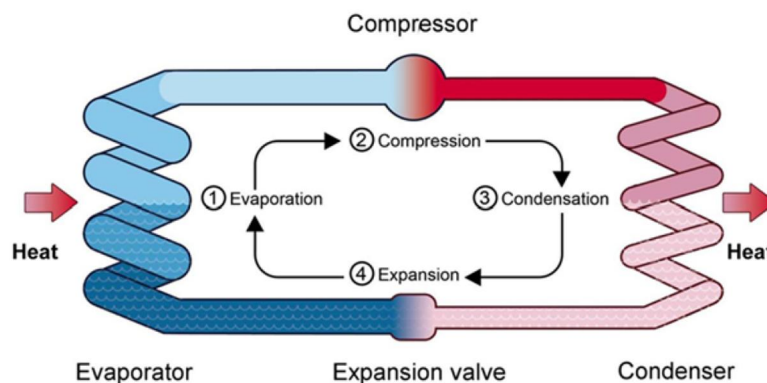
Figure 2-14. Schematic of a Heat Pump Cycle (Johnsston et al., 2011)

During the heating mode (winter), the fluid is cooler than the heat source (primary circuit in the ground) and absorbs heat from it. The refrigerant boils (Point 1) at relatively low pressure and passes through the compressor increasing the pressure and temperature (Point 2). Once the gas leaves the compressor, it condensates in the secondary circuit (inside the building) due to the outer lower temperature (Point 3). In this step, heat exchange occurs between the building and the secondary circuit heating the building. Then the hot and pressured refrigerant passes to and expansion valve returning to the initial conditions (Point 1). During the cooling mode (summer), the process is reversed; the refrigerant is cooled by the ground and heated in the secondary circuit (Johnsston et al., 2011).

c. Secondary Circuit

In GSHP's and energy pile systems, the secondary circuit is the heating and cooling delivery system which is installed inside the building. The maximum efficiency of the secondary circuit is obtained when the temperature increment between the primary and secondary circuit is minimal (Loveridge, 2012). In this way, ground energy systems reach the greatest efficiency when they are used with low temperature delivery systems inside the building (Table 4).

Table 4. Main types of delivery systems in secondary circuits and range of temperatures (Banks, 2008)

Type of Delivery System	Range of temperatures (°C)
Air heating	< +30
Underfloor heating	+30 to +45
Boilers and radiators	+45 to +55
Hot water	> +55

In the same way, for cooling purposes it is better to use a suitable cooling system which minimizes the temperature difference between the air conditioning system and the ground.

Thermal requirements inside a building could be different and depending on the requirements, there are different modes of operations. Ground thermal balance, which is related to the heating and cooling requirements inside the building, has to be taken into account for the performance of the system during the design of the heat exchangers and the delivery system (Loveridge, 2012). The efficiency of the system can be obtained by measuring the COP and the SSPF as explained above. The most important modes of operation are listed below:

1. Balanced systems: These systems use the ground temperature for cooling during the summer and for heating during the winter. Due to the thermal balance, the excessive heat during summer is used to recharge the ground for the winter extraction. The balanced situation makes the systems work more effectively and maximizes the energy extraction.
2. Only heating: This is the typical mode of operation in cold regions, where the heat requirements are needed only during part of the year. In these systems, it is important to keep ground thermal balance and avoid ground freezing due to high heat extraction. It is recommended that at least 70% of the heating energy need to be recharged during the summer time (Uotinen et al., 2012). Additional solar energy could be used to recharge the ground when the heat extraction exceeds the ground recovery capacity.
3. Free cooling: These systems work without the use of the heat pump and use directly the warm heat transfer fluid from the secondary circuit to the primary circuit during building cooling. Free cooling systems are highly efficient, but need small temperature differences between ground and the fluid inside the heat exchangers.

2.3 Heat Transfer in Soils

2.3.1 Introduction

In general, temperature difference between two points produces heat transfer, moving and transferring energy. According to the energy conservation principle, the heat transfer occurs until the system reaches equilibrium.

The addition or subtraction of heat and energy from a system changes its temperature. The quantity of heat (Q) required in order to increase the temperature of a mass of a certain material is shown in equation [2.4] (Bhalchandra & Robert, 1982):

$$Q = c\, m\, \Delta T \qquad\qquad [2.4]$$

Where:
  – Q : Quantity of heat [J]
  – m : Mass [kg]
  – ΔT : Temperature variation [K]
  – c : Specific heat capacity $\left[\frac{J}{kg \cdot K}\right]$

2.3.2 Mechanism of Heat Transfer

There are three different mechanisms of heat transfer, namely: conduction, convection and radiation. Conduction occurs between two systems in contact, convection depends on motion of mass from one place to another, and radiation is the heat transfer by electromagnetic radiation (Bhalchandra & Robert, 1982).

- Conduction: is the mechanism of heat transfer between bodies in contact due to the atoms in the hotter regions have more kinetic energy than the cooler, transferring part of their energy to their neighbours.
- Convection: is the heat transferred by a mass motion of a fluid from one region of the space to another. It occurs when a body is in contact with a fluid and a temperature difference exists between them. Convection process can be produced by circulating a fluid with a pump or blower. In the latter case it is called as forced convection, or caused by density differences due to the thermal expansion which is called natural convection or free convection.
- Radiation: radiation is the heat transfer by electromagnetic waves such as solar radiation, infrared and ultraviolet radiation. It does not require physical matter to be present between bodies for heat transfer like in convection or conduction heat transfer. The wave lengths of thermal radiation varies between 0,1-100 micrometres.

Mechanism of Heat Transfer in Soils

In soils, at ambient temperature, thermal conduction is the dominant mechanism of heat transfer; however, convection could become the dominant mechanism if there is ground water flow (Farouki, 1986). In the upper 10-15 meters of depth from the ground surface, other mechanisms are also involved as shown in Figure 2-15:

- Radiation due to the sun
- Convection (via water and air) due to climate factors
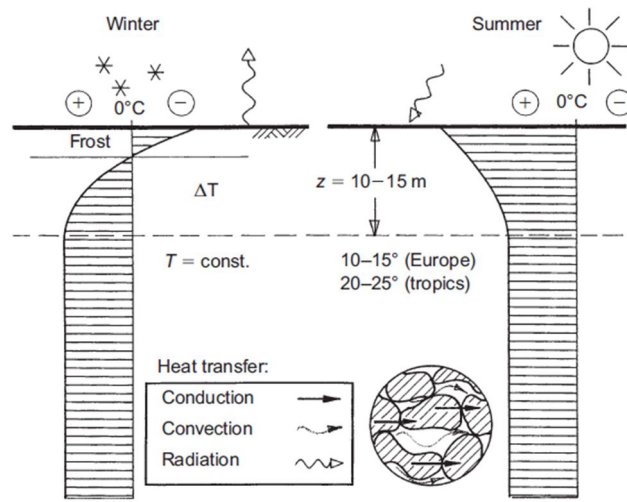- Latent heat transfer, result of a phase change of water processes

Figure 2-15. Mechanisms of heat transfer in the ground and temperature distribution (Brandl, 2006)

The solar radiation effects decrease with depth and are negligible at more than 15m below the surface. The total amount of heat transfer (q_{tot}) in the soil is given in [2.5] (Rees et al., 2000) (Brandl, 2006).

$$q_{tot} = q_{cond} + q_{l,conv} + q_{v,conv} + q_{lat} \qquad [2.5]$$

Where:

$$q_{cond} = \frac{Q}{A\,t}$$
$$q_{l,conv} = c_l\,\rho_l \boldsymbol{v_l}(T - T')$$
$$q_{v,conv} = c_v\,\rho_v \boldsymbol{v_v}(T - T')$$
$$q_{lat} = L_0 \rho_w \boldsymbol{v_v}$$

- In heat conduction (q_{cond}), Q is the heat flux for a volume through an area (A) during a certain time (t).
- In heat transfer by liquid and vapour convection ($q_{l,conv}$ and $q_{v,conv}$), c_l and c_v are the specific heat capacity, ρ_l and ρ_v are the fluid density and $\boldsymbol{v_l}$ and $\boldsymbol{v_v}$ are the vector of the fluid velocity of water and vapour respectively. T' is a reference temperature.
- In Latent heat transfer (q_{lat}), L_0 is the latent vaporisation heat at temperature T', ρ_w is water density and $\boldsymbol{v_v}$ is the vector of vapour velocity.
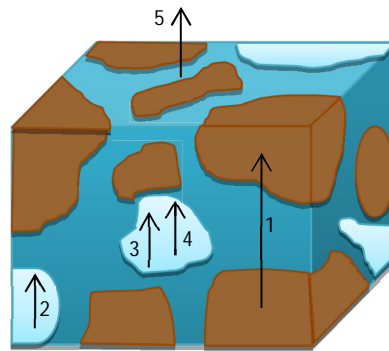
Figure 2-16. Different thermal transport mechanisms in soils (Sundberg, 1989). (1) Convection in pore air (2) Conduction in air (3) Radiation between particles (4) Vapour diffusion (5) Conduction in solid and liquid

There are other thermal transfer mechanisms involved in special cases such as, the radiation in coarse materials under dry conditions, natural convection under high temperature gradients and vapour diffusion in sands with high temperatures and gradients that produce moisture movement (Sundberg, 1989). Figure 2-17 explains the main heat transfer mechanisms in soils depending on the degree of saturation and the grain size.

The moisture migration induces changes in soil thermal properties, especially in unsaturated soils (Farouki, 1986). Evaporation of pore water in the soil induces vapour gradients and the water vapour moves through the soil towards the lower vapour pressure. If the temperature is lower in the new location it could condense by releasing the latent heat. This process of moisture migration affects the thermal properties of soils by changing the degree of saturation but it also contributes to heat transfer process. The process becomes important in soils with high porosity and high temperature differences.
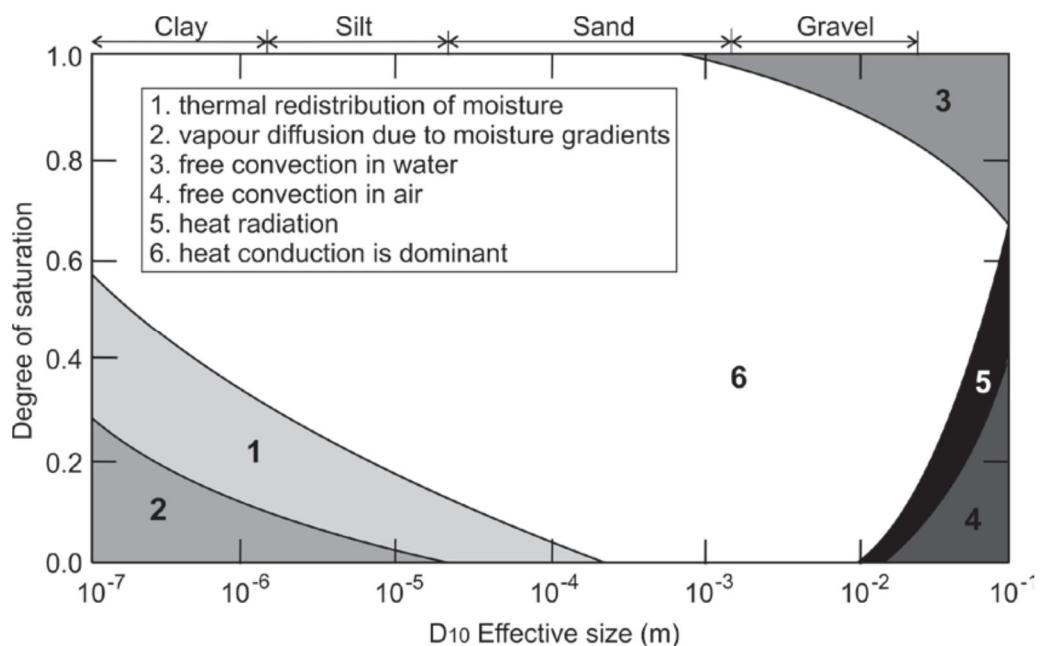

Figure 2-17. Predominant heat transfer mechanisms in soils depending on the degree of saturation and effective grain size (Farouki, 1986)

Heat transfer and heat energy balance depend on geothermal gradient and ground surface temperatures. The heat transfer has a great impact in many areas covering engineering problems.

There are two principal problems in the study of heat conduction: *heat flow rate*, which is the energy flow in a system when the temperature requirements are known, and the other is *temperature distribution*. Andersland et al., (1994) listed the followings as the factors that affect soils heat transfer in the soil surface:

– Climatic factors: The annual cyclic variations of the climate affect the ground surface temperature. In depths below 10-15m, the effect of climate is negligible and temperature remains constant throughout the year. Some of the climate factors that are involved in soil heat flow are:

  ▪ Surface radiation
  ▪ Temperature
  ▪ Convective heat flow
  ▪ Evaporation and condensation
  ▪ Heat flow into and out of the soil

– Freezing and thawing processes: In cold regions, freezing and thawing processes due to seasonal changes modify soil conditions, its properties and behaviour. The frost depth can be affected by:

  ▪ Air temperatures
  ▪ Precipitation
  ▪ Wind velocity

– Surface n-Factor: n-factor is defined as the ratio between the ground surface freezing index (I_{sf}) and the air freezing index (I_{af}) and it depends on:

  ▪ Vegetation
  ▪ Net radiation
  ▪ Surface relief
  ▪ Drainage
  ▪ Snow cover

2.4 Thermal Properties of the Ground

2.4.1 Introduction

In geotechnical engineering it is important to understand the physical, mechanical and thermal properties of frozen and unfrozen soils. Especially in cold regions like Finland and other Nordic countries where cyclic freezing-thawing processes occurs annually it is important to know the differences of soil behaviour and interrelationships between soil components. The knowledge of the thermal properties, the response of soils for thermal changes and the heat transfer mechanisms of soils and rocks are important in geo-engineering. The following are the main areas of geotechnical design where thermal properties of the ground are important:

- Geothermal heat flows
- Heat storage in the ground
- Ground freezing engineering
- Permafrost distribution
- Other engineering purposes such as buildings, roads and pipelines in cold regions.

Thermal properties of soils are dominated by the proportion of water, ice, air and soil itself (Farouki, 1986). Water content and soil dry density are the main parameters needed to determine the thermal conductivity (Kersten, 1952) (Figure 2-18). These parameters can be measured in the laboratory or in situ, because new technologies allow to measure soil thermal parameters on the field using special equipment.
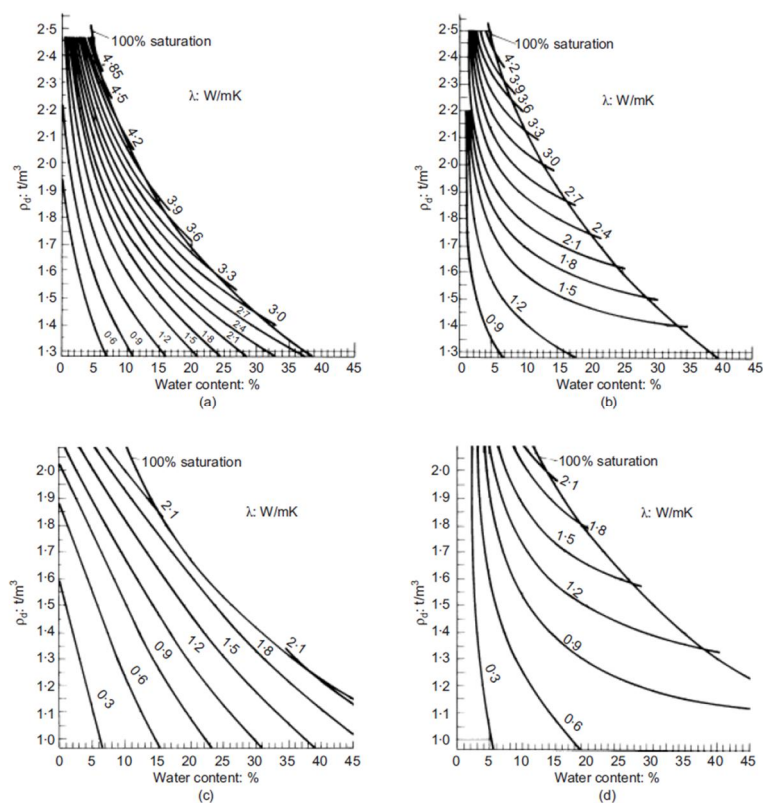

Figure 2-18. Relationship between thermal conductivity, water content and soil dry density (Brandl, 2006)

2.4.2 Thermal Properties of Soils

The thermal properties of soils are not constant and they vary with phase composition, water content or dry density. According to Andersland et al., (1994) the basic thermal properties of soils are:

- Thermal conductivity (λ) [W/mK]: Ability of the material to transport thermal energy [2.6]. It is defined as the amount of heat (Q) passing through unit area (A) of the soil in unit time under a temperature gradient applied in the direction of the heat flow ($\frac{dT}{dx}$).

$$Q = \lambda A \frac{dT}{dx} \qquad [2.6]$$

- Thermal diffusivity (α) [mm^2/s]: Ability of the material to level temperature differences and reach thermal balance in an unsteady state [2.7]. Where λ is the thermal conductivity, c is the specific heat capacity and ρ is the bulk density.

$$\alpha = \frac{\lambda}{c\rho} \qquad [2.7]$$

- Heat capacity (C) [kJ/m^3 K]: Capacity of the material to store thermal energy and is defined as the quantity of heat necessary to raise the temperature by 1°C [2.8]. Where, C_i is the volumetric heat capacity and x_i is the volumetric fractions of the soil, water, ice and air respectively.

$$C = C_s x_s + C_w x_w + C_i x_i + C_a x_a \qquad [2.8]$$

- Latent heat (L) [kJ/m^3]: Defined as the total quantity of heat required to melt the ice in a unit volume of soil without any temperature changes [2.9]. Where, ρ_d is the soil dry density, w is the water content, w_u is the unfrozen water content and L' is the mass latent heat for water (L'=333,7 kJ/kg).

$$L = \rho_d L' \frac{w - w_u}{100} \qquad [2.9]$$

Table 5. Thermal properties of soils and other elements (Sundberg, 1989; Andersland et al., 1994)

Material	Heat Capacity (kJ/m$^3 \cdot$K)	Thermal Conductivity (W/m$\cdot$K)	Latent Heat (kJ/m^3)
Air (20°C)	1,297	0,026	-
Water (0°C)	4,16 x10^3	0,56	333,5 x10^3
Ice (0°C)	2,20 x10^3	2,21	333,5 x10^3
Clay	3,0 - 3,6 x10^3	0,85 - 1,4	1,1 - 2,5 x10^5
Silty-Clay	2,9 - 3,3 x10^3	1,1 - 1,6	1,5 - 2,0 x10^5
Silt	2,4 - 3,3 x10^3	1,2 - 2,4	0,8 - 2,0 x10^5
Sand	2,5 - 3,2 x10^3	1,5 - 2,6	0,8 - 1,7 x10^5

The thermal properties depend on several properties of soils and rocks and they vary with temperature, water and ice content, density, degree of saturation and soil type. One of the most important thermal parameter of soils is thermal conductivity (Sundberg, 1989), which is related and influenced by factors such as:

- Temperature: In case of saturated soils, thermal properties differ totally in the positive and negative temperatures due to the different properties of water and ice. Depending on the presence of impurities, the surface tension and the confining pressure in fine grained soils, there is a certain amount of water that do not freeze at 0^oC. This unfrozen water could exist even at temperatures as low as -10^oC.

- Mineral composition: This property has higher effect on the thermal conductivity of rocks than soils. Especially, the presence of quartz, which has a high thermal conductivity (λ= 7,7 W/m·K) compared to other minerals, significantly affects the conductivity.

- Presence of air and water: Water is twenty times better thermal conductor than air and thus it affects the thermal properties of soils. This is the reason why dry soils have lower thermal conductivity than saturated soils. Thermal conductivity increases rapidly by adding small amount of water and even more in case of ice. However, thermal capacity increases with higher water content, but it decreases when the soil is frozen.

- Density of the soil: Thermal conductivity is related to the soil density, being a function of the dry density. The thermal conductivity increases when the soil dry density increases varying with the degree of saturation (or rather water content).

- Others:

  - Isotropy and anisotropy: depending on the isotropy of the material thermal conductivity can differ in vertical and horizontal directions, describing an elliptical function in anisotropic materials.
  - Porosity: Thermal conductivity of soils decreases with increased porosity.

2.4.3 Thermal Conductivity

a. Kersten Model

Kersten (1949 & 1952) established a relationship between thermal conductivity, the amount of water in the soil (water content) and dry density of frozen and unfrozen saturated soils. Thermal conductivity (λ) of soils increases when the degree of saturation or dry density increases (Kersten, 1949). Following empirical equations [2.10, 2.11 & 2.12] show the relationship for frozen and unfrozen soils:

- Unfrozen soil with more than 50% of silt and clay content:

$$\lambda = 0{,}1442(0{,}9\log \omega - 0{,}2)10^{0{,}6243\,\rho_d} \qquad [2.10]$$

- Frozen soil with more than 50% of silt and clay content:

$$\lambda = 0{,}001442(10)^{1{,}373\,\rho_d} + 0{,}01226(10)^{0{,}4994\,\rho_d} \qquad [2.11]$$

– Unfrozen sandy soils:

$$\lambda = 0,1442(0,7 \log \omega + 0,4)10^{0,6234 \rho_d}$$
[2.12]

Where:

- λ: Soil thermal conductivity (W/mK)
- ω: Water content
- ρ_d: Dry density (g/cm^3).

Kersten's correlations give reasonable results for frozen and unfrozen unsaturated soils (Farouki, 1986).

b. Johansen Model

Johansen (1975) introduced the Kersten number (K_e) to calculate the thermal conductivity of partly-saturated soils [2.13]. Johansen´s method is a technique to interpolate thermal conductivity of soils between dry and saturated soils and it does not take into account any moisture migrations (Johansen, 1975). This method has the advantage of its simplicity for calculation of thermal conductivity in partly saturated soils. It generally gives the best results with degree of saturations above 0.1 (Andersland et al., 1994). These factors are very important in case of highly porous materials. The Kersten number (K_e) to interpolate thermal conductivity (λ) in partly saturated soils follows the next relationship [2.13]:

$$K_e = \frac{\lambda - \lambda_{dry}}{\lambda_{sat} - \lambda_{dry}}$$
[2.13]

Then, Johansen established empirical correlations between K_e and the degree of saturation (S_r):

$K_e = 0,7 \log (S_r) + 1$ For unfrozen coarse grained soil
$K_e = \log (S_r) + 1$ For unfrozen fine grained soil
$K_e = S_r$ For frozen soil

The Johansen's equation [2.14] to calculate thermal conductivity (λ) of soils is:

$$\lambda = (\lambda_{sat} - \lambda_{dry})K_e + \lambda_{dry}$$
[2.14]

Where:

$\lambda_{dry} = \frac{0,135\gamma_d + 64,7}{2700 - 0,947\gamma_d} \pm 20\%$ For dry nature soils

$\lambda_{dry} = 0,039n^{-2,2}$ For dry crushed rock materials

$\lambda_{sat} = (\lambda_s)^{1-n}(\lambda_w)^n$ For saturated unfrozen soils

$\lambda_{sat} = (\lambda_s)^{1-n}(\lambda_i)^{n-w_u}(\lambda_w)^{w_u}$ For saturated and frozen soils

$$\lambda_s = \begin{cases} \mathbf{7{,}7}^q\,\mathbf{(2)}^{1-q} & If\ q > \mathbf{20\%} \\ \mathbf{7{,}7}^q\,\mathbf{(3)}^{1-q} & If\ q \leq \mathbf{20\%} \end{cases} \quad \text{Thermal conductivity of soil particles}$$

c. De Vries Model

De Vries (1963) established a method to calculate the thermal conductivity of soil based on the proportion of its constituents (x_i) and their thermal conductivities (λ_i) [2.15]. This method gives good results with saturated soils which have a low ratio between soil-fluid thermal conductivity. However, for dry soils the equation gives too low values (Farouki, 1986).

$$\lambda = \frac{x_w \lambda_w + F_A x_A \lambda_A + F_S x_S \lambda_S}{x_w + F_A x_A + F_S x_S} \qquad [2.15]$$

Coefficients F_a and F_s depend on shape, pore space and degree of saturation (De Vries model improved by Tang et al., 2008):

$$F_a = \frac{\mathbf{1}}{\mathbf{3}}\left[\frac{\mathbf{2}}{\mathbf{1} + g_a\left(\frac{\lambda_a}{\lambda_w} - \mathbf{1}\right)} + \frac{\mathbf{1}}{\mathbf{1} + g_c\left(\frac{\lambda_a}{\lambda_w} - \mathbf{1}\right)} \right]$$

$$F_s = \frac{\mathbf{1}}{\mathbf{3}}\left[\frac{\mathbf{2}}{\mathbf{1} + \mathbf{0{,}125}\left(\frac{\lambda_s}{\lambda_w} - \mathbf{1}\right)} + \frac{\mathbf{1}}{\mathbf{1} + \mathbf{0{,}75}\left(\frac{\lambda_s}{\lambda_w} - \mathbf{1}\right)} \right]$$

$$g_a = \mathbf{0{,}035} + \mathbf{0{,}298}S_r$$

$$g_c = \mathbf{1} + \mathbf{2}g_a$$

d. Improved Johansen Model

A new method to estimate thermal conductivity has been developed by Lu et al. (2007) improving the Johansen model to calculate the Kersten number (K_e) [2.16] and soil dry density [2.17]. In this new model new parameters are calculated for unfrozen soils with the following equations:

$$K_e = e^{\left[\alpha\left(1 - S_r^{(\alpha-\beta)}\right)\right]} \qquad [2.16]$$

$$\lambda_{dry} = -\mathbf{0{,}56}n + \mathbf{0{,}51} \qquad [2.17]$$

In this model, α and β are parameters obtained from the sand content of the soil and represent parameters related to the soil texture (α) and shape (β). For coarse materials $\alpha = 0{,}96$ and for fine soils $\alpha = 0{,}27$ meanwhile $\beta = 1{,}33$.
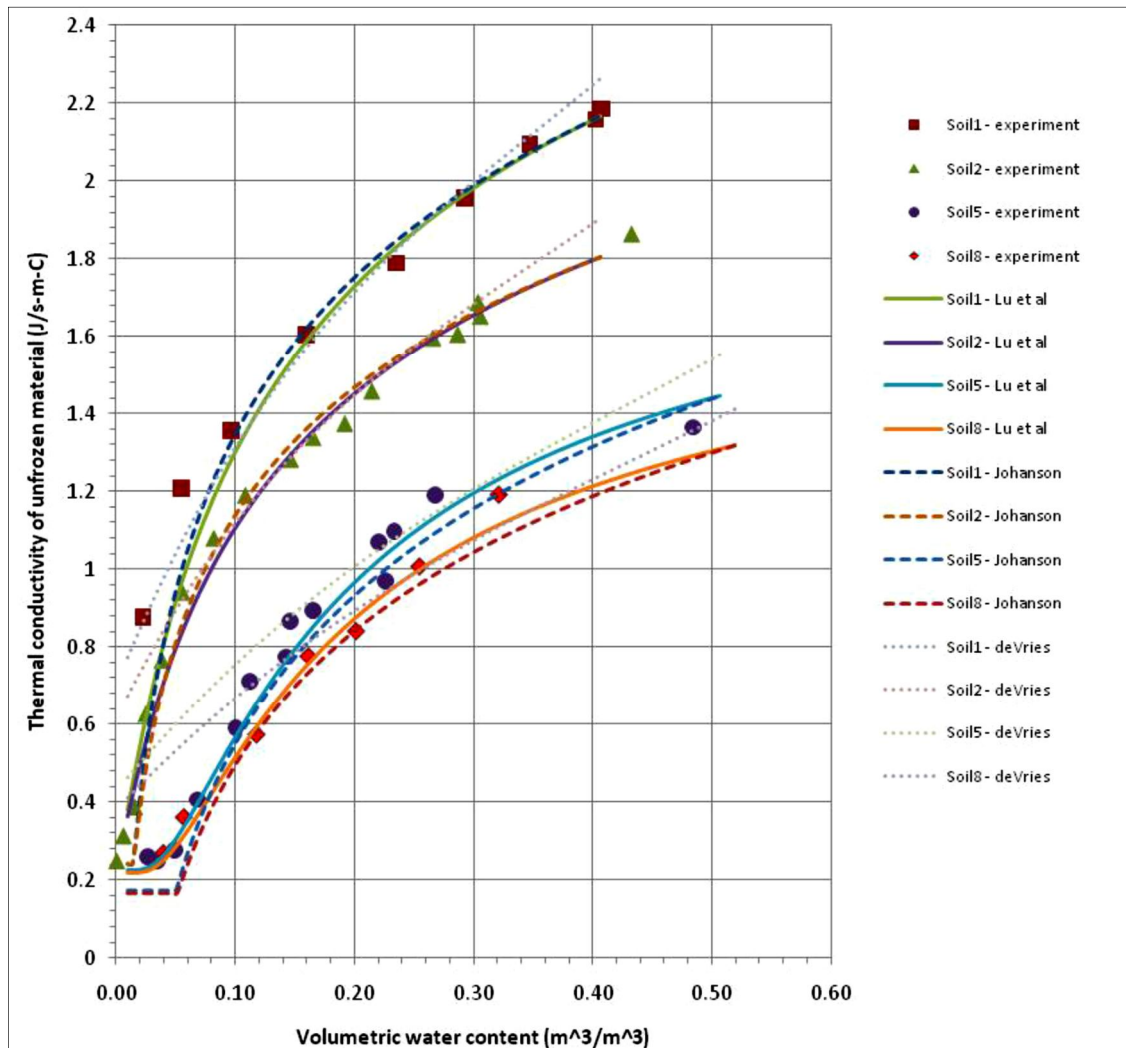
Figure 2-19. Calculation of the thermal conductivity of soils using different methods (SV Heat Theory Manual, 2012; Lu et al., 2007)

2.4.4 Heat Capacity

Heat capacity per unit volume is defined as the total amount of heat that is required to increase the temperature of a unit of volume by 1°C [2.18]. Heat capacity depends on the mass heat capacity (c) and the density (ρ):

$$C = c\,\rho \text{ (kJ/m}^3\text{ K)} \qquad\qquad [2.18]$$

In case of soils, the volume is occupied by soil grains, water, ice and air [2.19]. The volumetric heat capacity of the soil is:

$$C = C_s\,x_s + C_w\,x_w + C_i\,x_i + C_a\,x_a \qquad\qquad [2.19]$$

Where x_s, x_w, x_i, x_a represents the volumetric proportions of the ground components; soil, water, ice and air and C_s, C_w, C_i, C_a are the respective volumetric heat capacity of them.

2.4.5 Thermal Properties of Rocks

In case of rocks, as in soils, the principal mechanism of heat transmission is conduction and secondary mechanisms are convection and radiation. Thermal conductivity is easier to obtain in minerals than in rocks due to the defined crystalline structure and chemical composition. Thermal conductivity of rocks depends on many variables such as temperature, pressure, composition, porosity and water content. It is assumed that rocks are homogeneous and isotropic in many classifications which define thermal conductivity values. Other rock properties such as bedding, foliation, fracturing, and other variations in composition and structure are not taken into account (Clauser, 2006). The tables that provide the thermal properties of rocks are useful for its classification and to obtain thermal conductivity values for heat flow studies and research on geothermal sources.

The main factors that affect thermal conductivity in rocks are:

- Porosity and presence of water: The effect of the presence of water in rocks on the thermal conductivity is significant. Thermal conductivity increases as the water saturation increases. This relationship is nonlinear and it varies according to the type of rock, pore geometry and permeability of fluid.

- Composition: the presence of high-conductivity minerals in rocks increases the thermal conductivity of the rocks largely, especially with the presence of minerals such as olivine phenocrystals and even more the presence of quartz. On the other hand, clay minerals as kaolin or illite reduce thermal conductivity of rock.

Rocks can be divided in different groups based on the main factors that affect the thermal conductivity. Clauser (2006, 2009) proposes to divide rocks into four main groups based on the origin of the rock and the factors that cause or have more effect in thermal conductivity on each (Table 6).

Table 6. Rock types and thermal conductivity (Clauser, 2006)

Group of rocks	Factors
Sedimentary	Porosity and sediment type
Volcanic	Porosity
Plutonic	Dominant mineral (Feldspar content)
Metamorphic	Dominant mineral (Quartz content)

Other factors that influence the thermal conductivity of rocks are (Caluser, 2006):

- Pressure: Due to the increasing pressure fractures and cracks begin to close and this reduces the thermal contact resistance and porosity.
- Partial saturation
- Temperature: Thermal conductivity is a function of temperature and it varies inversely. The thermal expansion of the different minerals may create contact resistances that reduce the thermal conductivity of the rock for low temperature values.

Table 7. Thermal conductivity and heat capacity of rock types and minerals (Sundberg, 1989 & SV Heat Theory Manual, 2012)

Mineral or Rock	Heat capacity (J/kg·K)	Thermal conductivity (W/m·K)
Quartz	750	7,7
Quartzite	-	5,35 – 8,10
Granite	800	2,85 – 4,15
Granodiorite	-	2,95 – 3,85
Gneiss	-	2,70 – 4,40
Metamorphic	-	2,45 – 4,90
Sandstone	850 - 1000	2,30 – 6,50
Shale	950 - 2200	1,50 – 3,50
Limestone	850 - 2200	1,50 – 3,30

2.5 Mechanical behaviour of energy piles

Energy pile systems functions as foundation and as heat exchange elements in the ground with the aim to be a bi-function foundation. The two main functions of the systems are to support the static loads of the building and to heat or cool the building as required.

Temperature in the piles is generally designed between +2°C and +30°C (Loveridge, Amis & Powrie, 2012), but these values depend on the ground and air temperatures. Temperature changes in the ground caused by energy foundations in heating/cooling operation are small but their effects should be checked. Soil freezing surrounding the piles due to an excessive heat extraction may change soil properties considerably and has to be avoided (Brandl, 2006).

2.5.1 Mechanical Stresses

During heating and cooling cycles, thermal changes produce volume changes in the pile and in the ground surrounding it. The pile expands during heating and contracts during cooling causing axial tensile stresses and also affecting pile-soil interaction (Figure 2-20). During heating, the thermal expansion of the pile alters the pile-soil interaction, increasing the friction and adding compressive stresses to the pile. It has been shown in the past that the thermal expansion induces changes in the static behaviour of pile foundations after applying several cycling thermal loads (Amatya et al., 2011). In addition, the pile expansion also causes deformations in the surrounding soil. In order to avoid problems related with thermal effects in energy foundations it is important to understand the mechanisms of response better and provide indicative values of thermal effects.
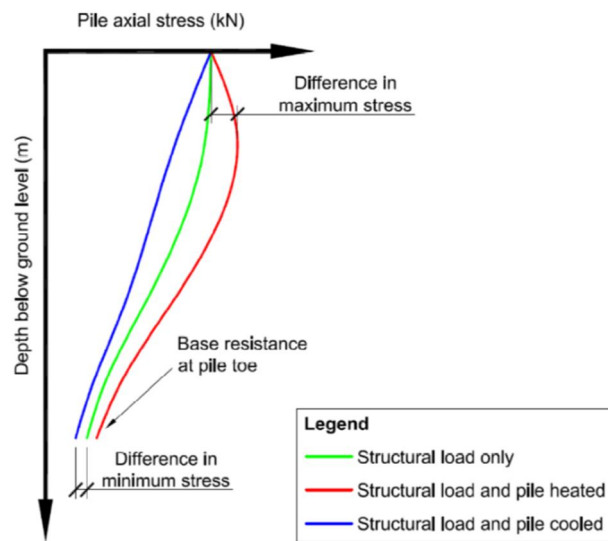
Figure 2-20. Variation of axial stress with depth of a pile due to thermal loading (GSHPA, 2012)

The volume change process in the soil and in the pile due to the temperature changes produces deformations (ε_{th}) in the materials. The deformations depend on the thermal expansion coefficient (α) of each material and the temperature variation as mentioned in the equation [2.20]:

$$\varepsilon_{th} = \alpha \Delta T \qquad [2.20]$$

If the mechanical load is less than 40% of the ultimate load, a perfect thermo elastic condition can be assumed (Kalantidou et al., 2012), and the total deformation (ε_{tot}) of the material is the sum of the elastic deformation (ε_{el}) and the thermal dilatation (ε_{th}).

$$\varepsilon_{tot} = \varepsilon_{el} + \varepsilon_{th} \qquad [2.21]$$

New deformations due to the expansion process induce compressive stresses to the pile. They can generate shear stresses between pile-soil and they should be considered in the structural design. Considering a perfect elastic condition, normal stress depends on the modulus of elasticity (E) and elastic deformation (ε_{el}). This is shown in the following equation:

$$\sigma = E\varepsilon_{el} = E(\varepsilon_{tot} - \varepsilon_{th}) \qquad [2.22]$$
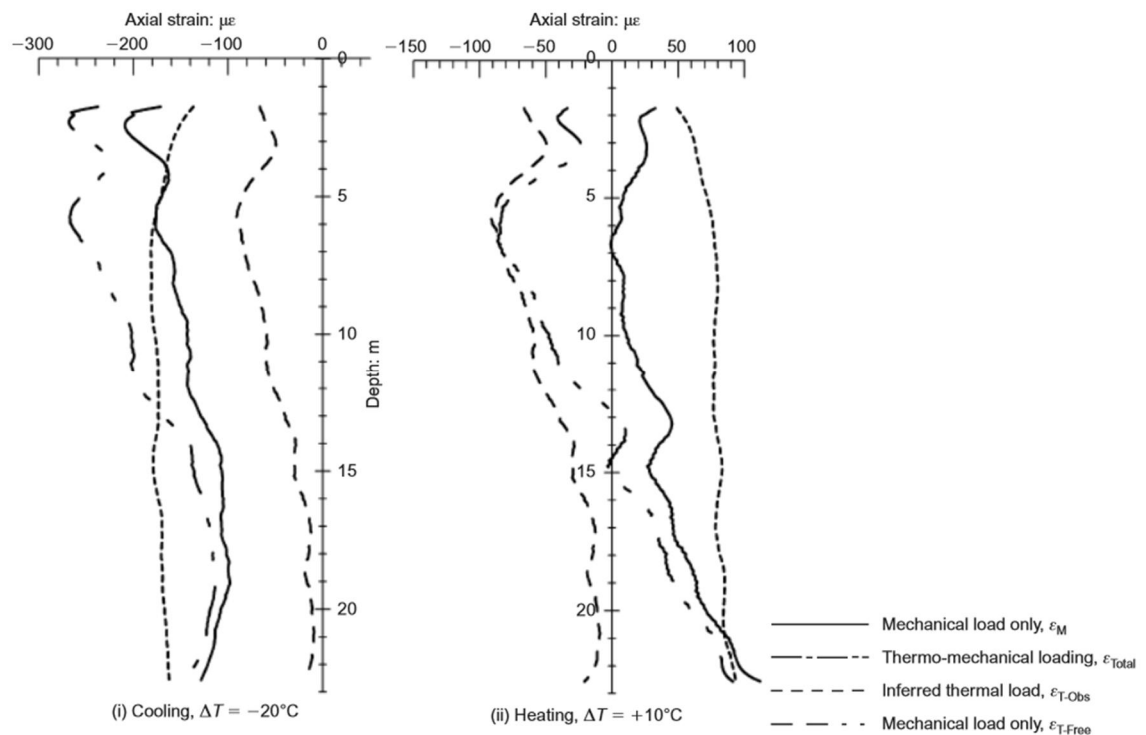
Figure 2-21. Measured axial strain profile of energy pile after thermal loading in London during heating (right) and cooling (left) (Amatya et al., 2012)

2.5.2 Deformations

Thermal loading also produces head settlement in the piles (GSHPA, 2012). After the initial settlement due to the structural load, the piles experiment deformations due to the cyclic thermal loading during heating and cooling (Figure 2-22). Repeated cyclic thermal loading reduces the shaft friction along the pile accumulating head settlement deformations, especially during cooling.
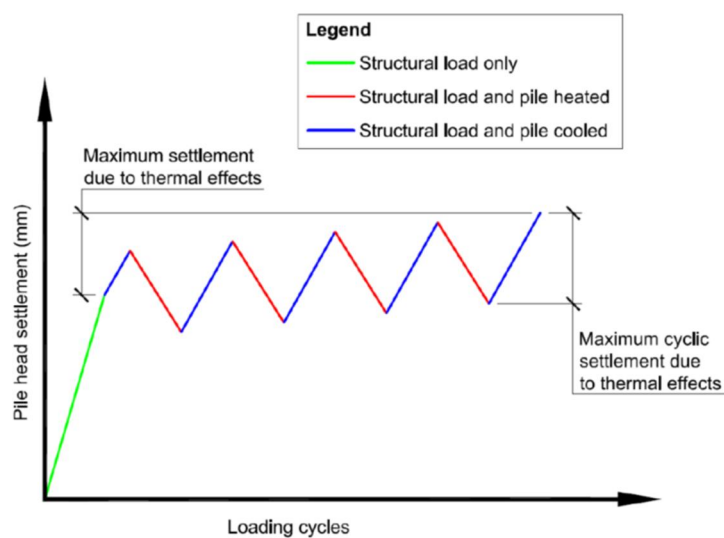
Figure 2-22. Variation in pile head settlement due to thermal load cycles (GSHPA, 2012)

Suryatriyastuti et al., (2011) reported that the energy piles subjected to thermal loads in seasonal operation produce uplift displacements and soil heave during heating (summer) and downward displacements in piles and settlements during cooling (Figure 2-23).
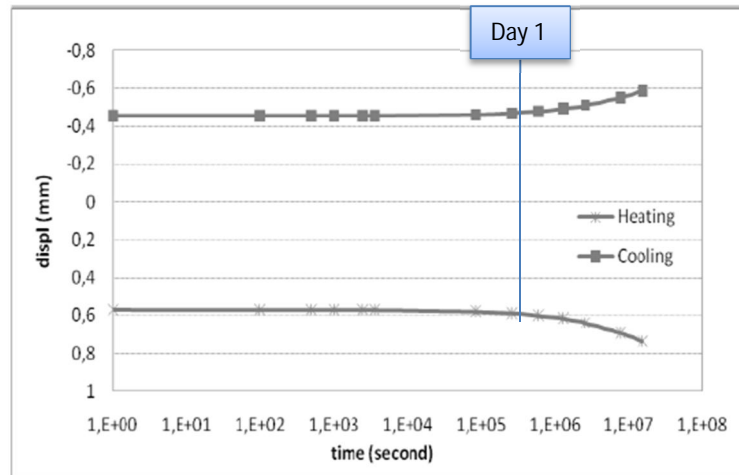
Figure 2-23. Evolution of uplift displacement in thermal loading during 6 months (Suryatriyastuti et al., 2011)

2.5.3 Other Considerations

Other consideration that has to be taken into account is that the thermal changes in the ground can produce water migration due to evaporation and condensation processes (Farouki, 1986). The water flow and the thermal expansion increases pore water pressure and reduce the effective stress of the soil. The presence of organic content increases the temperature sensitivity especially in clays (Brandl, 2006). Even though in the practice the effects are negligible, it must be considered in buildings sensitive to differential settlements.

In frictional piles, the response to vertical loads is strongly related to the interaction between pile and the soil. In this case the effects caused by thermal loads have to be taken into account. The changes in the pile-soil interface due to the temperature variations change the mechanical behaviour of the pile and the surrounding soil. If the phenomenon is repeated cyclically for a long time period it can produce a failure at the interface plane.
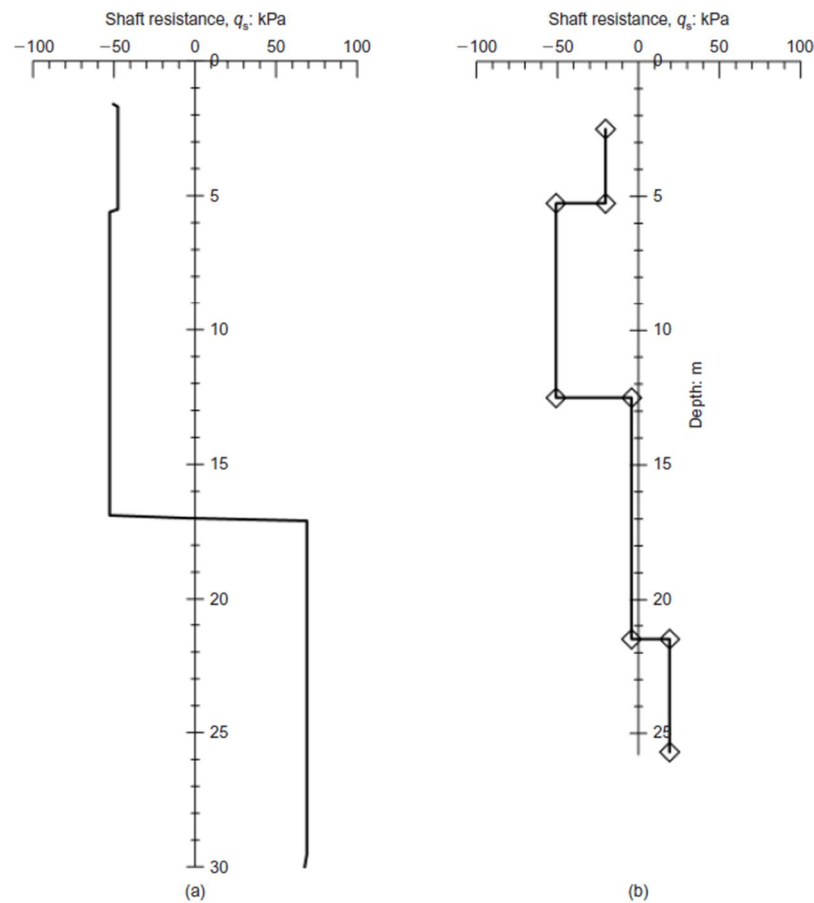
Figure 2-24. Mobilized Shaft friction in an energy pile due to thermal loading (heating); (a) London ; (b) Lausanne (Amatya et al., 2012)

Other important point in the design of energy piles is to avoid ground freezing surrounding the pile. It is important to keep soil-pile interface temperature above 0°C because if not, interface characteristics may change (Loveridge, Amis & Powrie, 2012).

In conclusion, thermal pile expansion/contraction during seasonal changes alters soil-pile interaction, mobilized shaft resistance and induces additional stresses and displacements. The displacements induced are mainly reversible and their effects are negligible (Brandl, 2006). Fine soils are more sensitive for temperature changes than coarse and granular soils. In addition, the presence of organic contents increases the temperature sensibility. On the other hand, irreversible settlements appear when the mechanical loads exceeds 40% of the ultimate capacity but still, conventional safety factors are adequate to avoid mechanical failure due to thermal loads (Kalantidou et al., 2012).

Table 8. Summary of piles response to thermo mechanical loading of different cases (Amatya et al., 2012)

	Location						
	London	Lausanne	London		Lausanne		Bad Schallerbach
Test ID	Heat sink pile	T-1	Main test pile		T-6	T-7	–
Thermal phase ΔT: °C	Heating 29·4	Heating 20·9	Cooling −20	Heating 10	Heating 18		Mixed +7 to −14
Max. thermal axial load: kN	−1550	−2150	670	−675	−3060	−2830	−300
Depth to point of max. thermal load: m	17	About 20	15	6	12·5	12·5	4·5
Max. thermally induced stress change: kPa/°C	−192	−104	177	−329	−153		*
Induced thermal stress at head: kPa/°C	~0	−50	~0	~0	−150		−27*
Induced thermal stress at toe: kPa/°C	~0	−87	~0	~0	−79		*
Thermally induced shaft resistance: kPa/°C	−2·1 (upper 17 m) 2·5 (lower 13 m)	−1·5 (soft clay) −0·5 (soft till) 0·9 (stiff till)	2·1 (6−15 m) −4·0 (20−22·5 m)	−5·9 (0−6 m) 1·5 (6−15 m) 5·4 (15−22·5 m)	−2·5 (soft clay) 0·5 (soft till) 5 (stiff till)		2·7* (4·5−6·5 m section)

Note: Compression negative; bgl = below ground level
* Indicative, or not possible to assess owing to non-uniform temperature profile

Otherwise, dimensioning process of heat exchanger piles is based on empirical considerations using conservative methods in order to be on the safe side (Boënec, 2009 and Johnsston et al., 2011). The knowledge of mechanical behaviour of heat exchanger piles makes the dimensioning process of energy pile foundations easier and more efficient. Currently there is no design method available that considers the complex interactions between cyclic thermal loads and the mechanical behaviour of energy piles.

2.6 Effects of Freezing and Thawing in Soils

2.6.1 Thaw Settlement:

Frozen ground contains ice in several forms as ice lenses or the massive frozen ground. In the thawing process, the ice disappears and the soil has to adapt to a new equilibrium situation. The study of this new equilibrium situation is important in the design of building foundations on frozen grounds.

Volume changes due to the freezing and thawing processes are a result from the phase change (ice to water) and due to the water flow (consolidation) from the soil. The magnitude of the settlement depends on many factors such as type of soil, ice content, density, excess pore pressure and compressibility of the soil (Phukan, 1985). Next figure (Figure 5-6) shows a typical thaw-settlement curve. As can be seen, during the thawing process at a constant pressure a big change in void ratio occurs due to the phase change from ice to water and the flow of excess water out of the soil (Point b to c). After this point (Point c), increasing the pressure new volume changes occur due to normal consolidation process (Point c to d).
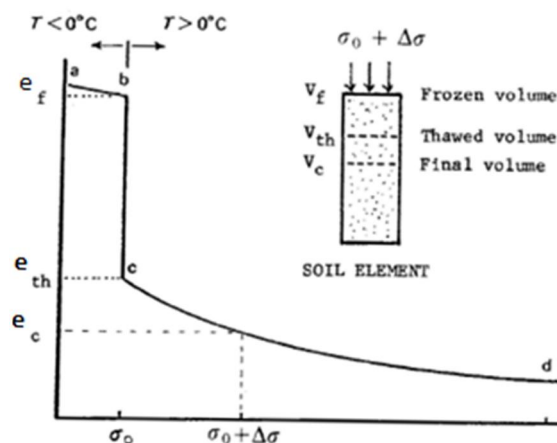
Figure 2-25. Typical void ratio versus pressure curve for frozen soils subjected to thawing processes. (Andersland et al., 1994)

The thaw settlement (ΔH) and the thaw strain parameter (A_o) are (Andersland et al., 1994):

$$A_o = \frac{e_f - e_{th}}{1 + e_f} \qquad [2.23]$$

$$\frac{\Delta H}{H} = A_o + m_v \Delta \sigma \qquad [2.24]$$

Where:

- e_f : Frozen void ratio
- e_{th} : Thawed void ratio
- σ : Effective stress
- m_v : Coefficient of volume compressibility

- H : Thickness of the soil strata

Freezing and thawing processes also produce changes in the consolidation properties of fine grained soils. Consolidation coefficient and hydraulic conductivity increases after freezing and thawing cycles (Paudel & Wang, 2010).

Some alternative correlations express thaw settlement using the relationship between settlement and basic physical properties of frozen soils. The next formula shows the thaw settlement as a function of the water content (Vähäaho, 1989):

$$A = \frac{w}{k_1} \qquad\qquad [2.25]$$

Where:

- A: Thaw settlement (%)
- w: Water content: (%)
- k_1: Thaw settlement factor. Range [2-6] depending on field conditions.

The previous formula gives good results for estimating the thaw settlement as a function of the water content. Other experimental equations, like Speer et al. (1973) and Watson et al. (1973) use the unit weight to estimate thaw settlement (Figure 5-7).
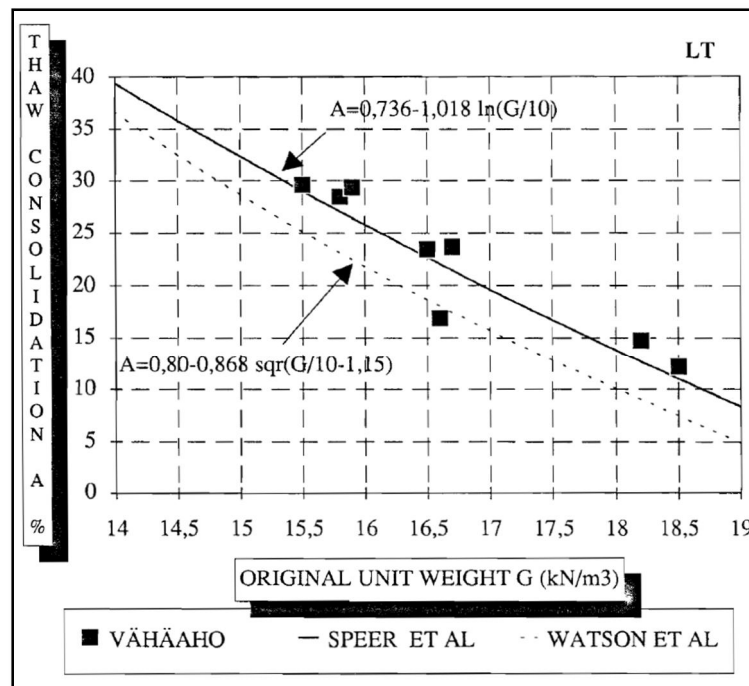
Figure 2-26. Thaw settlement as a function of the original unit weight (Vähäaho, 1989)

For further freezing-thawing cycles, the thawing settlement is smaller than in the first cycle. Vähäaho (1989) proposes following formulation for the second and third freezing-thawing cycles:

$$\Delta\epsilon_2 = \frac{w}{k_2} \qquad\qquad [2.26]$$

$$\Delta\epsilon_3 = \frac{w}{k_3} \qquad\qquad [2.27]$$

Where:

- $\Delta\epsilon_i$: Increment of thaw settlement in the cycle number i (%)
- w: Water content: (%)
- k_i: Thaw settlement factor. Recommended k_2=20 and k_3=40

2.6.2 Shear Strength Changes:

Thaw consolidation produces changes in the shear strength of clays. After thawing process, the shear strength decreases rapidly but when the soil dries, the shear strength is higher than in the initial situation. The increment after thaw consolidation is even bigger in remoulded shear strength (Vähäaho, 1989). The values for estimate the shear strength after thaw consolidation are:

Shear strength: $S_v(t)= r_t\ S_v$

Remoulded shear strength: $S_{vr}(t)= 4\ r_t\ S_{vr}$

Where r_t is a factor which during the thaw takes a value of 0,5 and in the final consolidations it varies between 1,35-1,9.

The increasing of the shear strength is due to the effect of the thaw consolidation in cohesion and friction angle. The cohesion of the soil increases after thawing processes on average by 100% and the friction angle by 10% (Vähäaho, 1989).

2.6.3 Changes in the Mechanical Properties of Clay:

Thawing and freezing processes produce changes in almost every mechanical property of clays due to changes in the clay microstructure (Vähäaho et al., 1989). The main changes are shown in the following Table 9.

Table 9. Main changes in mechanical properties of clay due to thaw consolidation (Vähäaho, 1988)

Property	Change	Range of value
Unit weight	Increase	10-15%
Water content	Decrease	33-40%
Liquid limit	Decrease	15-25%

3 Numerical Methods and Modelling in Geotechnical Engineering

The computing power available has resulted in advanced software products for engineers and scientific analysis. They made it possible to use powerful technique such as a finite element analysis in engineering practice, opening a new window as an application tool in numerical modelling.

Finite element codes are extremely powerful calculation tools and they help to resolve complex problems in relatively short time. However, the result depend on the input provided by the user and thus is essential that the user has a complete understanding of the input parameters and know the limitations in order to produce a reliable output. Software provides the ability to do highly complex computations that are not otherwise humanly possible, but obtaining useful results depends on the user ability to interpret the results. Furthermore, the results from numerical analysis should not be applied to an engineering design or practice without being filtered through professional engineering judgment.

A numerical model is a mathematical simulation of a real physical process. It is a simulation of real process and it is an attempt to take our understanding of the process and translate it in mathematical terms. It is purely mathematically and it differs very much from the scaled physical modelling in laboratory or full-scaled field modelling. Mathematics can be used to simulate real physical process because physical process follows mathematical rules and we can use them to develop a deeper understanding of the physical processes.

3.1 Advantages and Limitations of Numerical Modelling

Numerical model has many advantages over physical modelling but it would be wrong to think that numerical models do not have limitations. Some of the more obvious advantages are:

- Save time: Numerical models can be set up quickly than physical models which may take months to construct meanwhile numerical models can be created in hour or days.
- Scenarios: Physical models are usually limited to fixed or narrow conditions meanwhile numerical models can be used to investigate different scenarios.
- Scale effect: Physical model can have problems scaling some parameters like the gravity, but numerical models have not got this difficulty.
- Information: Physical models only provide information and data at discrete instrumented points. Numerical modelling provides information and results in any location.

Otherwise, associated to the thermal heat flow there are also many limitations that have to take into account. These limitations are for example: changes in pore-water pressure, volume changes and perhaps chemical changes. In the other hand, describe mathematically the constitutive relationships is not possible due to its complexity but

still some of these difficulties can be overcome with greater and faster computer processing power.

3.2 How to Model

A numerical model is a mathematical simulation of a real process but as in a real problem, careful planning involved in a site characterization or measurements is also required for modelling.

It is important to have conceptual model of the problem and make a guess or have some basic or empirical calculations of the solution before starting to model. Planning is necessary before start to model and have a mental picture and think about how results will look like. After that, if there is not any similarity between the results and what is expected is easier to understand what is wrong in the modelling process. If there is not any preliminary guess solution, then it would be difficult to judge the validity of the results.

Another important part of modelling is to define the main objective of the modelling process. Depending on the main objectives, some parameters can be determinate with accuracy meanwhile there is no needed to spend a lot of time establishing some other.

Numerical model is a simulation of a real physical process and need to be a simplified abstraction of the field conditions. In the field, ground profile, stratigraphy and boundary conditions may be complex and irregular but in a numerical model they need to be simplified. Numerical model should not become too complex and include all the detail that exists in the field. It is a tendency to make geometry too complex, but increasing the complexity does not always lead to a better and accurate solution because geometric details can even create numerical difficulties and difficult the interpretation of the results.

A general rule to make a model is to start with the simplest model geometry and judge its results. Then if the solution is valid, you can add details and more complex elements to the model. It is much more efficient to start from simple and build the complexity into to the model in stages, than to start with a complex model. Otherwise, in the early stage of the numerical models simplicity has to be applied to the material properties, too. It is a good idea to start with estimated material properties in order to obtain understandable and reasonable solutions and for checking that the model has been set up properly. After the preliminary models the input parameters also need to be determinate with accuracy. Better and more accuracy results can be obtained combining laboratory and field test to get material parameters for the new available software tools.

3.3 Numerical Modelling in Geotechnics

Nowadays numerical methods are used in geotechnical design and in ground engineering to solve many problems related with:

- Slope stability and limit equilibrium slope analysis to determine the critical slip surface

- Stress state and deformations simulating the behaviour of soils and rocks with elastic or plastic analysis
- Ground water flow in saturated and unsaturated soils
- Vapour flux and infiltration in saturated soils
- Transport and seepage of contaminants in saturated and unsaturated soils
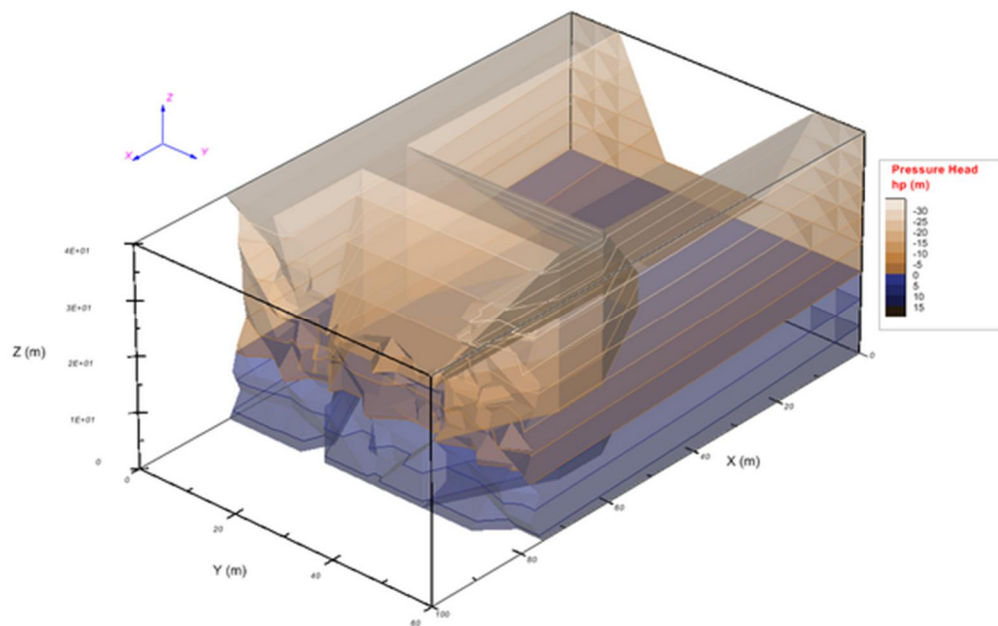- Geothermal analysis and convective and conductive heat flow in soils and rocks

Figure 3-1. Illustration of a 3D model of a dam in a valley using SoilVision (SoilVision 2012)

Concerning the geotechnical engineering and heat flow in soils and rocks, finite element software and numerical methods are important tools which can be used to model thermal changes in ground. Environmental chances or the construction of buildings and facilities can produce thermal variations in the ground. It is important to know ground thermal behaviour and keep the ground thermal balance. Numerical methods make it possible to analyse simple and complex geothermal problems, freezing and thawing process or heat transfer through any type of porous material containing soil, water, ice and air at the same time.

Recently, numerical methods and models have been applied in order to investigate and develop long time ground temperatures behaviour and energy foundations operations. Develop numerical models and methods for heat transfer in ground are useful to investigate thermodynamic aspects and ground temperature distribution surrounding heat exchangers in long-time period operations in order to keep ground thermal balance. These tools are also a good alternative combined with results of experiments in situ and laboratory tests.

4 Case Histories from Literature

4.1 Energy Pile Testing in Hämeenlinna

A test site was constructed by the company Ruukki in Hämeenlinna for the testing and performance of energy pile systems (Kesti, 2012). Characteristics of the test site:

- Type of piles: Steel piles (RR170/10 and RR140/8) filled with loose concrete-mix
- Length of the piles: 20 m
- Diameters: 170mm (RR170/10) and 140mm (RR140/8)
- Thickness: 10mm (RR170/10) and 8mm (RR140/8)
- Distance between piles: 5-10m
- Pipes configuration: Simple U-tubes (40mm and 25 mm diameter)
- Carrier fluid: 28% water-ethanol liquid
- Soil profile: 20m depth of clay (λ=1,8 W/mK) above the bedrock
- Soil temperature measurements at 1m from the pile at depths: 5m, 10m, 15m and 20m

For heating, the results of the pile testing shown that the power of the piles was between 0 to 300-500 W/pile that corresponds to a maximum between 15-25 W/pile-m. The average values for the test period were 9.5-12 W/pile-m with an average difference between the inlet and outlet liquid temperature of 0.5-0.6^{o}C. The temperature difference between the ground and the carrier fluid was between 0°C to +4.2^{o}C, with an average of +2.6^{o}C.

During the cooling season the inlet heat transfer liquid was heated by a small boiler with temperatures between +12°C to +18°C. In one of the piles the fluid was heated at +55°C during a short period. The average power values for the test period were between 5.8-18.6 W/pile-m with an average difference between the inlet and outlet liquid temperature of +0.3^{o}C to +1.2^{o}C. In case of the pile with the fluid heated at +55°C, the average power was 62.2 W/pile-m with a temperature difference between the ground and the liquid of +33.3^{o}C (Kesti, 2012).

The case studied with high fluid temperature during the cooling season (ground loading period) was studied to know ground thermal behaviour to store seasonal heat. This heat storage can be done with solar panels or other systems than can collect the wasted heat and pump it into the ground.

4.2 Office Building in Jyväskylä

A new 6-storey office building (Technopolis Innova 2) was built in Jyväskylä in 2012. It is the first building in Finland using an energy pile foundation and has an area of 1700m^2 (Uotinen, 2012).

The building is located on reclaimed lake area and the ground is divided in four soil layers. The top soil layer is a coarse-grained fill mixed with soft sediments of the lake with thickness between one and three meters. Under it, there is a 3-6 meter thick layer

of soft material, mainly clay and silt, with high organic content and water content between 30-60%. Under the soft layer there is a dense silt layer with 15m thickness. Finally, under the silt layer there is a dense layer of moraine with lot of boulders.

The building has a foundation with 246 driven piles with lengths between 22-29m. Three types of steel piles were used: RR220/12.5, RR220/10 and RR170/10 with diameters between 220mm (RR220/12.5) and 170mm (RR170/10). The bearing capacity of the piles is between 1350kN and 691kN. The pile foundation has 38 energy piles, using at least one pile per column as an energy pile with approximately a total length of 1050 of energy piles in contact with the ground. The distance between piles varies between 5.5 to 7.8m and each energy pile covers $40m^2$ of base area. Heat collecting pipes (Uponor PE-Xa U-shape) with outside diameter of 25mm were installed inside the piles and after the installation the piles were filled with mortar. Seven different manifolds collect all the pipes from the piles. The manifolds were also connected to the heat pump in order to control the system.

The energy consumption of the building per year is 318 MWh for heating and 427 MWh for cooling. Energy production simulations were carried out with different thermal conductivities of the soil (1.1, 1.8 and 2.2 W/mK) considering the initial temperature of the ground at $+8^oC$. These simulations show that using a ground thermal conductivity of 1.8W/mK the energy savings were:

- Heating: 165 MWh per year, almost 50% of the energy required
- Cooling: 160 MWh per year, about 38% of the energy required.

A monitoring system is installed in order to control the temperature of the soil in three different points. Temperature measurements are observed every one meter until 15m depth. The efficiency of the system will be evaluated with the temperature measurements and energy consumptions of the building. The payback period would be between 9-10 years according to the energy savings, the investment cost and price of the energy (Uotinen, 2012).

4.3 Energy Pile Simulations for Buildings done by Ruukki

Some simulations for heating and cooling buildings with energy pile foundations have been carried out by the company Ruukki to show the benefits of this system. These simulations were done to see the benefits of the energy savings that can be obtained with energy pile systems in commercial and office buildings. Next examples present the results for the models and simulations carried out for a one-storey commercial building and three-storey office building (Ruukki, 2012).

- One-storey commercial building:

A hardware store building was selected as the one-storey commercial construction. The level of the thermal insulation corresponds with the national energy regulations of 2010. The efficiency of the ventilation and the heat recovery system is at good level. The secondary circuit for heating and cooling the building consists in water circulation in pipes embedded in the floor.

With the energy pile solution, the building obtains 71% of the energy required for heating and 100% of the cooling energy used in the building. The heating and cooling benefits could be improved if the heat from refrigerator equipment would be stored in the ground. This can be applied in supermarkets and building with cooling equipment.

Main characteristics of the building:

- Total area: 8400 m^2
- Number of energy piles: 264
- Length of the piles: 20 m
- Thermal conductivity of the ground: 1,1 W/mK
- Heating energy: 34 kWh/m^2 a
- Cooling energy: 10,4 kWh/m^2 a

– Three-storey office building

In this case, a small three-storey office building was simulated. It was assumed that the energy efficiency and the thermal insulations were according to 2010 national regulations. The energy piles heating and cooling system was compared with a common district heating solution.

For cooling purposes, building requirements were relatively high compared with others buildings in Finland. For cooling, the free energy from the soil using an energy pile system can be 88 per cent.

For heating purposes, the geothermal pile system cover nearly 80 per cent of the building's energy needs and the remaining 20 per cent will be covered by district heating.

The calculated carbon footprint of 25-year for the energy pile system period was only about 40 per cent compared to a district heating solution. In addition, the effects of the production method of the electrical energy for district heating were no taken into account.

Main characteristics of the building:

- Total area: 2700 m^2
- Number of energy piles: 30
- Length of the piles: 15 m
- Thermal conductivity of the ground: 1,6 W/mK
- Heating energy: 54 kWh/m^2 a
- Cooling energy: 53 kWh/m^2 a

5 Kupittaa case in Turku

5.1 Introduction

In Kupittaa case, an energy pile system was studied for heating and cooling purposes of a new building for the Turku University of Applied Sciences. The goal is to build a sustainable and energy efficient campus. The main objective of this study was to determine the total amount of usable energy that can be used without breaking ground thermal balance. Besides, Turku University of Applied Sciences has patented several inventions to install underground barriers without excavations and the Kupittaa case is possibly the first time to model the effects of and underground insulation barrier in Finland. For this reason simplified models were created in order to know the energy that can be extracted/pumped from the soil keeping ground thermal balance.

The building design has not started yet, so this is a preliminary study of the possibilities to use an energy pile foundation in Kupittaa. The size of the building, the structural solutions for the building or the foundation as well as the energy requirements are not known at the moment. An energy pile foundation could be one of the best solutions for cooling and heating this building. Besides, there is no ground investigation from the site available, so the thermal properties of the ground that were used in the models explained below were estimated from experience and literature.

Main characteristics of the building for the study of the model:

- Concrete slab without insulation: 800 mm
- Vertical insulation barrier: 200 mm. Thermal conductivity 0.046 W/mK
- Pile diameter: 200 mm
- Pile lengths:
    - Normal Piles: 40m reaching the bedrock working as foundations and as energy pile heat exchanger.
    - Short piles: 15m long (working only in summer time pumping additional solar energy to the ground)

5.2 Modelling

5.2.1 Objectives

The main objective of this preliminary study was to evaluate the ground thermal behaviour and response for a building foundation with energy piles. In this study, ground energy storage capacity for cooling and heating of the building was evaluated in order to know the total amount of usable energy capacity in Kupittaa under the local climatic and environmental circumstances. Several 2D and 3D models were carried out to define the energy that can be extracted from the soil during the winter time and pumped during summer without breaking the ground thermal balance. Prevent ground from freezing due to a non-balance heat extraction was also an objective. In addition, the efficiency of a vertical insulation barrier of 5m depth and 200mm thick surrounding pile foundation was studied.

5.2.2 Model Geometry and Characteristics

This case was a preliminary study to evaluate thermal storage capacity of the ground. The thermal properties of the ground were estimated and based on literature. Thus the reliability of the results could be affected by the accuracy of the thermal properties used in the modelling process. For the study two different models were done. The first of them was a symmetric 2D model (Figure 5-1) for the study of the ground thermal behaviour in a big scale in a transient analysis. This model simplifies the building geometry and focuses in the effect of the piles heat extraction, the effect of the insulation barrier and the study of the amount of energy needed to keep ground thermal balance. This 2D symmetric model was studied in two different cases: with and without the insulation barrier in order to compare the results and see if the construction of a vertical insulation barrier (5m depth) helps to maximize thermal energy storage below the building. In this 2D model two different types of piles were modelled, long piles (40m long) working during the whole year and short piles (15m long) working only during summer time for recharging thermal energy storage. The second model was a 3D model of one pile and its influence area. This model was done in order to know ground thermal behaviour surrounding the pile.
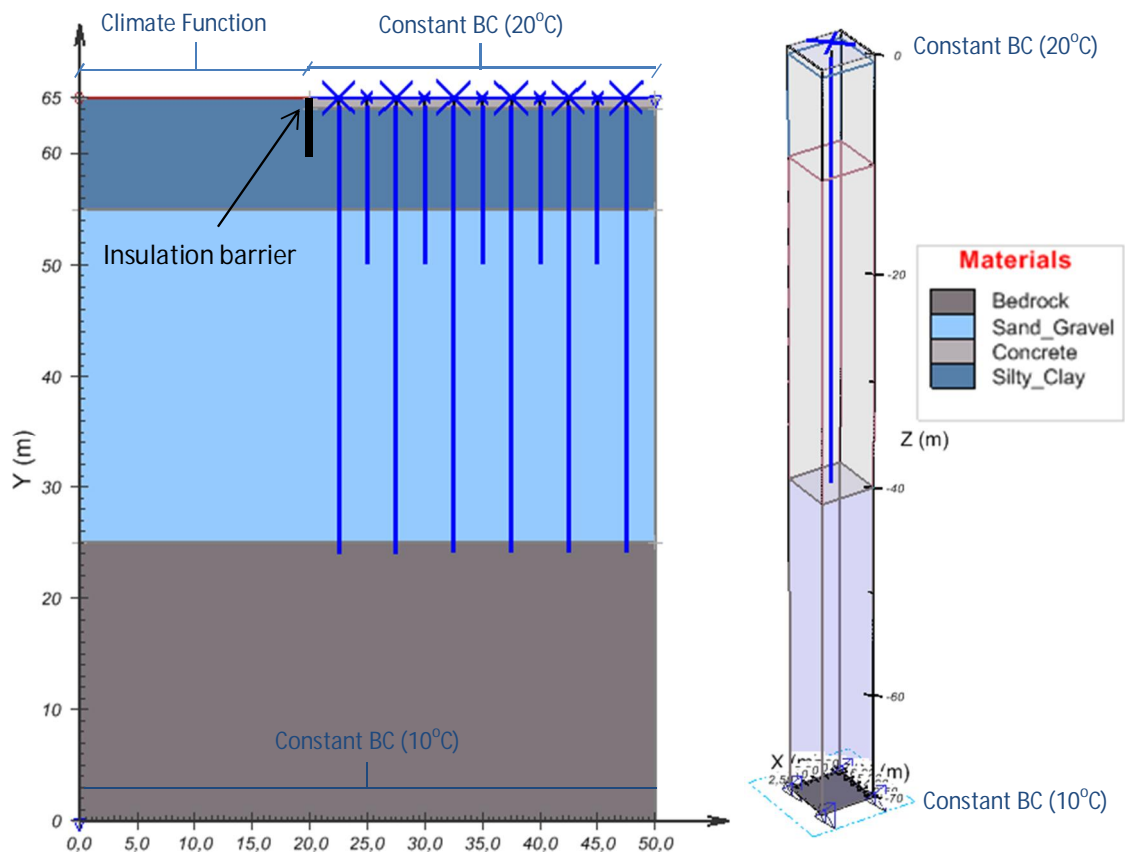
Figure 5-1. Geometry, characteristics and boundary conditions of the 2D (left) and the 3D model (right)

In both models a ten years transient analysis was studied. The initial conditions were established with two constant boundary conditions. First of them was applied in the ground surface and the temperature was the annual average temperature. The second boundary condition was applied down to 65m below ground surface and its value was +10°C. This temperature was applied in the model due to the ground water temperature measurements done in situ at the depth of 20 metres, which shown that the average ground water temperature was around +10°C.

Other characteristics of the model were:

- Long piles: Modelled as a *well boundary condition* pumping heat to the ground during summer operation and extracting during winter. Length of the piles was 40m and the distance between them is 5m (25m^2 per pile).
- Short piles: Modelled as a *well boundary condition* pumping the additional solar energy collected to the ground in summer time. Length of the piles is 15 m. They were located in the middle point between long piles only in one direction (distance 2.5m) and the distance between short piles is 5m (25m^2 per pile).
- Ground: The ground was divided into three layers:
    - Silty-Clay: Upper 0-10 m depth
    - Granular material (calcio-fluvial sand and gravel): 10-40 m depth
    - Bedrock (granodiorite)

5.2.3 Materials

The soil profile was divided into three layers and their material properties are shown in the following Table 10.

Table 10. Thermal parameters of the ground

Soil		Thermal Conductivity	Heat capacity	Vol. Water Content
		W/m K	kJ/m^{3}K	m^3/m^3
Clay	Unfrozen	1,22	2400	0,55
	Frozen	1,74	2000	0,55
Granular	Unfrozen	1,97	2800	0,35
	Frozen	3,01	2000	0,35
Bedrock	Unfrozen	2,89	1980	0,05
	Frozen	3,36	-	0,05

Other construction materials were also used in the model. Table 11 shows the properties of the construction materials used.

Table 11. Thermal parameters of the construction materials

Material		Thermal Conductivity	Heat capacity	Vol. Water Content
		W/m K	kJ/m^{3}K	m^3/m^3
Concrete	Unfrozen	1,63	2150	0,1
	Frozen	1,75	2000	0,1
XPS	Unfrozen	0,046	45	0,01
	Frozen	0,046	45	0,01

5.2.4 Boundary Conditions

a. Constant boundary conditions

In the model some constant boundary conditions were applied during transient analysis.

- Building: The building was represented in the model as a line with a constant temperature of +20°C. This value was the average value of indoor temperature during the year. No insulation was considered under the concrete slab in the modelling, even though in Finland floors need to be insulated.
- Temperature in the depth of 65m below surface: at this depth ground temperature was constant and the value is +10°C during the whole analysis.

b. Climate function

During the transient analysis a cyclic Turku climate boundary condition was used (Figure 5-2). This climate boundary condition was calculated from monthly average temperatures during the last 30 years. This climate situation is repeated annually during the transient analysis. The climate function is applied on the ground surface which is not in contact with the building.
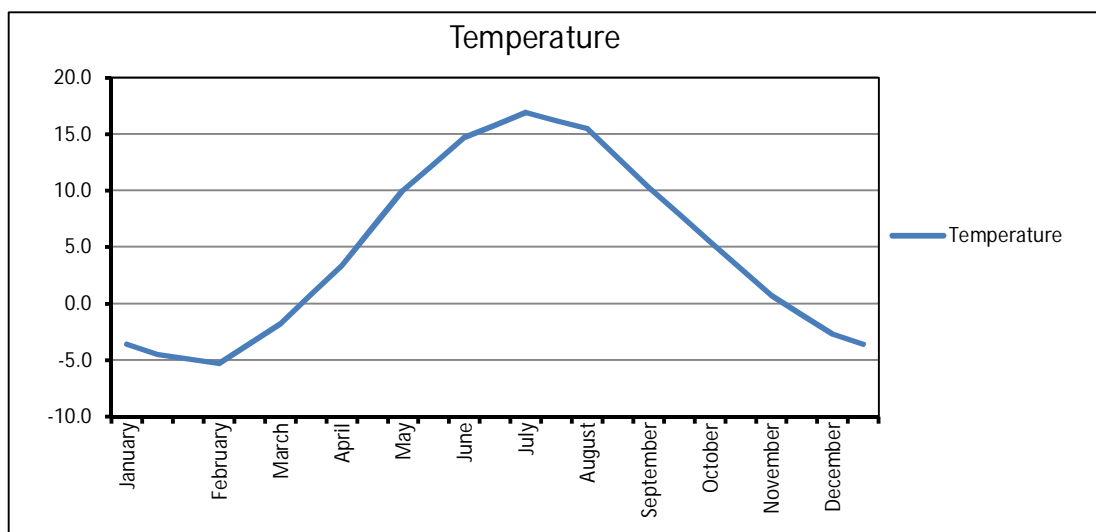
Figure 5-2. Turku cyclic climate function based on average air temperature

c. Energy function

The energy function represents the boundary condition of the heat exchangers for heating and cooling purposes during the different seasons of the year (Figure 5-4). Energy piles are used to extract or pump heat depending on the seasonal operation. The piles are absorbing or pumping different values of heat flux depending on the energy requirements of the building on each season.

The values of the energy extracted or pumped for energy functions created for the model were based on previous studies done in Finland (Figure 5-3). These studies show the energy that can be extracted or pumped from the soil depending on the thermal conductivity (Nyholm, V., 2011).
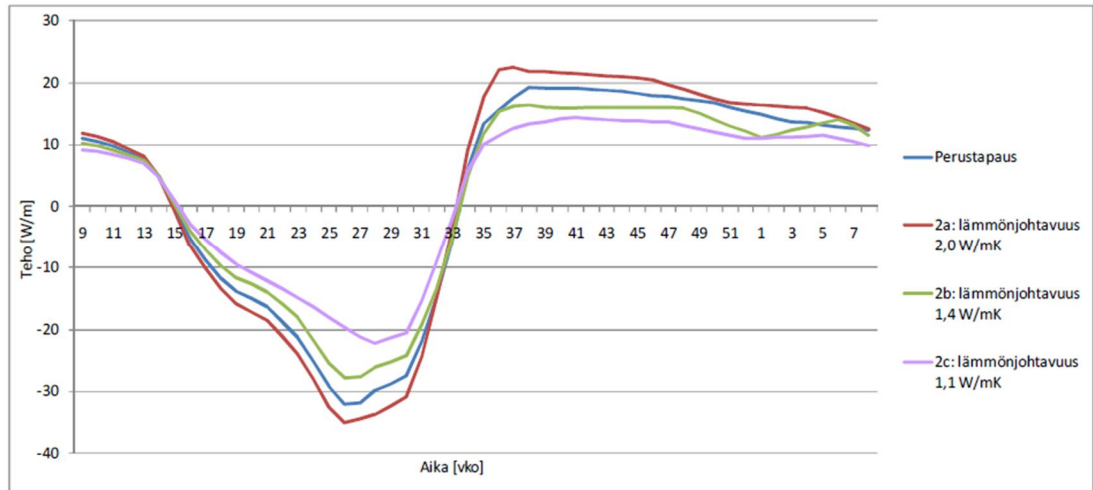
Figure 5-3. Values of energy extracted or pumped depending on thermal conductivity (Nyholm, V., 2011)

Next figure (Figure 5-4) shows the energy function calculated according to the thermal properties of the ground. The energy function for long piles was calculated by interpolating the thermal conductivity of the clay and the calico-fluvial sand (λ=1.76 W/mK). For the short piles, the energy function was calculated with the thermal conductivity of the clay (λ=1.22 W/mK). The sign criteria are positive in case of heat extracted from the soil and negative for heat pumped to the ground.
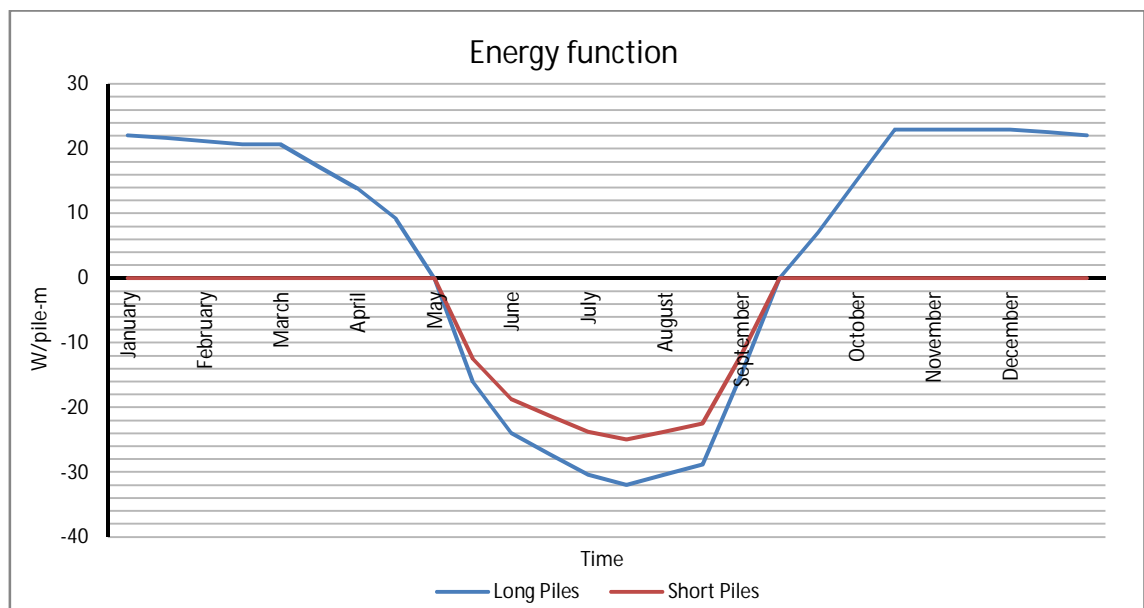
Figure 5-4. Energy functions calculated according to the thermal conductivity of the ground for long piles (L=40m) and short piles (L=15m) which only work during the summer time

Following figure (Figure 5-5) shows the energy functions used in the models according with the input parameters and sign criteria of the software used (Soil Vision/Heat). Converted to SoilVision input units from Figure 5-4.
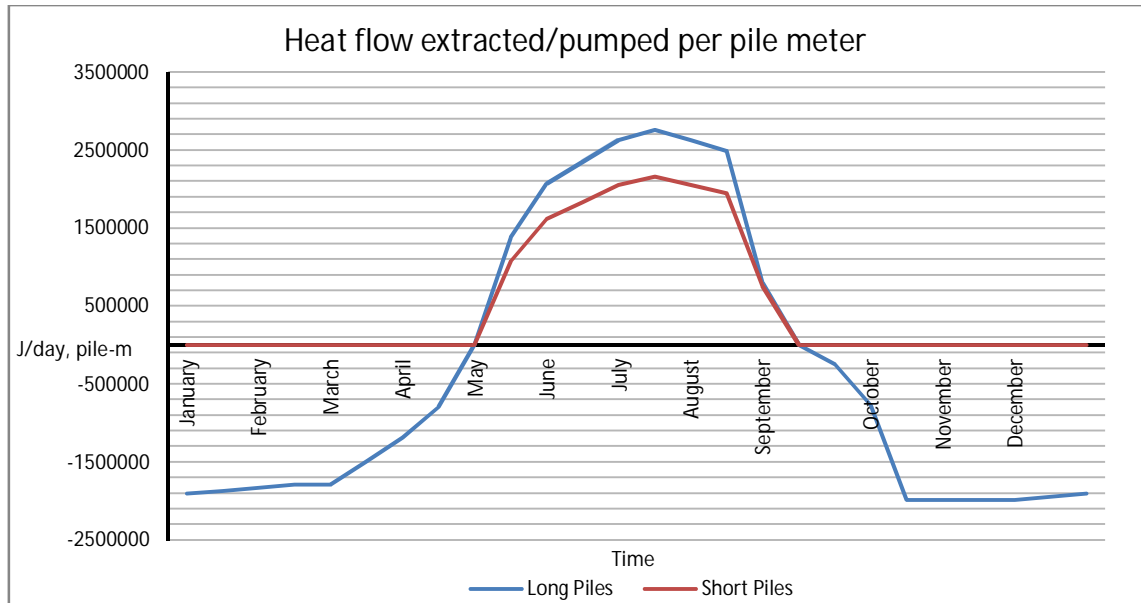
Figure 5-5. Energy piles function for SoilVision Heat. Long piles function (L=40m) and short piles (L=15m)

The software used for modelling (Soil Vision/Heat) uses the following sign criteria:

- Cooling: In summer energy piles are pumping heat to the soil (positive heat flux values)
- Heating: For winter operation energy piles are absorbing and extracting heat from the ground (negative heat flux values).

As can be seen in figures 5-4 and 5-5, in Kupittaa case, the maximum estimated value of heat flow extracted by a pile during the winter time was 23W/m for long piles. For summer time the maximum value of heat flow pumped was 32W/m. For short piles, that only work during the summer time, the maximum value of heat flow pumped into the soil was 25W/m. The values of energy extracted obtained from the energy function are similar to the typical values that can be found in literature (Brandl, 2006). These typical values of heat flux for energy piles were between 20-50 W/pile-meter.

Calculating the area under the blue curve and multiplying with pile length 40m (Figure 5-5), the energy function for the long piles presents an annual deficit of 3.77 GJ (1047kWh) per pile. Due to this asymmetric heat extraction from the soil, additional solar energy is collected by solar panels in order to keep the thermal balance. This annual deficit has to be compensated with the energy supply by the solar panels during the summer. In the model it is assumed that all the energy collected by the solar panels is pumped in the soil only by the short piles during summer time. Applying the same method in the energy function for short piles (area under red curve times 15m), the total amount of energy pumped by them annually was 8,206 GJ (2279kWh) per pile, which is more than the energy required to keep the thermal balance.

If the peak energy for one square meter of solar panel is around 125W/m^2 and annual average efficiency is about 15%, it means that annually the total amount of solar energy produced is 160kWh/m^2 (0,576GJ). The additional solar energy required to keep ground thermal balance is 3.77 GJ (1047kWh) thus it is necessary to have less than 7m^2 of solar panels to supply the additional solar energy needed. Besides, the effective area of the short piles is 25m^2/pile, more than three times the area needed for the solar panels, so using the roof area for solar panels should be sufficient.

Following tables (Table 12 and Table 13) summarizes the boundary conditions applied in the different models carried out and where they were applied.

2D Model:

Table 12. Summary of the boundary conditions applied in the 2D model carried out with SoilVision

Boundary condition	Applied
Climate	Ground surface outside the building
Energy function for short piles	Short piles
Energy function for long piles	Long piles
Constant +20°C	Ground surface inside the building
Constant +10°C	Ground at 65m depth

3D Model:

Table 13. Summary of the boundary conditions applied in the 3D model carried out with SoilVision

Boundary condition	Applied
Climate	-
Energy function for short piles	-
Energy function for long piles	Long piles
Constant +20°C	Ground surface inside the building
Constant +10°C	Ground at 65m depth

5.3 *Results*

5.3.1 Thermal Balance

Studying the energy function of the long piles (40m length), every year exists an annual deficit of 3,77 GJ (1047kWh) per pile. To keep the thermal balance it is important to avoid ground freezing due to the massive heat extraction. The energy deficit has to be compensated with the energy supply by:

- Geothermal energy that comes from the earth.
- Solar energy pumped into the ground by the piles working in summer time.
- Thermal losses through the building basement.

Next figure (Figure 5-6) shows soil profile temperature after ten years transient analysis.
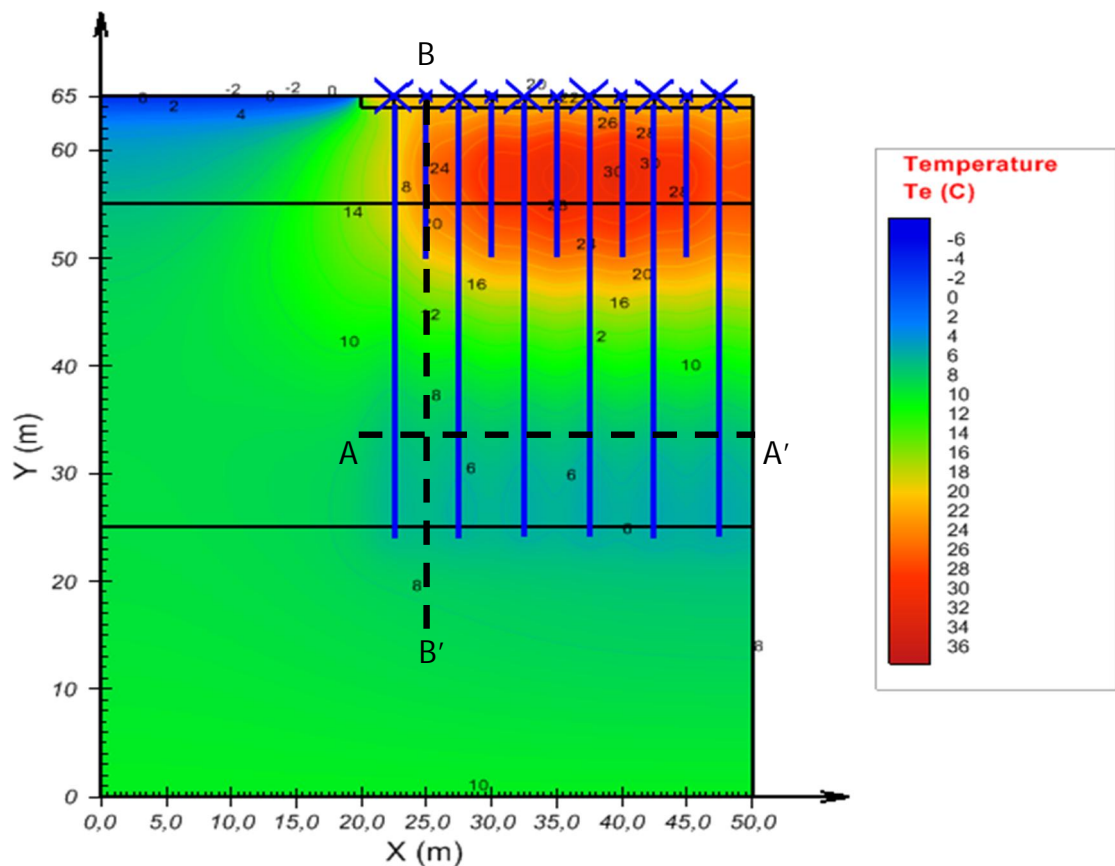
Figure 5-6. Ground temperatures after ten years under continous operation (1st January)

As can be seen in the figure 5-6, after ten years of transient analysis the soil reaches the highest temperatures in the depth of 0-15m. This is due to the additional thermal energy that comes from the short piles pumping thermal energy collected by the solar panels and energy losses through the basement (without insulation) of the building.

Otherwise, few metres above the border between the coarse grained granular (calico-fluvial) materials and the bedrock the ground reaches the lowest temperature but as can be seen, the temperature remains positive. Next plot (Figure 5-7) shows the

temperature of different points (represented by the "X" coordinate) located at the depth where the temperatures are lower (Section A-A'):
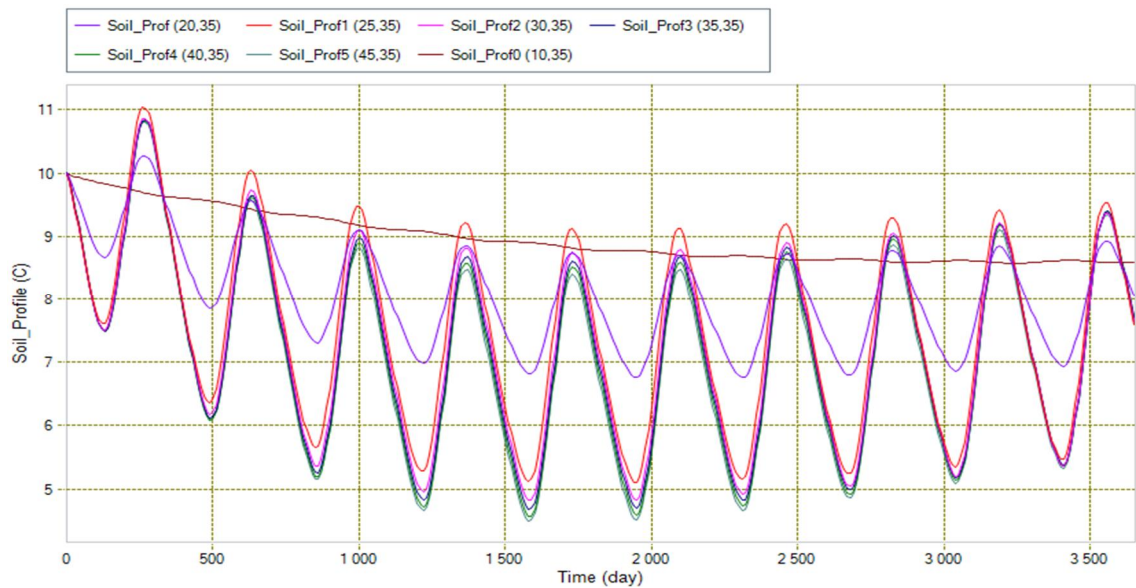
Figure 5-7. Temperature profile at 30m depth after ten years operation

The following plot (Figure 5-8) shows the temperature evolution of points located in the middle point between piles at different depths represented by the "Y" coordinate (Section B-B'; ground surface Y=65):
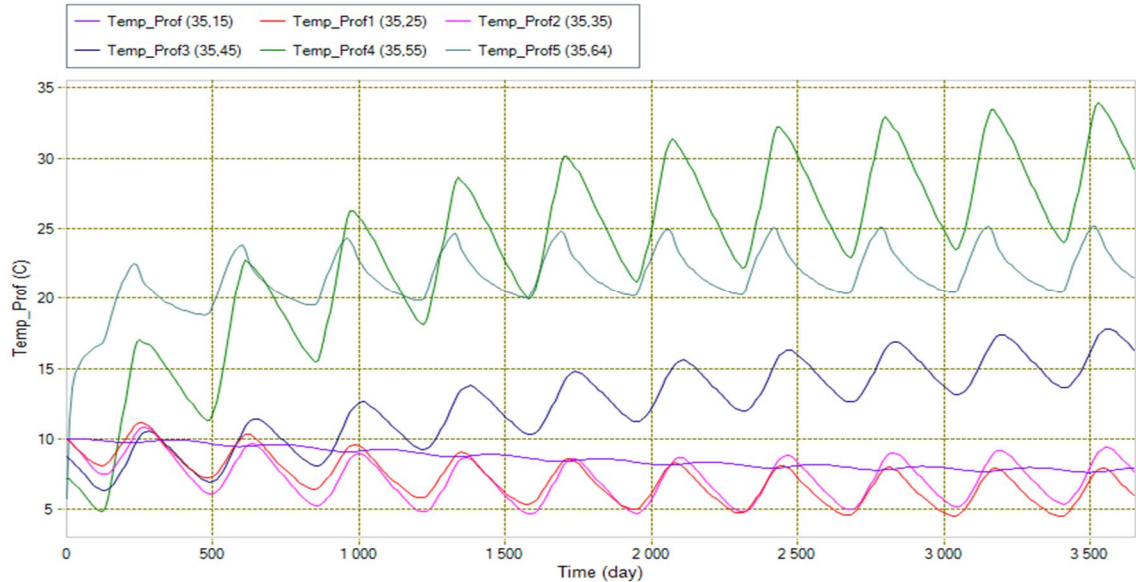
Figure 5-8. Ground temperature at different levels in points located between piles

3D Modelling

In the 3D model, only one long pile in its influence area was modelled. In this case, the solar energy collected and supplied by the short piles was not considered. In this way was possible to study if the geothermal energy that comes from the earth and the energy losses through the basement are enough to keep the thermal balance. Following figures show the temperature of points located at different depths represented by the "Z" coordinate:
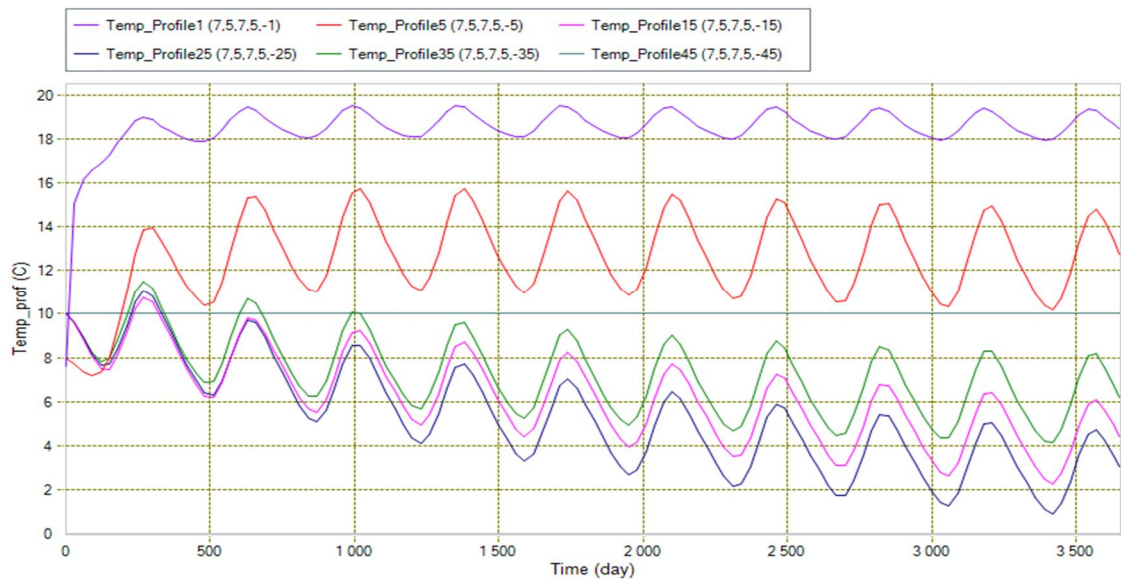
Figure 5-9. Ground temperature at different depths from the ground surface in points located between piles
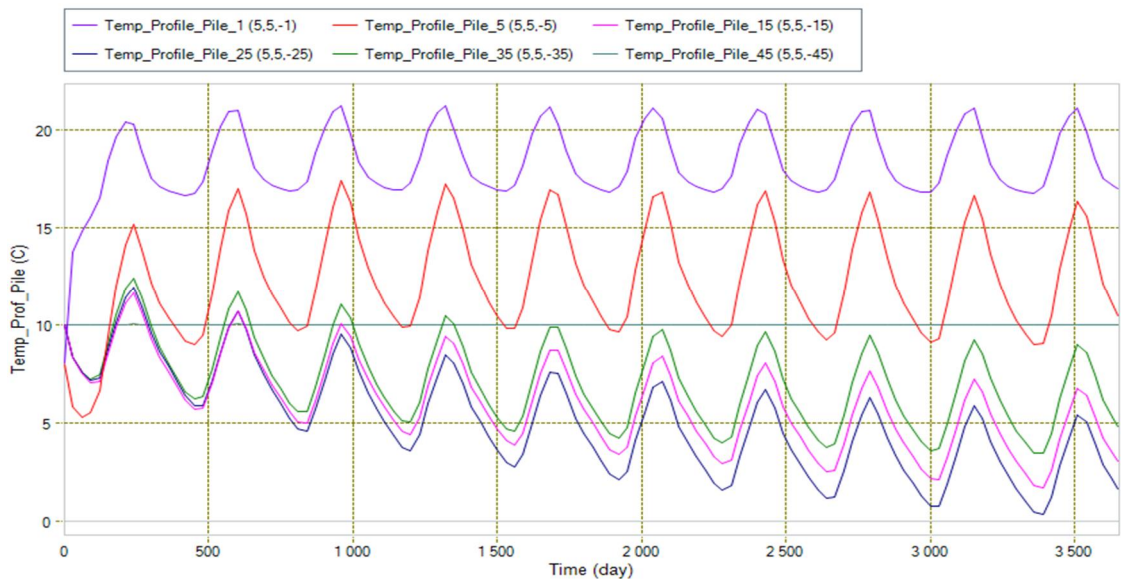
Figure 5-10. Ground temperature at different depths in points located next to a pile

In the results of the 3D models (Figures 5-9 and 5-10) the ground does not reach negative temperatures around the pile after 10 years operation. In the other hand, the temperature tends to go down gradually and reaches low temperature values close to zero in deeper points. This means that in the long term there is a need to compensate the asymmetric heat extraction keeping ground thermal balance and avoiding negative temperatures surrounding the piles.

Next figures show the temperature profile obtained in the 2D model in the points located in the middle of piles at different depths. The plots show ground temperatures when the soil has the highest (Figure 5-11) and the lowest (Figure 5-12) temperature after one, two five and ten years. As can be seen in the figures, the maximum temperature difference appears at 10 meters depth due the additional energy collected during the summer operation and pumped by the short piles.

62
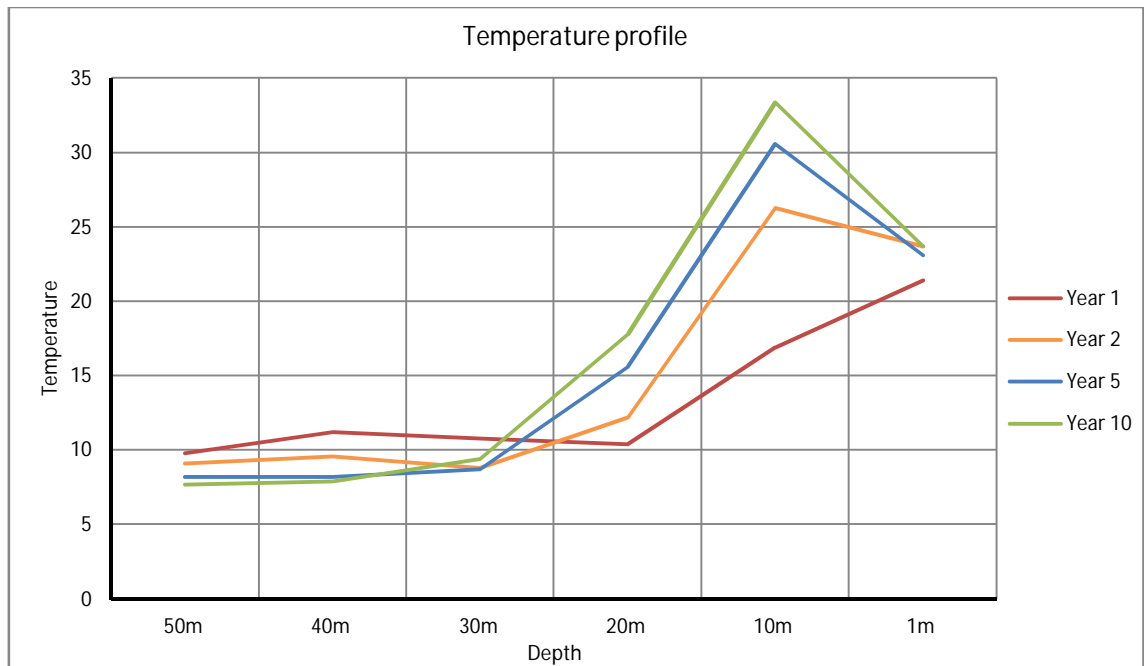
Figure 5-11. Ground temperature profile between piles after summer, when the cooling operation has ended (October)
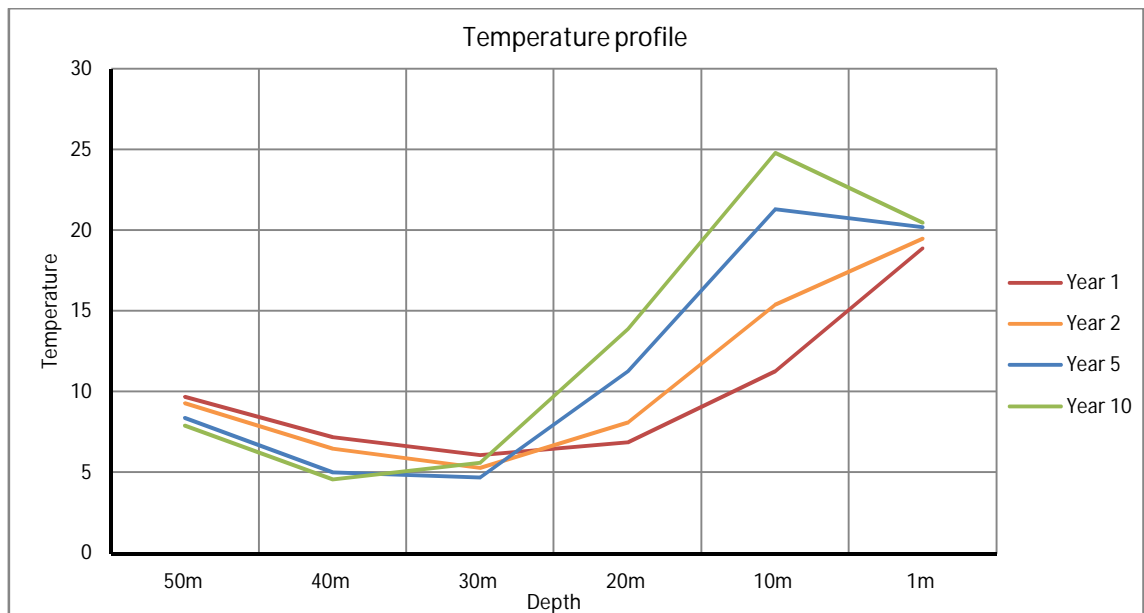
Figure 5-12. Ground temperature profile between piles after winter, when the heating operation has ended (April)

Next plot (Figure 5-13) shows the monthly ground temperature profile obtained in the 2D model in the points located between piles at different depths after 10 years of continuous operation. The maximum ground temperature is reached in the beginning of October, after the loading season during the summer. The lowest temperature is reached in April when the heat extraction from the ground finishes.
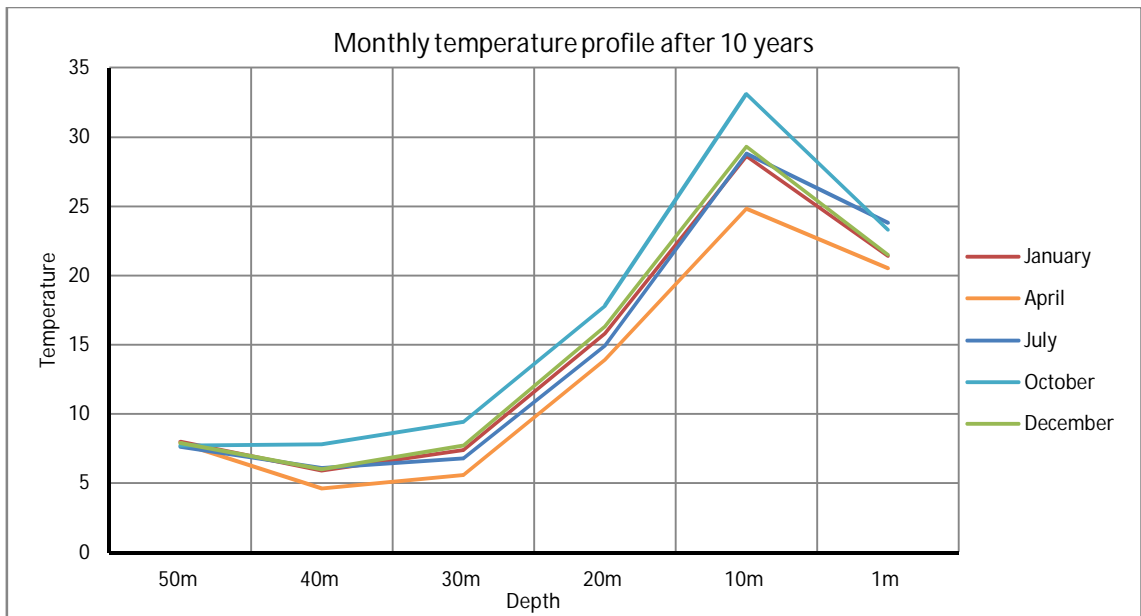
Figure 5-13. Monthly ground temperature profile after 10 years of operation
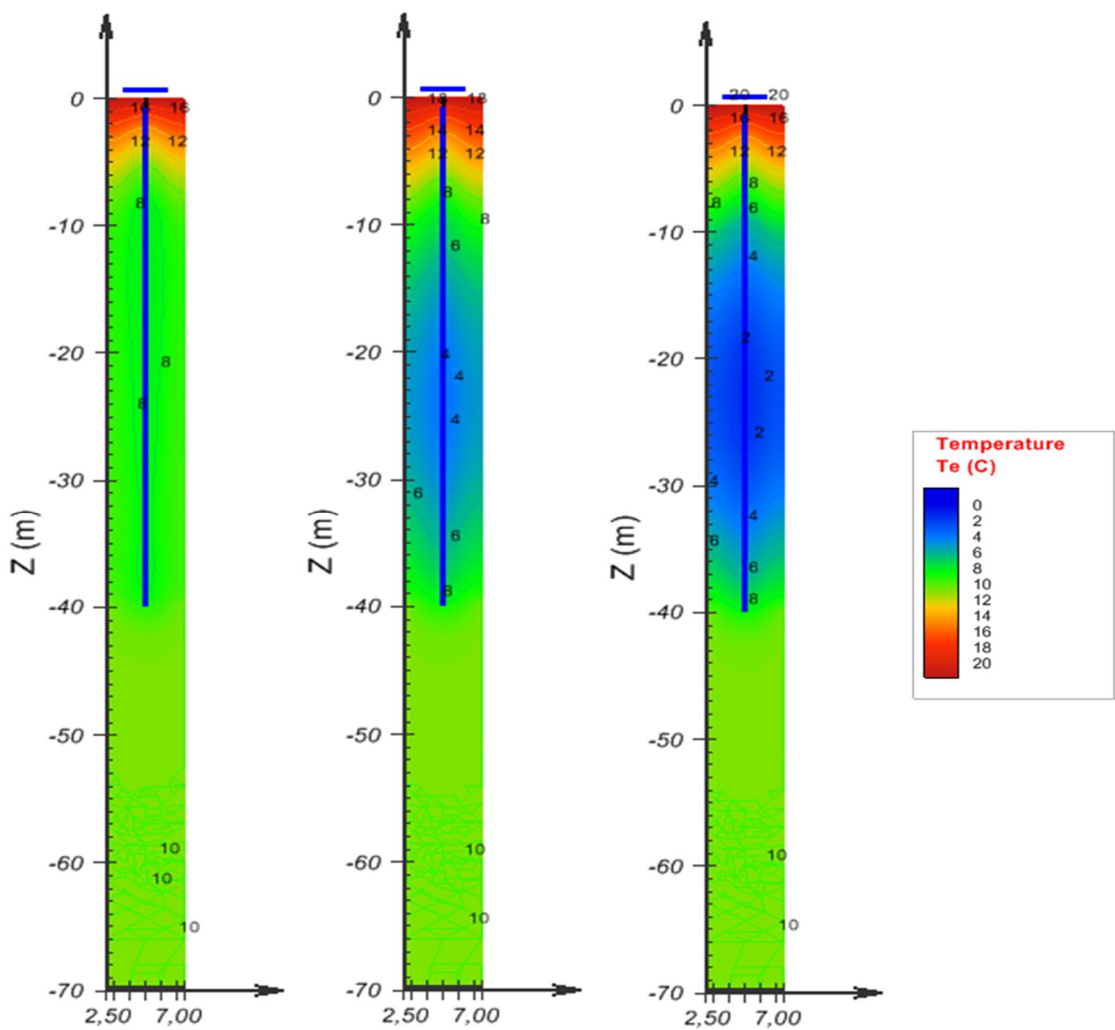
Figure 5-14. Ground temperature evolution the 1st of January after one year (left), five years (middle) and ten years (right) operation

5.3.2 Efficiency of the Vertical Insulation Barrier

The efficiency of a vertical insulation barrier, which was supposed to be a 200mm thick XPS slab reaching the depth of 5m surrounding the building, was studied in this point. In order to compare the efficiency of the insulation barrier the same 2D model was used with and without the insulation. Following Figure 5-15 shows ground temperatures in both cases.
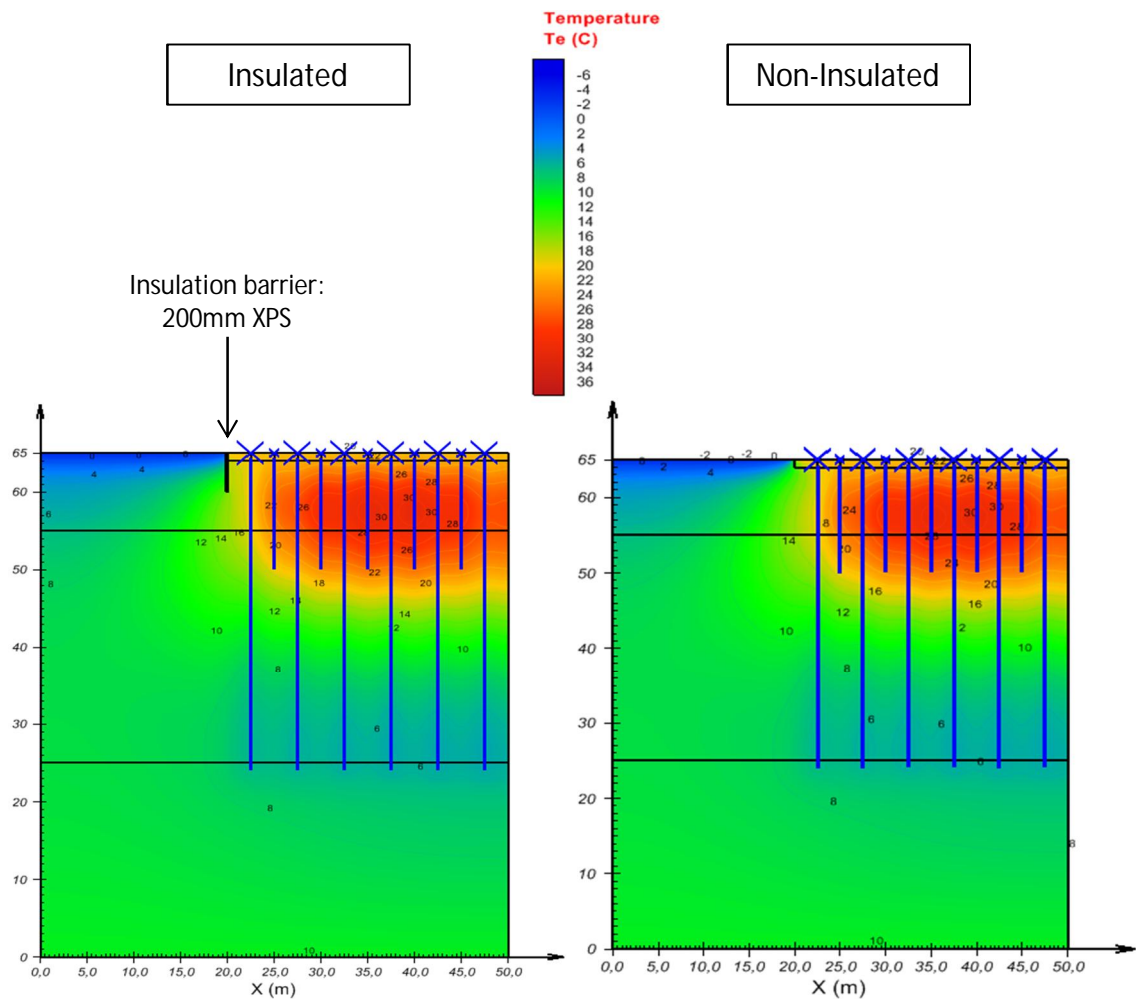
Figure 5-15. Comparison of the ground temperature after ten years with (left) and without (right) insulation

As is shown in the previous figure (Figure 5-15), in a big scale there is not an important temperature difference below the building using or not an insulation barrier surrounding the foundation. Due to the shallow depth of the insulation barrier its effect was limited few meters below the building. In both cases ground temperatures were practically the same and the effect of the insulation barrier seemed to affect only to the points located close to it, reducing its effect with distance. The temperature modelling results were examined at different depths in the inner and outer part of the insulation (Figure 5-16 and 5-17) in order to understand better the effect of the insulation barrier.
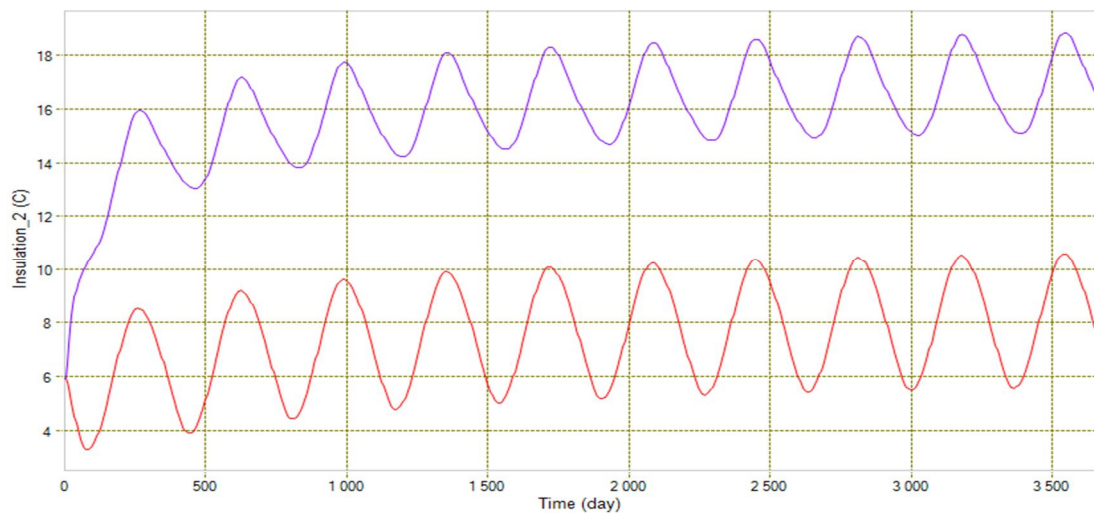
Figure 5-16. Comparison of inner and outer temperature at 2m depth after ten years operation. Red and lilac lines show temperature in the outer and inner part of the insulation barrier, respectively
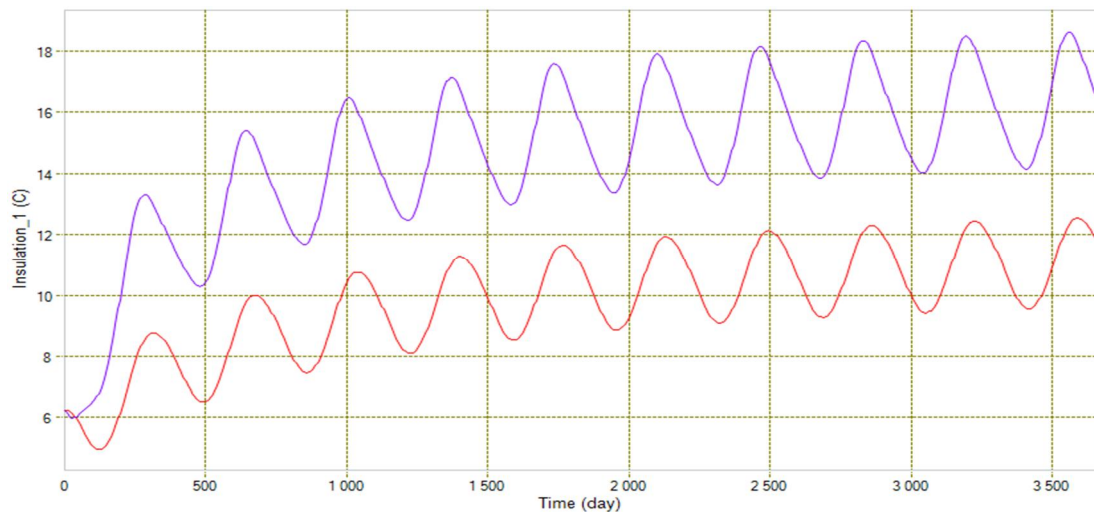
 Figure 5-17. Comparison of inner and outer temperature at 4m depth after ten years operation. Red and lilac lines show temperature in the outer and inner part of the insulation barrier, respectively

As it is shown in the previous figures, the temperature difference between the inner and the outer part of the insulation decreases with depth. Next plot (Figure 5-18) shows the temperature differences between the inner and outer temperature at different depths. It shows that:

- After ten years operation, the temperature difference increases gradually (see linear regression in figure 5-18).
- In long term analysis, ground temperature increases faster with depth even though the temperature difference between both sides of the insulation decreases.
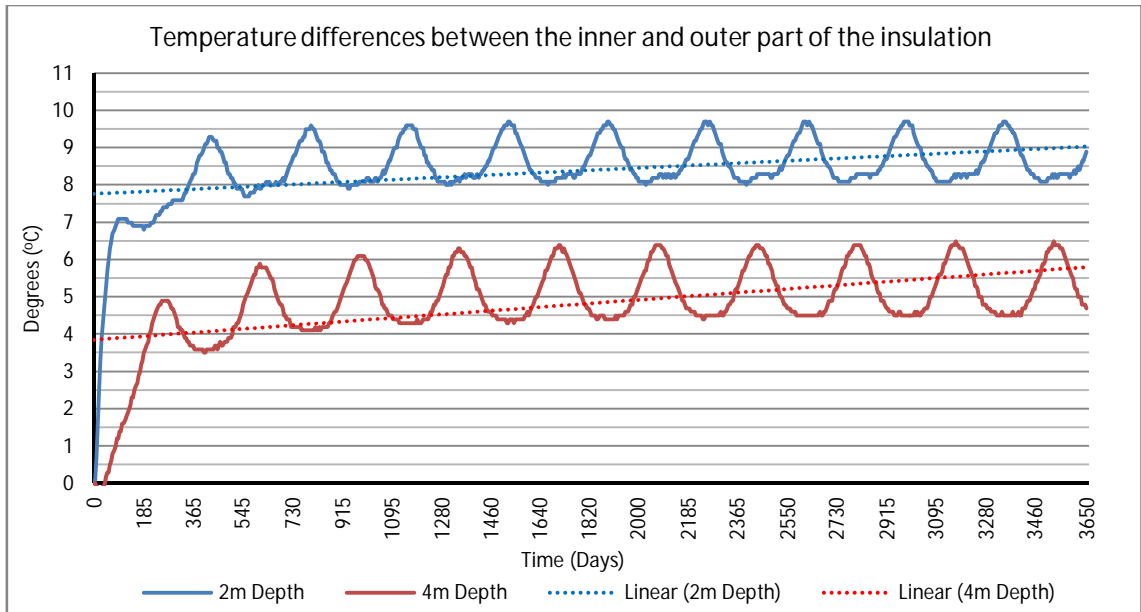
Figure 5-18. Ground temperature differences between the inner and outer part of the insulation by depth

Following figure (Figure 5-19) shows the temperature differences of the ground with and without the underground insulation barrier. As can be seen, depending on the depth the temperature difference varies between +1.5 to +3.5°C. The energy stored is related to temperature differences (depending on depth) and the heat capacity of the soil. Thus considering the heat capacity of the clay and this ground temperature increment, thermal losses through the building floor reduces around 1.0-2.3kWh per cubic meter of soil in points located close to the barrier. As it was mentioned before, the effect of the insulation barrier reduces with distance and also the energy stored reduces with the distance from it.
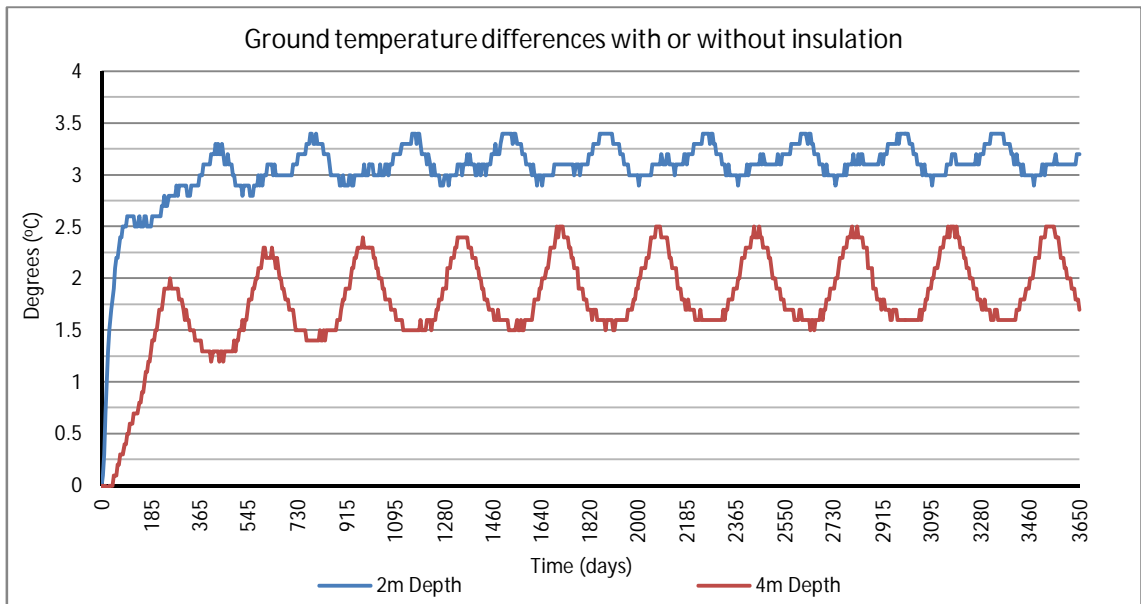
Figure 5-19. Ground temperature differences at different points with and without underground insulation barrier by depth. Point A at 2m depth(X=20,1; Y=63) and Point B at 4m depth (X=20,1; Y=61)

6 Myllypuro Ice Rink in Helsinki

6.1 Introduction

Myllypuro ice rink is an ice rink facility built in 1976. It is located in the east part of Helsinki, Finland (Figure 6-1). The facility was designed and built to give more opportunities for the young people to enjoy ice sports and hobbies because they depend on outside temperatures and only are available during the winter (Vähäaho et al., 2012).

The facility was founded on the clay deposit so that ice rink areas were built directly on the clay using a thin EPS insulation layer (100 mm) and a heat wires system in order to prevent ground freezing and frost heave. Myllypuro ice rink is an example of horizontal ground loop system where energy has been extracted from the soil since 1976 to 2012. But the energy extracted was not used to give any benefit for the owner, only to keep the temperature of the ice rink facility as required.
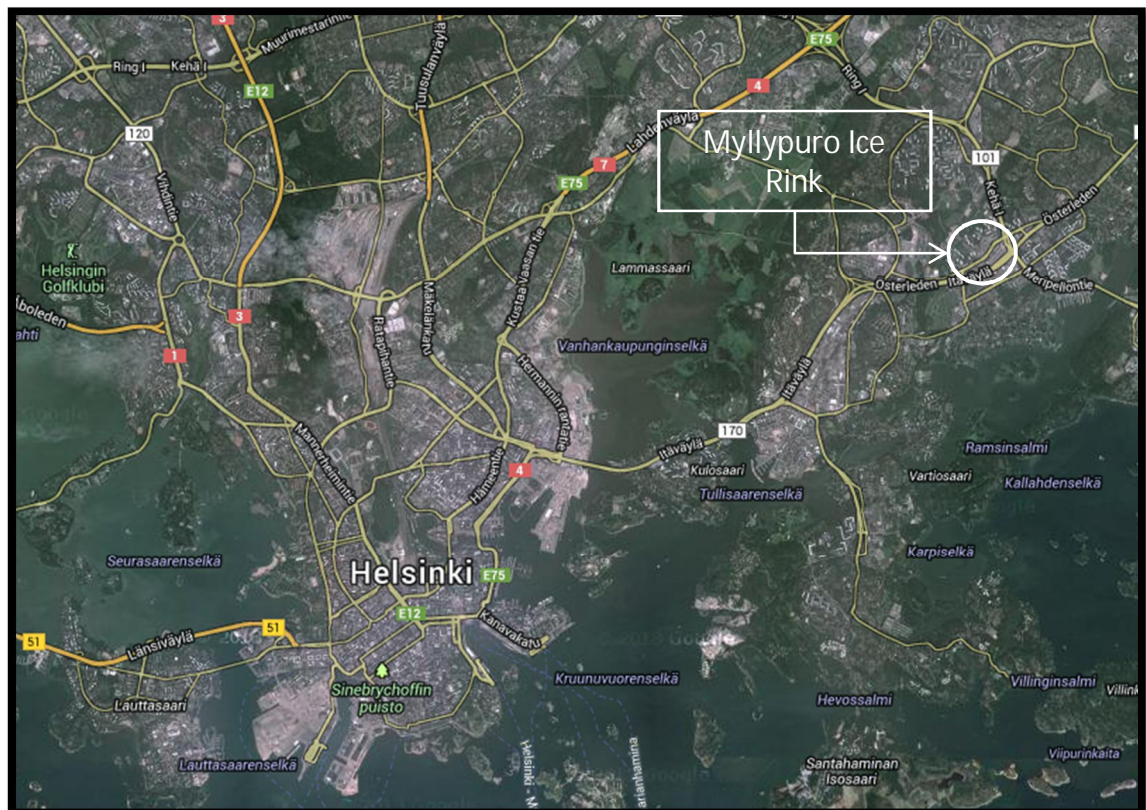
Figure 6-1. Location of Myllypuro ice rink in Helsinki city (Google Maps)

During the first years, the facility was closed in summer time and the ice rink was melted. Later on, due to the demand to continue practicing time of winter sports during summer time it was decided to keep the rink open during all the year (Figure 6-2). Over the time, heating system with warming wires stopped working and the EPS insulation layer was not thick enough to prevent the freezing process of the ground. Ground freezing process advanced over the time and uneven ground deformations

started to appear causing continuous problems and increasing maintenance cost (Figure 6-4).

Figure 6-2. Picture of one of the ice rinks inside Myllypuro ice rink (Myllypuro Jäähalli, 2012)

Description of the Problem:

In 1996 it was decided to monitor the situation and a wide measurement program was designed. The program included the installation of temperature and settlement sensors and lateral deformation indicators. Also some drilling tests were done to define the extension of the frozen area below the ice rink. In 2000 the measured frost depth was 6.3m resembling permafrost (Vähäaho et al., 2012).

The deformation measurements in the foundations located in the middle of the hall supporting columns showed that columns had started to uplift and in 2012 the middle columns had risen 88mm. In addition, in the middle of the ice rink there was frost heaving (about 0.5m) and horizontal movements (Figure 6-3).
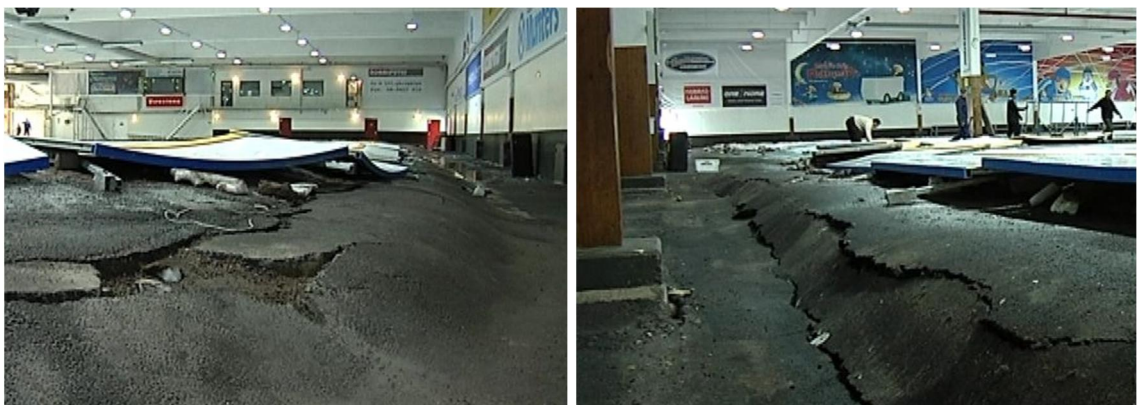
Figure 6-3. Pictures of the frost heaving before starting the renovation process (Myllypuro Jäähalli, 2012)
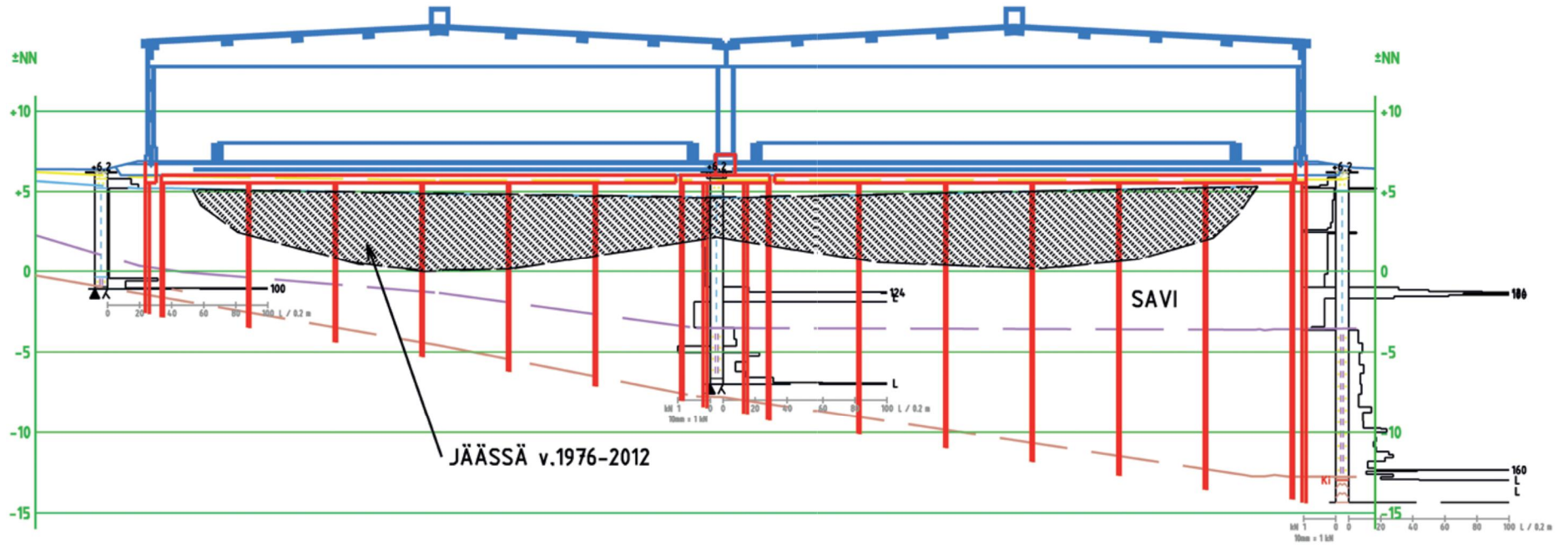
Figure 6-4. Cross section of Myllypuro ice rink; Soil profile and frost penetration below the ice rink after more than 30 years of operation (Vähäaho et al., 2012)

Description of the Solution:

A renovation process was planned. A new foundation system was designed and one of the most important points in the design process was to control the melting process of the frozen layer of clay. The new foundation system consisted of a well-insulated concrete slab and steel piles (Vähäaho et al., 2012).

   – A well-insulated concrete slab:

The concrete slab connects all the piles and also prevents the effects of the thawing process of the subsoil. The concrete slab separates the cooling pipes (located in the upper part the concrete plate) used to keep the ice rinks frozen and two other pipe system systems (horizontal and vertical inside the piles) used to prevent soil freezing which are located in the lower part of the concrete slab. In addition, an insulation layer of 100mm and a drainage system have been designed to avoid heat transference and to keep the structures dry (Figure 6-5).
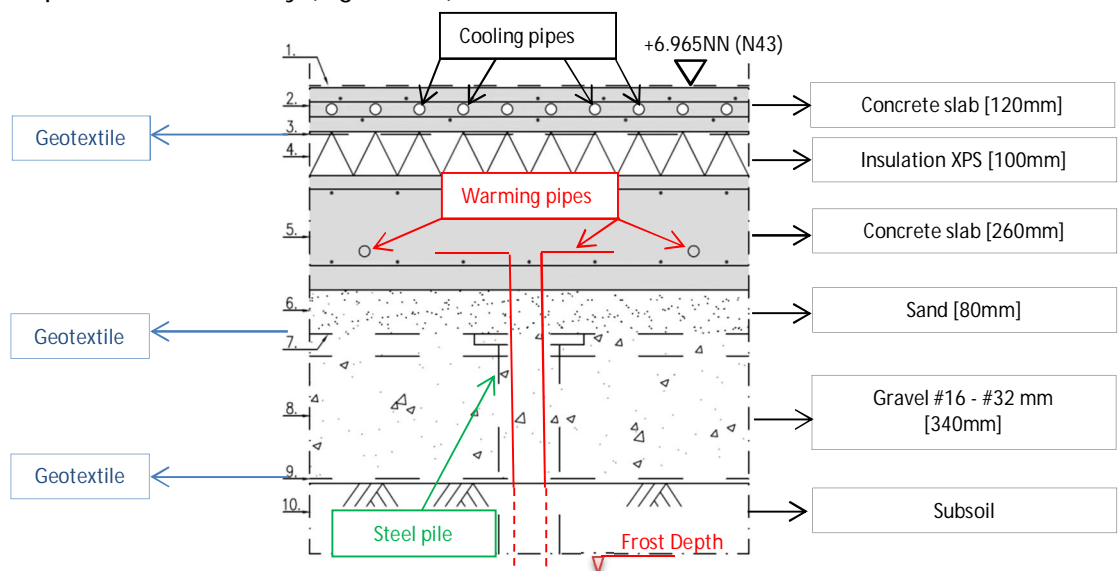
Figure 6-5. Cross section and material layers of the concrete slab designed in Myllypuro ice rink (Modified from Mehto, 2010)

   – Steel piles:

A new foundation system was designed with 240 steel energy piles with lengths varying between 12-25m, outer diameter of 140mm and 10mm wall thickness. The steel pile foundation was installed in a 5,5m mesh reaching the moraine below the clay layer (Figure 6-6). In addition, the old concrete piles below the centre line of columns were substituted by new steel piles in order to carry the superstructure loads.

The final solution to melt the frozen ground below the ice rink and to prevent the frozen soil to stick to the piles was to pump hot liquid into pipes installed inside the piles. The steel piles were equipped with plastic U-type pipes inside the piles to enable the circulation of warm liquid. The pipes were installed inside the piles (U-type configuration) up to the frost depth that was assumed to be (about 5-6m) and also embedded in the concrete slab (Figure 6-5).
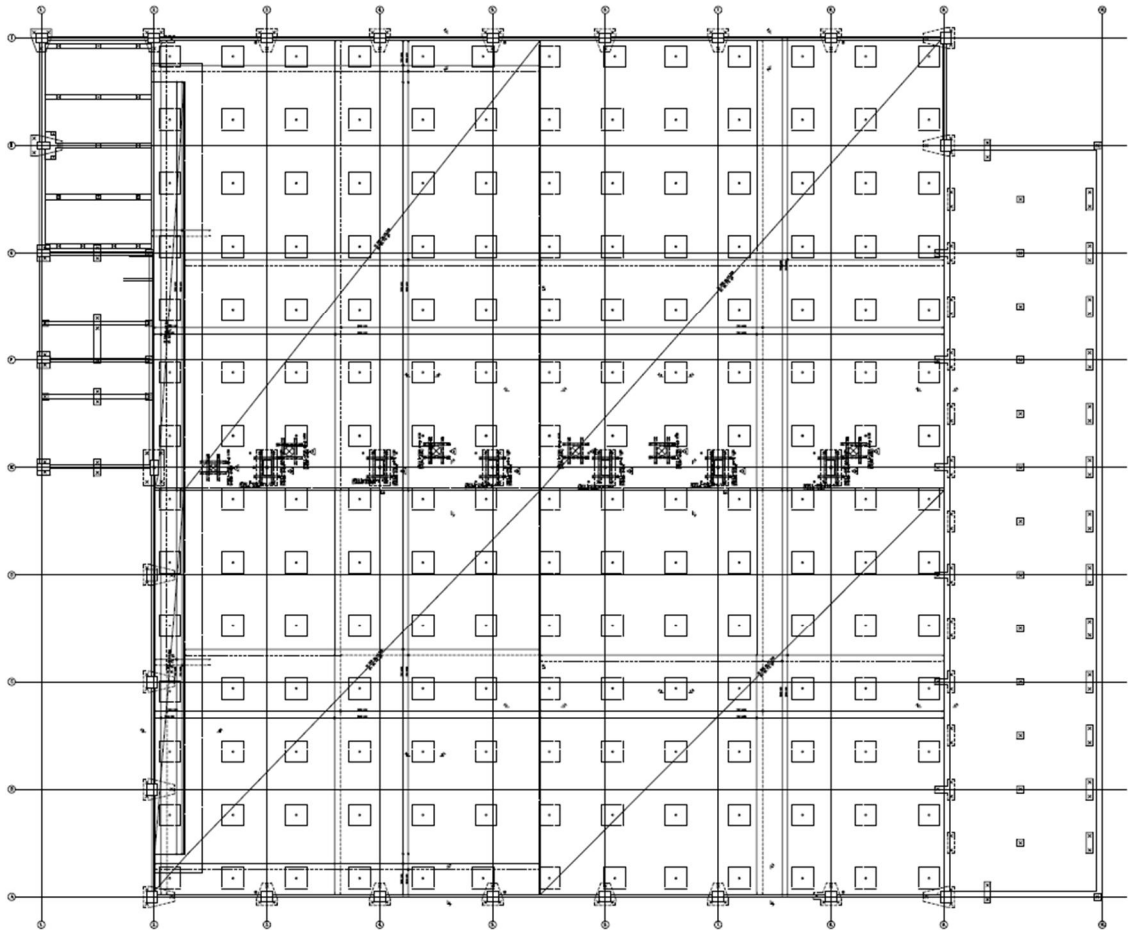
Figure 6-6. Configuration of the pile foundation mesh. Distance between piles: 5.5m (Mehto 2010)

This system pumps heat into the ground in order to prevent the soil surrounding the piles from freezing, thus reduces the possible additional load. This additional load is caused by negative shaft friction because of the thaw settlements in lower clay layers. Nowadays, the warming system is pumping heat only to the piles, circulating warm liquid from +28 (in) to +28°C (out). Horizontal pipes are not in use, but they could be used in the future. This system is very energy efficient and cheap compared to other solutions with piles heated directly by electricity because this system uses the wasted heat from the cooling system.

When the new foundation system started to pump heat into the ground, frozen soil below the ice rink started to thaw. This thawing process of the frozen soil increases the load of the piles and it has and it will also produce settlements due to the thaw consolidation. The effect of the thaw consolidation was evaluated with empirical formulations. Based on the water content of the clay (average about 100%) a maximum of two meters settlement was expected. One important effect that could occur due to the thawing process was the increasing of the negative shaft friction produced by the thaw consolidation settlements.

Renovation Process:

The repair works started in May of 2012 by removing the old structures, old insulation systems and removing one meter sand layer used for levelling. The place had favourable conditions for the formation of ice lenses, because of the soil grading and the close ground water level to the surface. Therefore, the thickest ice lenses were measured to be about 0.5 m.

The next step was to reinforce the centre line columns and to start the pile driving. The installation system of the steel piles was a mixture of drilling and driving. In the first meters it was decided to drill through the frozen clay layer because the pile driving would have been difficult. After that, the installation process of the piles continued with a pneumatic hammer into the pre-drilled hole.

Because the renovation processes started during the end of the spring and the early summer, quick thawing and the use of heavy machine produced settlements of 800 mm (Figure 6-7). The driving of the piles in pre-drilled holes increased the soil temperatures due to the friction. After the pile installation process was ready, the surface was insulated with crushed aggregate. After that, the settlement speed was decreasing down to 20 mm week.
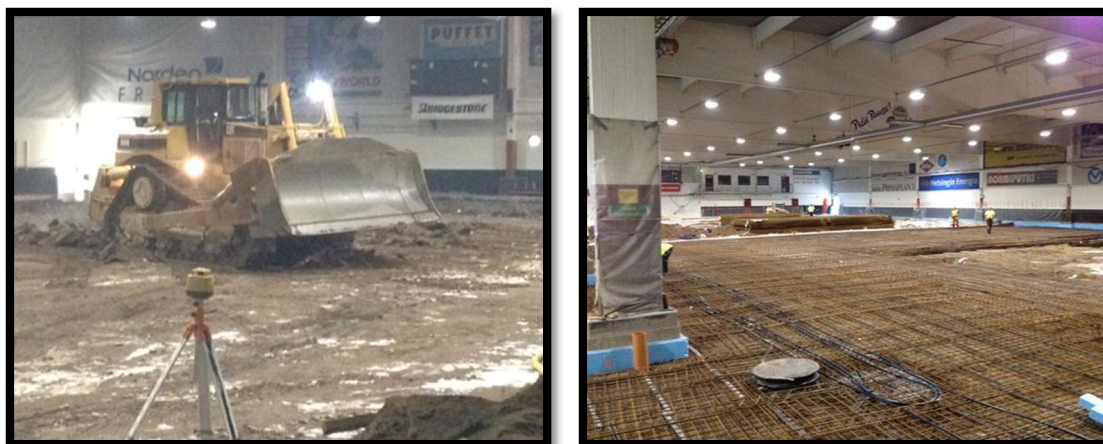
Figure 6-7. Renovation works inside Myllypuro ice rink (Myllypuro Jäähalli, 2012)

The renovation process was finished in November 2012 and now the facility is open again. In order to control soil temperatures profile and the frozen area below the ice rink there are six temperatures measuring points.

73

6.2 Sampling and In Situ Observations

6.2.1 Sampling

For the sampling campaign, it was not possible to take samples below the ice rink because the facility was already in use. For this reason, at the site, the samples were taken from unfrozen ground located few meters outside ice rink building (Figure 6-8).

The coordinates of the sampling point were (6677704.638 ; 25503913.666 ; 6.144) NN system (N43). The floor level in Myllypuro ice rink was at +6.965 NN systems (N43). NN system is 305mm lower than N2000 system. Weight sounding diagrams done nearest the sampling point in appendix 2.
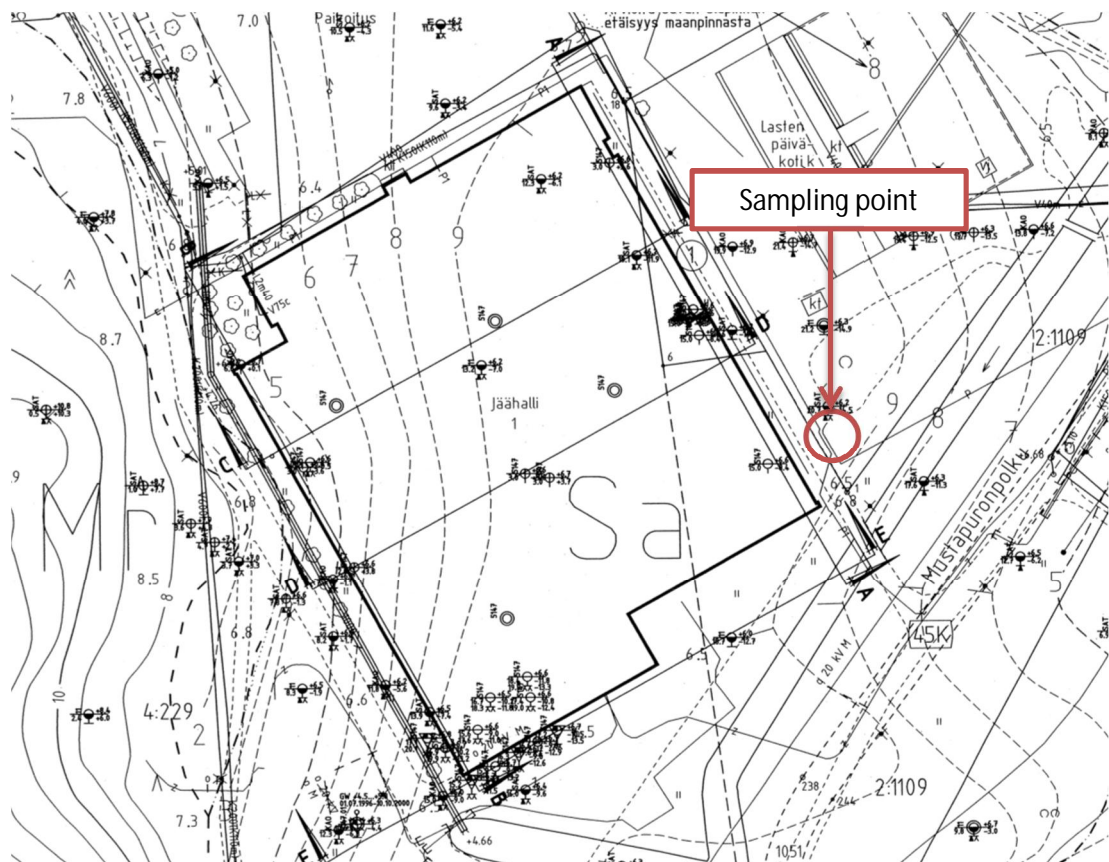
Figure 6-8. Location of the sampling point in Myllypuro ice rink (Helsingin kaupunki, 2009). Soil profiles in Appendix 1

The unfrozen undisturbed sample was taken with a piston sampler into a thin steel tube with an internal diameter of 86mm and height of 660mm. The sample was taken by pushing the tube into the soft clay in order to keep the soil structure as natural as possible. The tube was pushed down further and the sampling continued until the tube was full of undisturbed soil (Figure 6-9). Once the tube with the sample was extracted the ends of the tubes were wrapped with plastic bags and sealed with caps. The tube was identified and registered and it was transported in vertical position. Once in the laboratory, the samples were stored in the cold room in vertical position (average temperature +7°C).

Figure 6-9.Pictures of the sampling process (left) and the storage (right) of the sampler tubes in the cold room (average temperature +7°C)

6.2.2 In Situ Observations

Temperature Measurements

The temperature of the ground below the Myllypuro facility has been monitored at six points below the building floor with five T-type thermocouple sensors in each point (Figure 6-10). All the temperature sensors were connected to a register box to monitor the temperature readings. Several in situ observations have been done to monitor and control the melting process of the frozen ground below Myllypuro ice rink. The temperature transducers were located up to a maximum depth of 5.2m and ground temperature was registered in different time periods in order to control the melting process (see Appendix 2). The ground temperature measurements were also used to establish the initial conditions of the models carried out. In addition, the results obtained in the models carried out were based on the measurements done in the different time periods.

Deviation of the In Situ Temperature Measurements

The results obtained in the models explained below may be different of the real situation because of the deviation of the temperature measurements. Thermocouple sensors were used to measure ground temperatures. Thermocouples measure the voltage difference between two cables made of different metals joined to produce a voltage at a given temperature. The measured voltage difference can be converted to temperatures of the different points. Absolute temperatures are not measured and

because of this the calibration of the equipment is really important. The accuracy of the equipment used to monitor ground temperatures in Myllypuro ice rink was between ±0.5 to ±2°C (Eutech EcoScan Temp JTK meter). Besides, the temperature readings could vary even more than one degree depending on the moment that they were taken (see Appendix 2). Temperature measurements should be done after the thermocouple measuring equipment reaches a constant temperature, otherwise voltage measurements can be affected.

The effect of time to the measured values was studied 3.10.2013 and 11.10.2013 by taking many readings during one hour when the equipment was reaching steady state temperature (air temperature inside the rink building). Last temperature readings were taken two times after arriving to the site and twice again one hour later in order to see the reliability of the temperature measurements and validate the old readings. The difference between the readings was in some cases even more than one degree until the measuring equipment reaches the steady state temperature. In the earlier temperature measurements done in situ the waiting time has possibly been too short affecting the reliability of the temperature measurements.
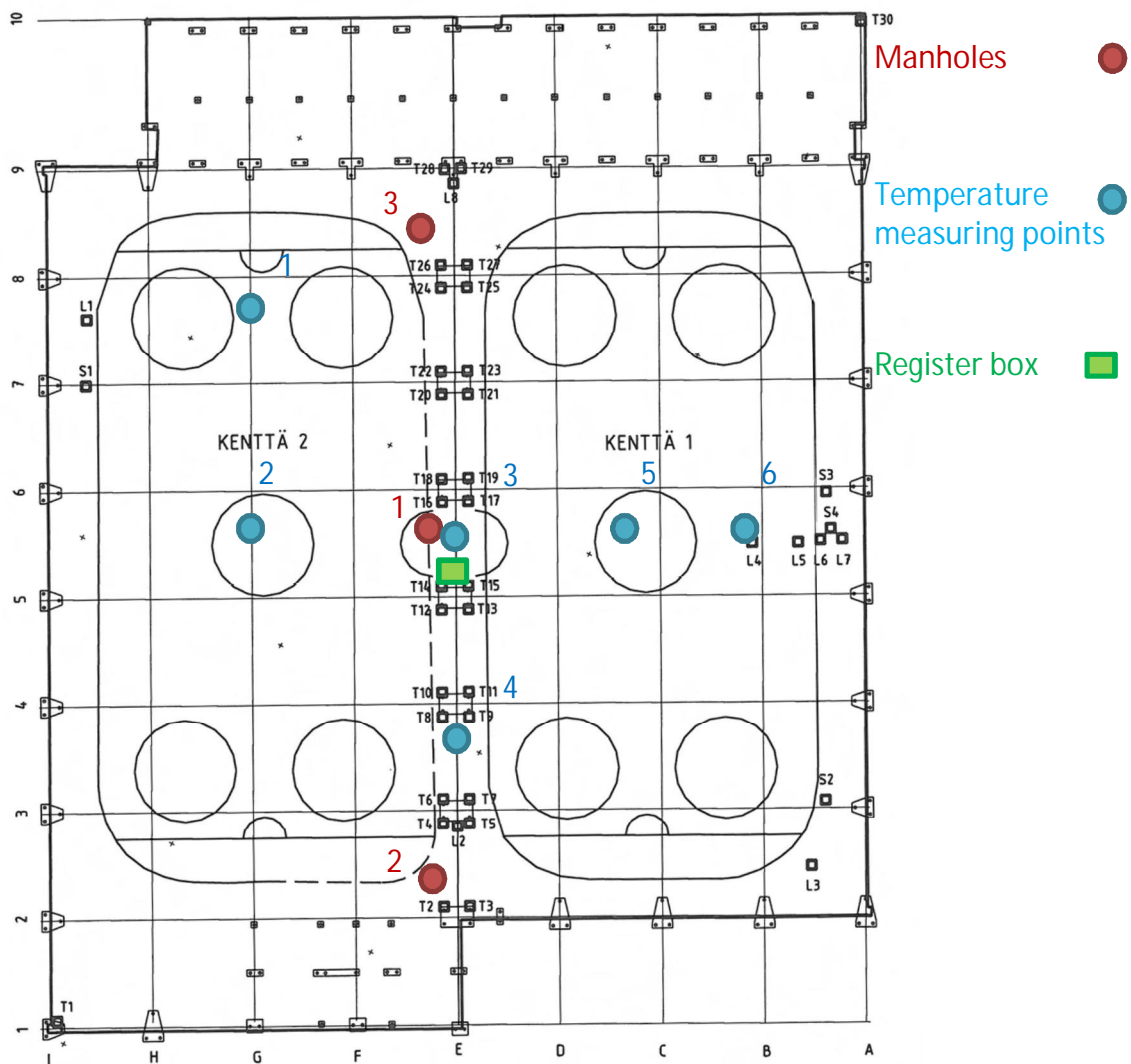
Figure 6-10. Location of the temperature sensors and observation points in Myllypuro ice rink (Gotekniikka, 2009)

Observation points

A field visit in Myllypuro site was done the day 30.9.2013 to monitor the melting process below the ice rink. During the site visit, three different trap doors located between the ice rinks were opened for the inspection of the manholes in order to control the evolution of the melting process (Figure 6-10). Water temperature, water table level (h_w) and the thawing settlement were measured in the three different points (Figure 6-11). Following table-14 shows the measured parameters.

Table 14. In situ observations in the three manholes in Myllypuro ice rink.

	Point 1	Point 2	Point 3
Water temperature (^{o}C)	+8.7 to +9.0	+6.0 to +6.1	+9.0 to +9.3
Settlement (mm)	440	350	270
Water table level from the surface (m)	-1.28	-1.29	-1.30

Inside the manholes it was possible to see that the water level was around 1.3m below the ground surface. In addition, in the bottom of the manholes there was a steel mesh

at 1.75m depth (h). This steel mesh was in the beginning (after the renovation works) in contact with the ground. The thaw settlement produced until date was calculated by the difference between the depth of the ground surface and the steel mesh (Figure 6-11).

During the site visit it was also possible to observe that the originally horizontal drainage pipes were inclined certain angle (α) that varied between 45° to 55°. The drainage pipes were not connected to the lower part of the concrete slab and due to this and because of the thaw settlement occurred until that day the drainage pipes were inclined.
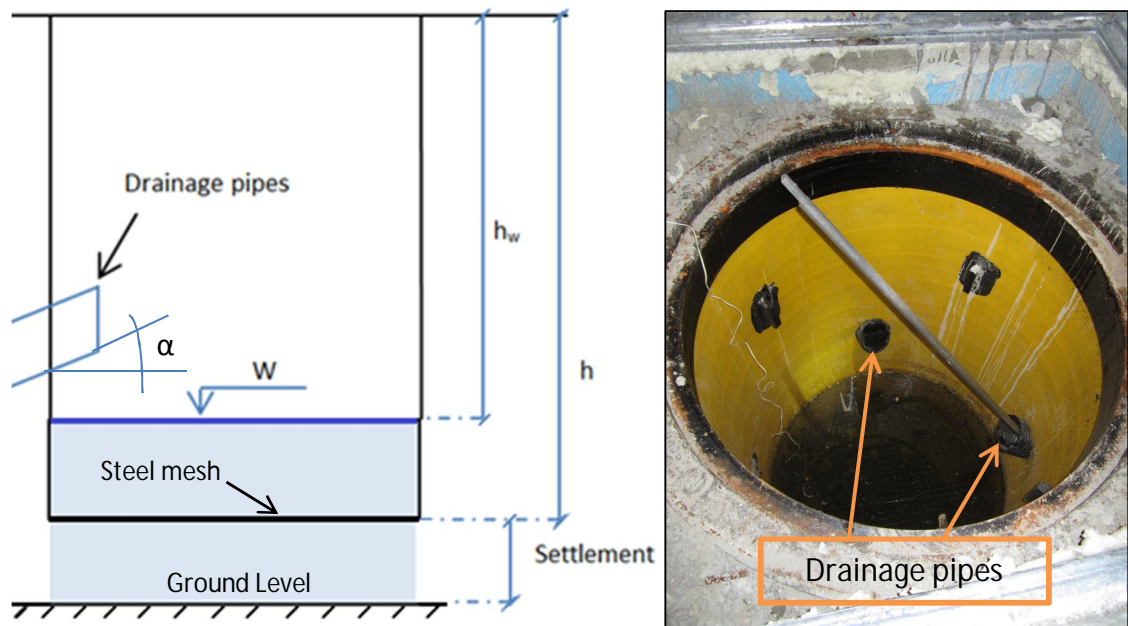
Figure 6-11. Schematic and picture of the trap door inside Myllypuro ice rink

6.3 Classification Test

In the laboratory, the samples were stored in a cold room at +7°C temperature in vertical position. Soil classification tests were done in order to determine soil parameters such as:

- – Water Content
- – Natural Unit Weight
- – Specific Gravity
- – Dry Density
- – Degree of Saturation

- – Organic content
- – Grain size distribution
- – Porosity
- – Void ratio

Grain size distribution test were done in order to estimate the frost susceptibility of the soil according to the Finnish standard SFS-EN ISO 13793:2001. Figure 6-12 and 6-13 show the frost susceptibility of the ground on the basis of grain size distribution, which shows the percentage of grains passing through the sieves of different sizes.
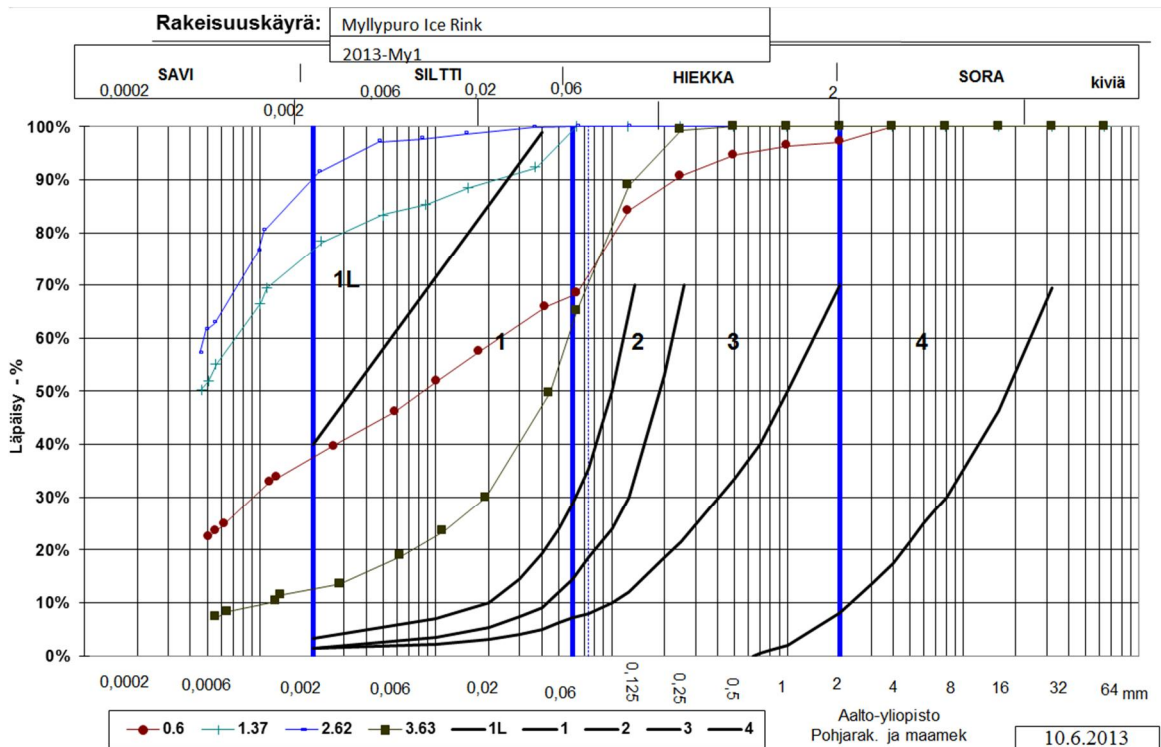
Figure 6-12. Estimation of the frost susceptibility on the basis of grain size distribution. From 0 to 3.63m depth
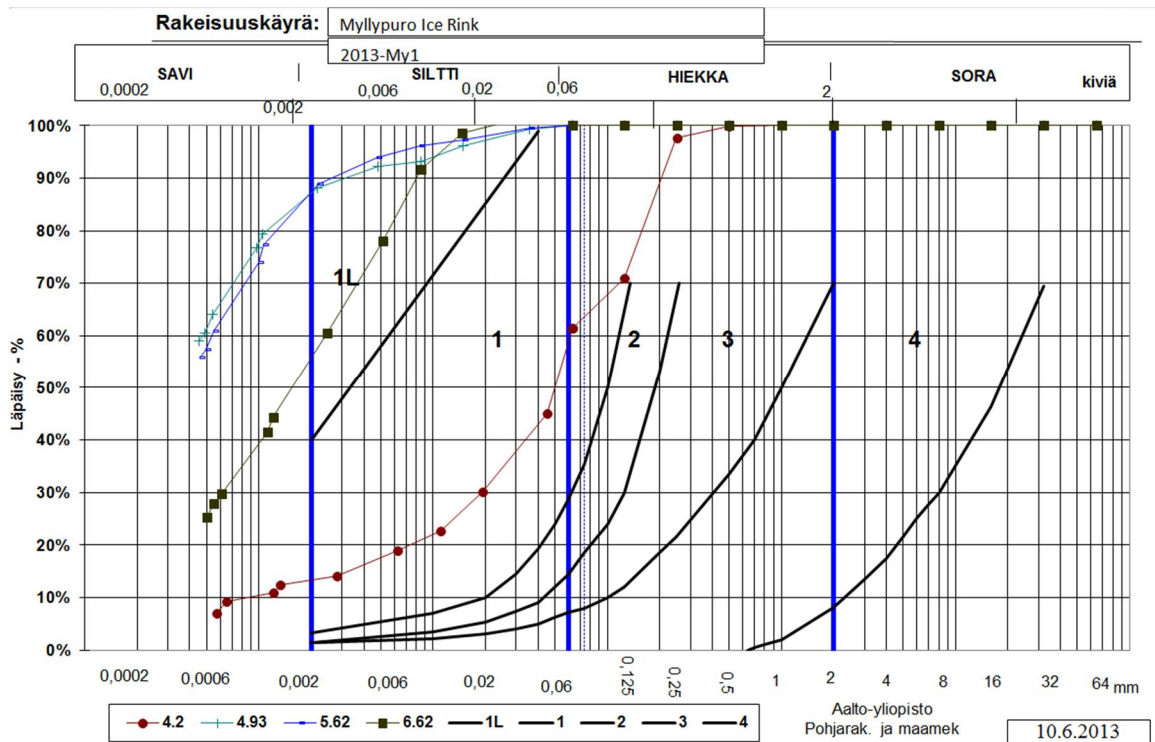
Figure 6-13. Estimation of the frost susceptibility on the basis of grain size distribution. From 4.2 to 6.62m depth

Depending on the grain size distribution curve it is possible to know the frost susceptibility of the soil. If the grain size curve falls completely inside regions 2, 3 or 4, the soil is non–susceptible to frost. If the grain size curve falls completely inside regions 1, the soil is frost-susceptible, except for "fat clay" (region 1L) where the frost susceptibility is low. As can be seen in the grain size distribution curves (Figure 6-12 and Figure 6-13), the soil is composed of fat clay at depths between 1.3-2.7m and 4.7-5.7m. This soil has low frost susceptibility. The soil below the surface and between 2.7-4.2m depth has higher content of silt increasing the frost susceptibility of the soil.

The following table 15 shows geotechnical parameters obtained in the classification test done in the laboratory with the samples from Myllypuro Ice Rink. The soils were classified according to the Finnish standard SFS-EN ISO 14688-2. The parameters obtained in the classification test were used to estimate the thermal properties of the soils for the modelling process explained later.

Table 15. Table with geotechnical parameters obtained from classification test done with Myllypuro samples

Parameter	Symbol	Depth (m)								Units
		0,6	1.2-1.3	2.5-2.6	3.5-3.6	4.2-4.3	4.7-4.8	5.5-5.6	6.5-6.6	
Water Content	ω	60,100	76,000	92,150	17,880	18,100	114,630	108,090	66,240	%
Density	ρ	-	1,538	1,484	2,045	-	1,454	1,450	1,629	g/cm3
Dry Density	ρ_d	-	0,908	0,753	1,712	-	0,665	0,677	0,927	g/cm3
Specific Gravity	ρ_s	2,640	2,810	2,810	2,700	2,700	2,820	2,820	2,720	g/cm3
Natural Unit Weight	γ	-	15,090	14,550	20,060	-	14,260	14,220	15,980	kN/m3
Porosity	n	-	67,700	73,200	36,600	-	76,410	75,980	65,670	%
Void ratio	e	-	2,093	2,726	0,577	-	3,240	3,160	1,913	-
Degree of Saturation	S_r	-	100,000	100,000	83,960	-	100,000	100,000	100,000	%
Organic content	H	5,778	3,600	3,760	0,730	0,849	4,090	4,070	2,700	%

Grain size classification:

Classification (SFS-EN ISO 14688-2)	saCl	Cl	Cl	sasiCl	saclSi	Cl	Cl	Cl

6.4 Thermal Conductivity

Thermal parameters of the soil were obtained from the results of the classification test (Point 6.3) and the formulations explained in Point 2.4.3. The following tables (Table 16 and Table 17) and figures (Figure 6-14 and Figure 6-15) show thermal conductivities calculated for the frozen and unfrozen soil at different depths. These thermal conductivity values obtained were used for the calibration of the models.

Table 16. Values of the thermal conductivity of the unfrozen soil at different depths (W/mK)

Depth (m)	Water Content (%)	Dry Density (g/cm^3)	Kersten	Johansen	De Vries	Imp. Johansen	Average
1.2-1.3	76	0,908	0,794	0,947	1,049	0,974	0,9408
2.7-2.8	92,15	0,753	0,667	0,889	0,955	0,889	0,85
3.5-3.6	17,88	1,712	1,566	1,530	1,765	1,562	1,60575
4.7-4.8	114,63	0,665	0,620	0,843	0,903	0,843	0,80225
5.5-5.6	108,09	0,677	0,623	0,881	0,952	0,881	0,834125
6.5-6.6	66,64	0,927	0,787	1,063	1,152	1,063	1,01625
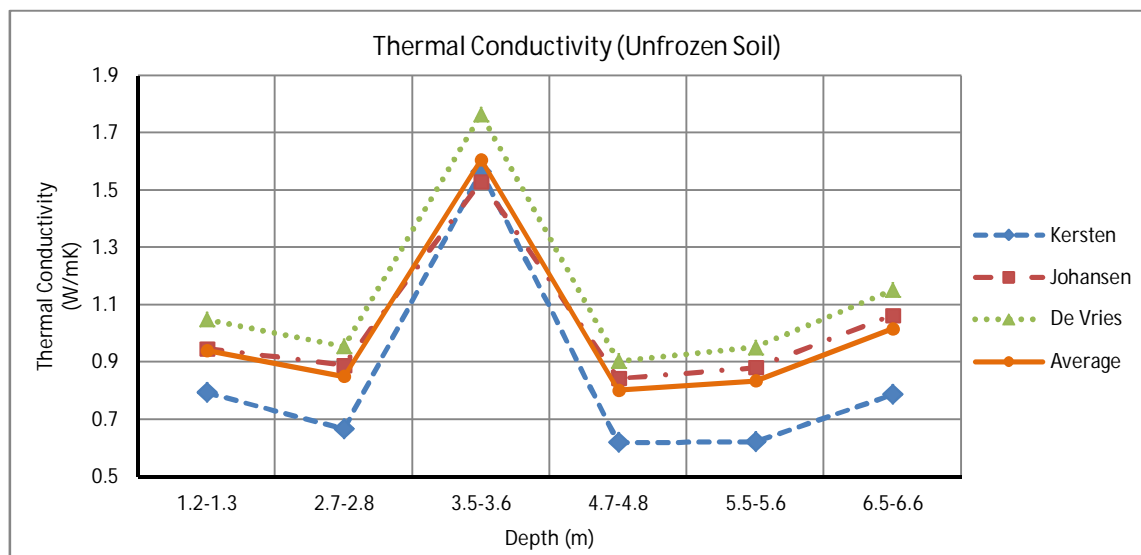
Figure 6-14. Graph with the values of the unfrozen thermal conductivity calculated by different formulations with depth

Table 17. Calculated thermal conductivity values of the frozen soil at different depths (W/mK)

Depth (m)	Water Content (%)	Dry Density (g/cm^3)	Kersten	Johansen	De Vries	Imp. Johansen	Average
1.2-1.3	76	0,908	2,671	2,389	2,49	2,389	2,48475
2.7-2.8	92,15	0,753	2,701	2,228	2,448	2,328	2,42625
3.5-3.6	17,88	1,712	1,892	2,361	2,789	2,628	2,4175
4.7-4.8	114,63	0,665	3,031	2,294	2,423	2,294	2,5105
5.5-5.6	108,09	0,677	2,899	2,298	2,426	2,298	2,48025
6.5-6.6	66,64	0,927	2,418	2,411	2,512	2,411	2,438
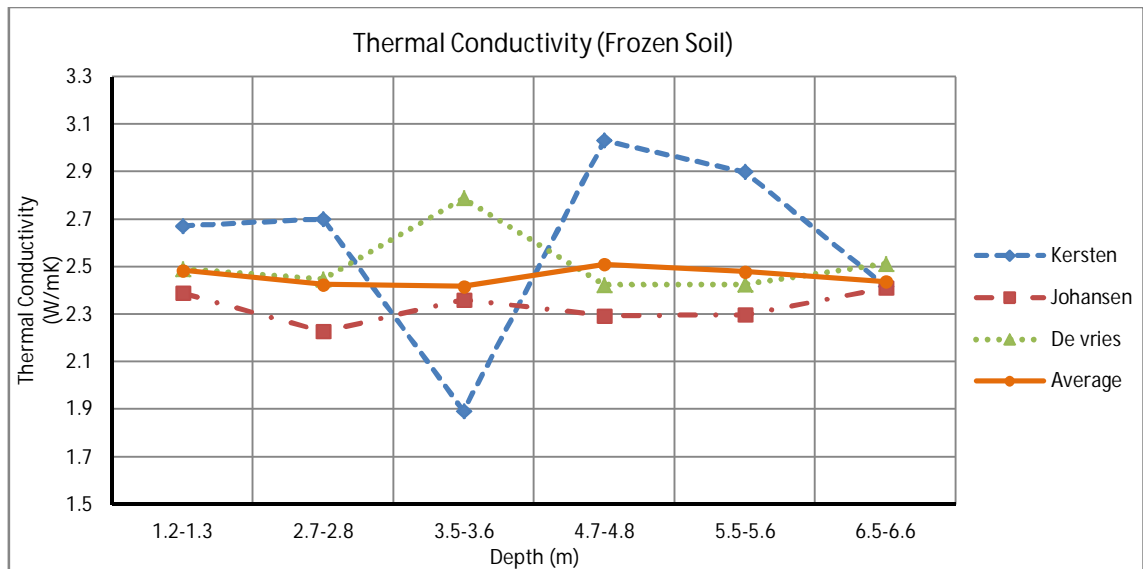
Figure 6-15. Graph with the values of the frozen thermal conductivity calculated by different formulations with depth

6.5 Frost Heave and Thawing Settlement Test

6.5.1 Material and Methods

The purpose for the Frost Heave test is to determine the frost susceptibility of the soil and the settlement due to the freezing and thawing processes. During the test, frost penetration, frost heave as well as the change of the sample height is monitored. The test results are used to estimate frost heave and thaw consolidation of the structures on the tested soils (Onninen, 1999).

1. Parameters:

The following parameters are measured and monitored during the test:

- Frost heave (h): Change of the sample height during the test. It is the difference between the current reading and the initial reading before the test.
- Height of the unfrozen part of the sample (Z_s): It is calculated at the height of the 0^oC isotherm from the measured temperature profile
- Depth of frost penetration (Z_j): It is calculated at the depth of the 0^oC isotherm using the measured temperature profile.
- Frost heave ratio (h/ Z_j): It is calculated from the ratio between the frost heave and frost depth and it is expressed as percentage.
- Thawing settlement: It is the change of the height of the sample during the thawing test. It is calculated as the difference between the current reading and the initial reading before the test.

2. Method description

  ▪ Equipment:

The equipment used for the thawing settlement test and frost heave test is shown in the figure (Figure 6-16) and is composed by:

– Test cell: It was a cylindrical, thermally insulated split barrel cell with an inner diameter of 80mm. In the internal walls of the cell there were five temperatures transducers installed for the monitoring of the temperature profile.
– Bottom and top caps: The sample was installed between two caps with a temperature gauge for the temperature monitoring. Within the caps, cryomat-cooled liquid was circulating to freeze the sample from top to down keeping the sample bottom unfrozen.
– Loading frame: It was used for loading the cap and the soil sample at the level that correspond the estimated vertical stress in situ.
– Displacement transducers: Electrical and manual displacement transducers were located in the top of the sample for monitoring the frost heave and settlement of the sample during the test.
– Data logging device: Consist of a data logger and a computer to save all the data for the devices.
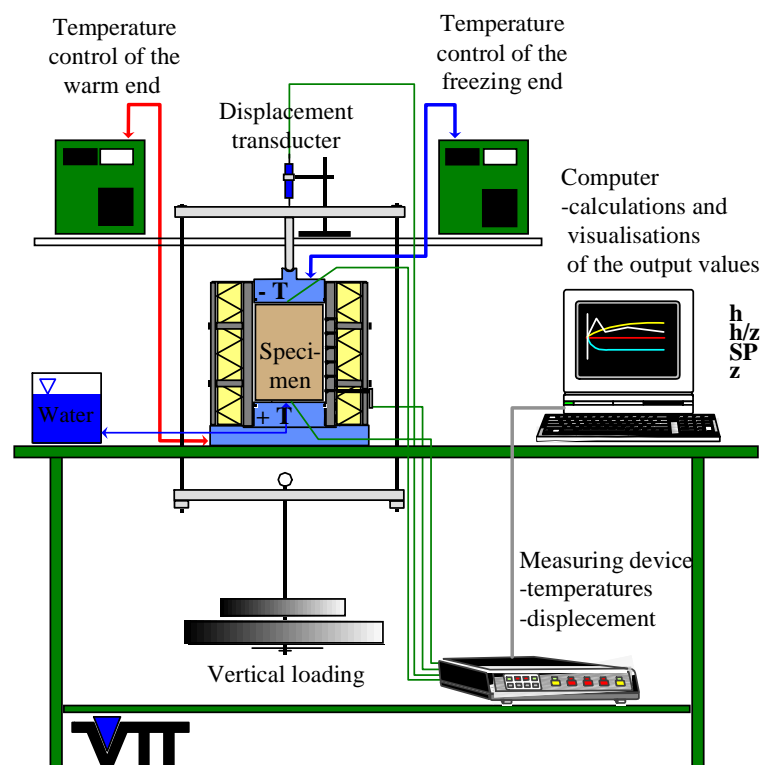
Figure 6-16. Description of the elements and devices used for the frost heave and thaw consolidation test (Onninen, 1999)

- Calibration:

A mix of ice and water was used for the calibration of the temperature gauges in the test cell. Calibration was done in order to adjust the energy loses through the pipes and cables due to:

- Insulation defects
- Room temperature
- Continuous thermal losses due to the length of the pipes
- Electric resistance due to the length of the cables

During the calibration all the temperature transducers of the test cell were submerged in the mixture of water and ice during 24h. After the calibration, the average temperatures of each temperature transducer were calculated (Table 18).

Table 18. Average temperatures of the sensors after 24h submerged in water and ice at 0^oC

	Sensor 1 (Top)	Sensor 2	Sensor 3	Sensor 4	Sensor 5	Sensor 6	Sensor 7 (Bottom)
Temperature	-0,547134944	1,115752	0,836191	1,486401	1,15562	1,008005	-0,591482467
Calibration	-0,547134944	1,115752	0,836191	1,486401	1,15562	1,008005	-0,591482467

3. Installation of the sample:

Myllypuro undisturbed samples were inside 86mm diameter tubes. A hydraulic piston was used to take the sample out of the sampling tube. After that, the samples were cut with a steel wire in order to get the correct diameter (80mm) and height (100mm) of the frost cell. Once the preparation of the sample was done, the installation continued in a cold room with air temperatures +3^oC.

The sample was installed on the bottom cap of the test cell. Between the bottom and the top caps of the test cell a filter paper and a filter stone were installed. The sample was installed in the test cell covered with a rubber membrane which also covered the filter stone and the bottom and top caps. The membrane pressed tightly the top and the bottom caps with O-rings.

The sample covered by the rubber membrane was placed inside the frost cell (Figure 6-17). The walls of the test cell were greased with a thin silicone layer. The sample was closed within the insulated test cell and the displacement transducers as well as the loading frame were installed in the top of the cell.
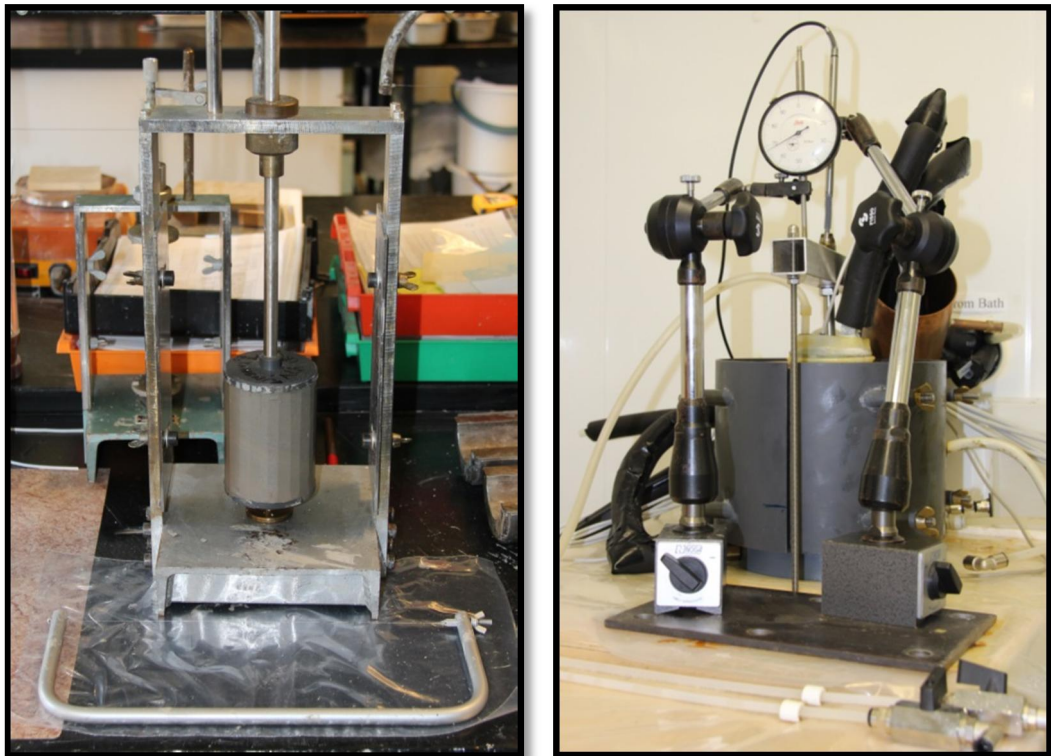
Figure 6-17. Picture of the preparation of the sample (left) and the frost cell with the displacement transducers (right)

4. Frost Heave Test

Frost heave test started with consolidating and saturating the sample. For this first part of the test, room temperature remained constant at +3°C and top and bottom cryomats were turned off. The water level was kept higher than the top level of the sample in order to saturate it. The sample was loaded using the loading frame with the vertical stress that the sample has in situ. Consolidation stopped when the height of the sample remained constant during more than four hours.

Once the consolidation was finished, frost heave test started. The cryomats were switched on and the temperature of the cooling circulation was adjusted. In the top cap the temperature is -3°C and in the bottom +1°C keeping these temperatures constant during the test. During the test, temperature and displacement measurements were monitored with a frequency of 5 min. Frost heave test finishes when the net frost penetration is zero during more than four last hours. The value of the segregation potential obtained when the net frost depth remains constant is used to calculate the frost heave.
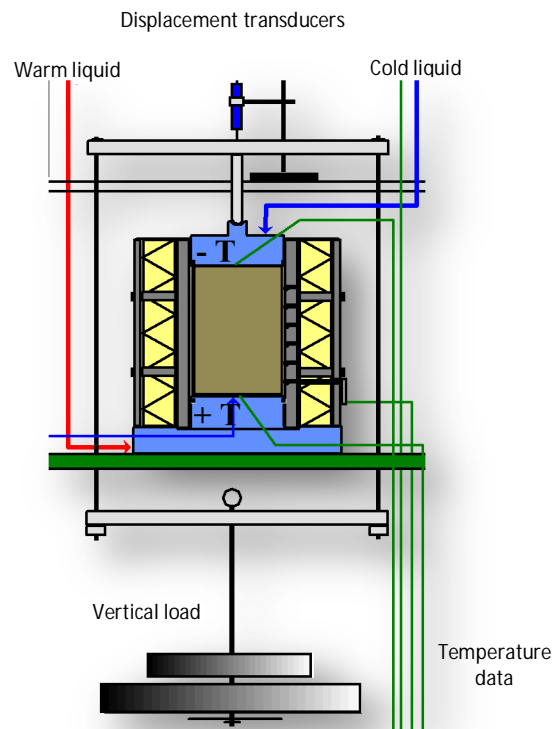
Figure 6-18. Main parts and cross section of the frost cell (Modified figure from Onninen, 1999)

5. Thaw settlement test

Thaw settlement test was used to determine the thaw consolidation properties. After the frost heave test the thaw consolidation test started. During thawing test the loading frame was still loaded with the vertical stress that the sample has in situ. The sample was totally saturated keeping the water level higher than the top of the sample. The room temperature was $+3^{o}C$ and the cryomats were adjusted again with temperatures of $+15^{o}C$ in to top and in the bottom cap. During the test, temperature and displacement measurements were monitored with a frequency of 5 min. Thaw settlement test finished when the vertical displacement was zero which means that the height of the sample remained constant.

When the thaw settlement has finished, the vertical load was removed and the sample started freezing in order to measure the frost heave without load. The cryomats were adjusted with temperatures of $-3^{o}C$ in the top and $+1^{o}C$ in the bottom. For this part of the test, temperature and displacement measurements were monitored with a frequency of 5 min. Again, unloaded frost heave test finished when the net frost penetration was zero during more than four last hours.

6. Ending of the test

All the data was registered using a data logger in the frost heave and the thaw consolidation tests. After saving the data, the cell was opened, the rubber membrane was removed and the height of the sample was measured. The frozen and unfrozen part of the sample was measured in order to calculate the percentage of the thaw consolidation. The sample was photographed (Figure 6-19) and other visual observations were recorded (ice lenses, layers etc.). The moisture content of the frozen and unfrozen part of the sample can be defined by putting the separated samples in the oven during 24 hours.

Figure 6-19. Picture of the frozen sample after the freezing-thawing test (Initial height 100mm)

6.5.2 Results of the Frost Cell Test

Six Frosts Heave and thawing settlement test were done at different depths (Table 19). The main objective of the tests was to estimate the thawing settlement due to the melting process of the frozen soil below the ice rink. Other parameters such as frost depth, frost penetration, frost heave and segregation potential were calculated in order to validate the initial conditions of the models explained later.

Thaw Settlement due to Melting Process

The thaw settlement is calculated in the frost cell and compared with the empirical results obtained with the formulations explained above (Point 2.6). The following tables and figures show the thawing settlement calculations.

Table 19. Empirical thawing settlements in percentage calculated with different formulations

Method	Depth (m)					
	1,2	2,5	3,6	4,8	5,8	6,8
Vähäaho	25,33	30,72	5,96	38,21	36,03	22,08
Speer et al.	31,73	35,42	2,70	37,47	37,73	25,88
Watson et al.	28,01	32,06	0,00	34,40	34,70	21,90
Average (%)	28,36	32,73	2,89	36,69	36,15	23,29
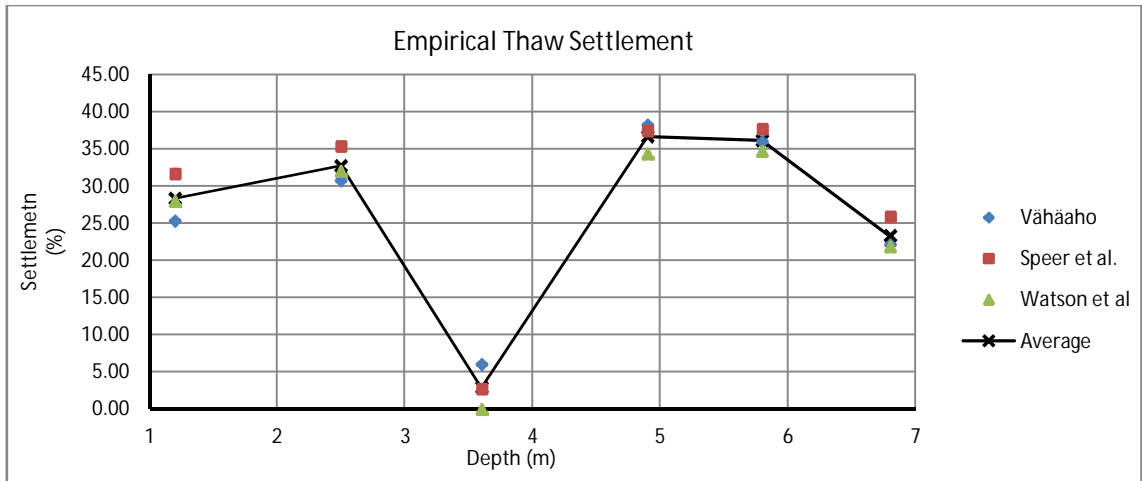
Figure 6-20. Thawing settlement in percentage by depth calculated by different empirical formulations

Table 20. Real thaw settlement and frost depth by depth defined from the frost cell test

Frost Cell	Depth (m)					
	1,2	2,5	3,6	4,8	5,8	6,8
Thaw Settlement (mm)	22,59	19,51	10,34	18,48	21,58	19,005
Frost Depth (mm)	73,7	69,87	76,42	60,07	65,99	72,11

Settlement in %	30,651	27,923	13,530	30,764	32,702	26,356
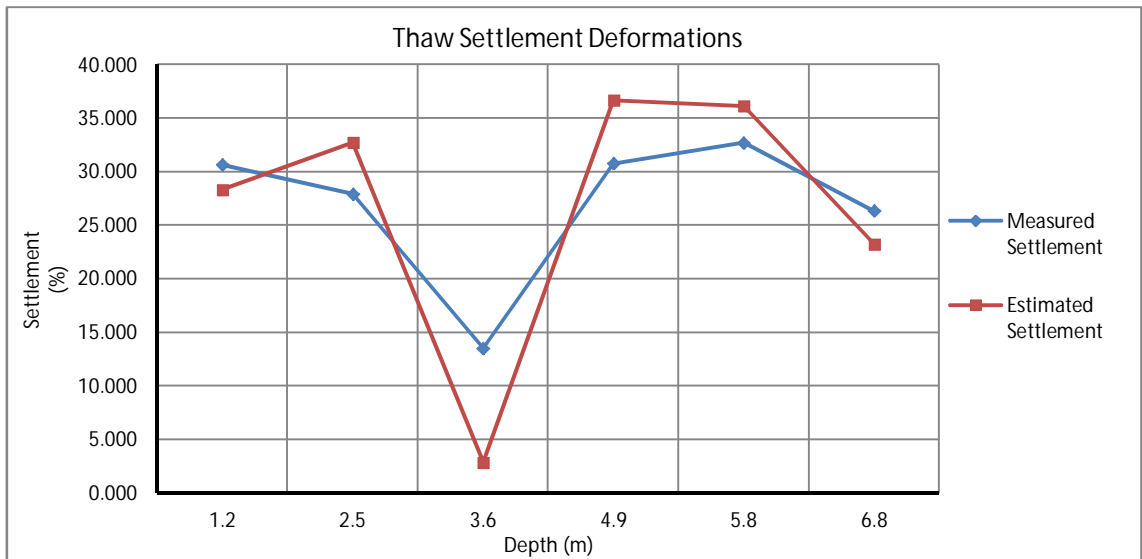
Figure 6-21. Comparison of the estimated thaw deformations calculated with empirical formulation and the measured values obtained in the frost cell

As can be seen above (Figure 6-21), the comparison of the measured values obtained in the frost cell with the thaw settlement calculated by the empirical calculations is overestimated in the points where the water content is high. Otherwise, empirical calculations underestimate settlements when the water content is low.
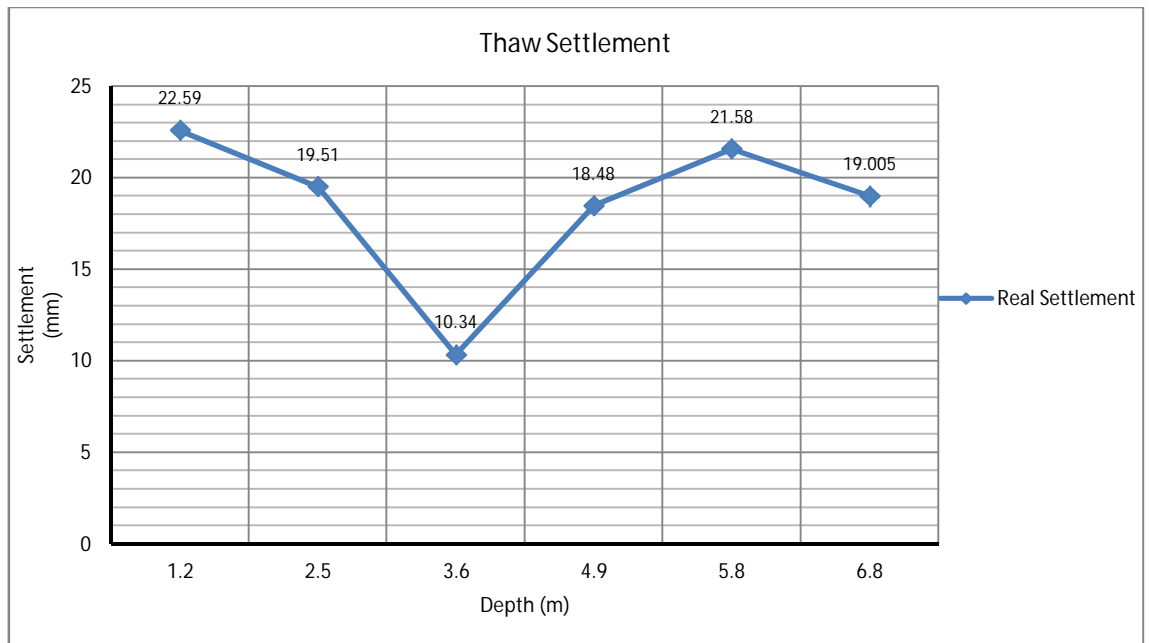
Figure 6-22. Real thaw settlement measured in mm obtained in the frost cell by depth

Next plot (Figure 6-23) shows the thawing settlement evolution in hours of the different samples. As can be seen in the figure, the thawing settlement occurs rapidly and more than 90% of the total settlement in the frost cell test occurs during the first 5 hours.
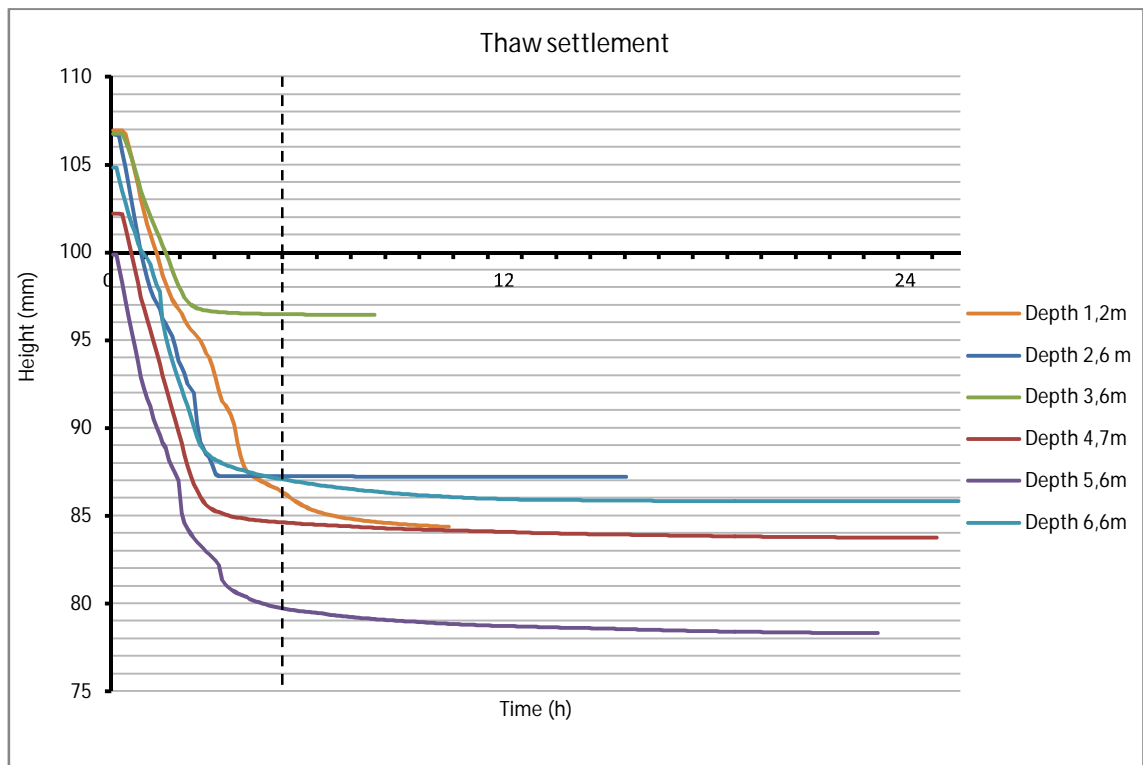
Figure 6-23. Thaw settlement evolution in time (hours) of the different samples

Frost Heave and Frost Depth

The frost cell test is divided in four different time steps where the height of the sample varies (Figure 6-24). In the plot it is possible to difference the loading phase [1] where the sample is loaded with the in situ stress, the first freezing cycle (loaded) [2], the thawing phase [3] and the second freezing cycle (unloaded) [4]. The plots of all the samples are shown in Appendix 4.
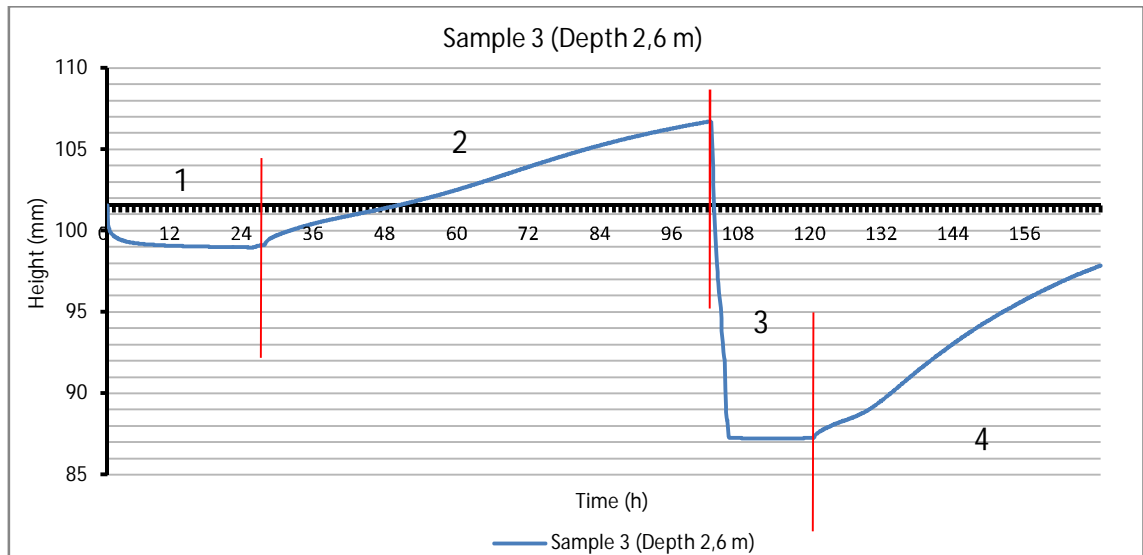
Figure 6-24. Example of the evolution of the height of the sample in the frost cell test

The frost susceptibility of the soils due to the freezing and thawing processes is shown in next figures where the frost heave and the frost depth are represented. A complete table with the values calculated in the frost cell tests is shown in Appendix 4.
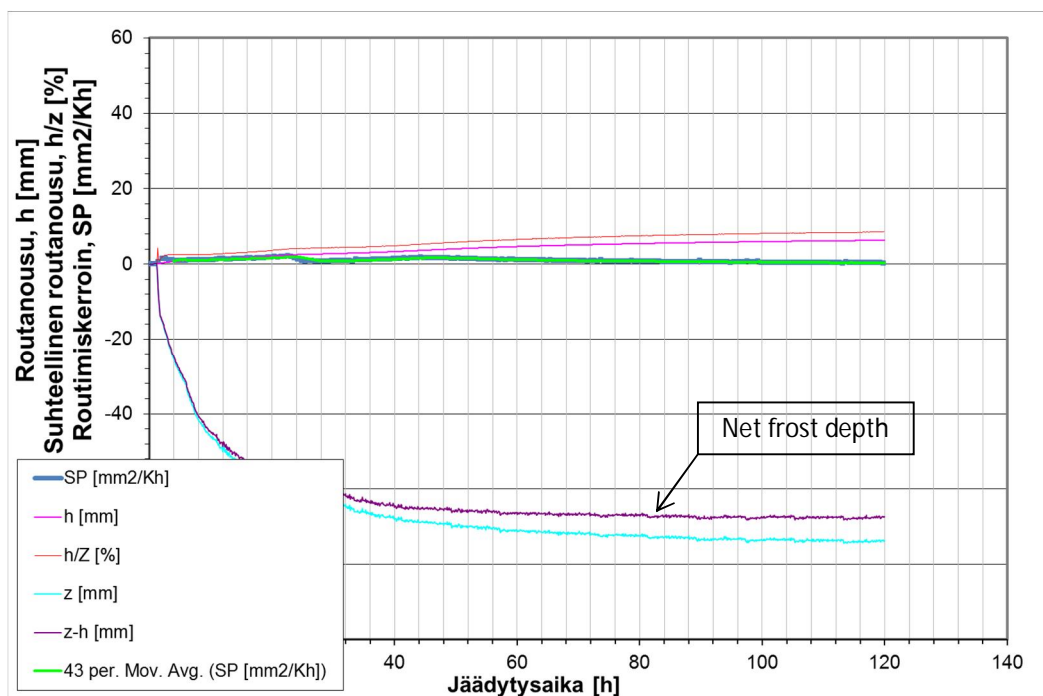
Figure 6-25. Example of a test result at 1.2m depth obtained in the frost cell

Next figures (Figure 6-26 & 6-27) show the total frost heave of the tested samples after the first (loaded) and the second (unloaded) cycle. As the frost heave is continuosly increasing, figure 6-28 shows the frost heave of the tested samples after 24 hours. In the following figures (6-28, 6-29 & 6-30) the frost susceptibility of the soil is compared by measuring the frost heave and frost depth after 24 hours. The figure shows that the soil at 3.6m depths produced the highest frost heave after 24 hours being the most frost supceptible sample (Nurmikolu, 2006).

Table 21. Classification of the frost susceptibility of soils (Nurmikolu, 2006)

	SP_0 (mm^2/Kh)	h_{24h} (mm)	h_{96h} (mm)
Non frost-susceptible	<0.5	<0.6	<1.2
Slightly frost-susceptible	0.5-1.6	0.6-2.2	1.2-3.7
Moderate frost-susceptible	1.6-3.3	2.2-4.5	3.7-7.4
Hight frost-susceptible	>3.3	>4,5	>7.4
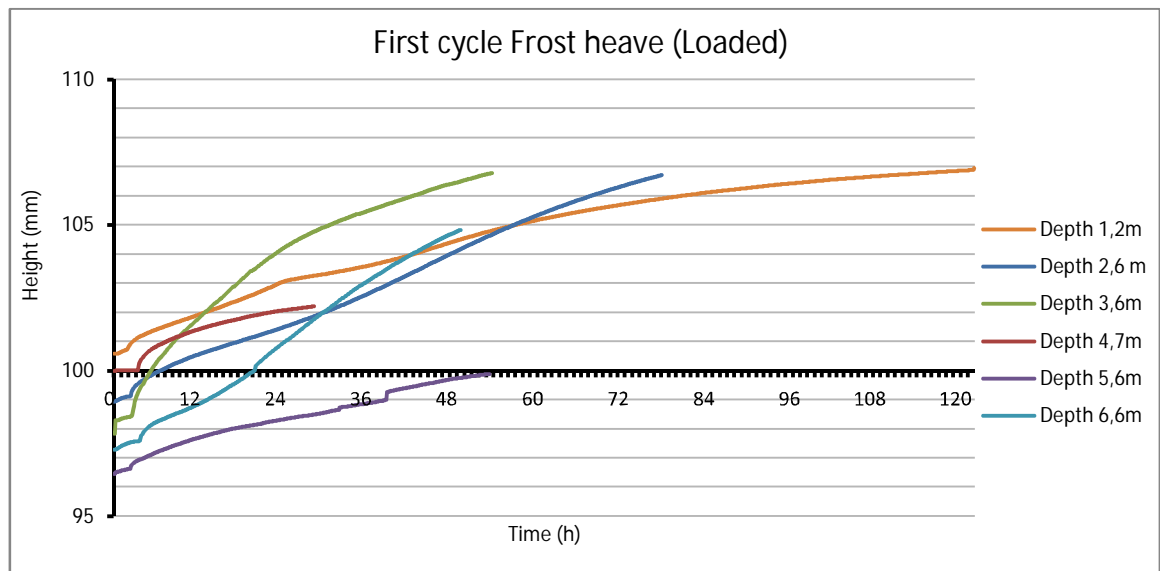
Figure 6-26. Comparison of the first cycle frost heave (loaded) by time
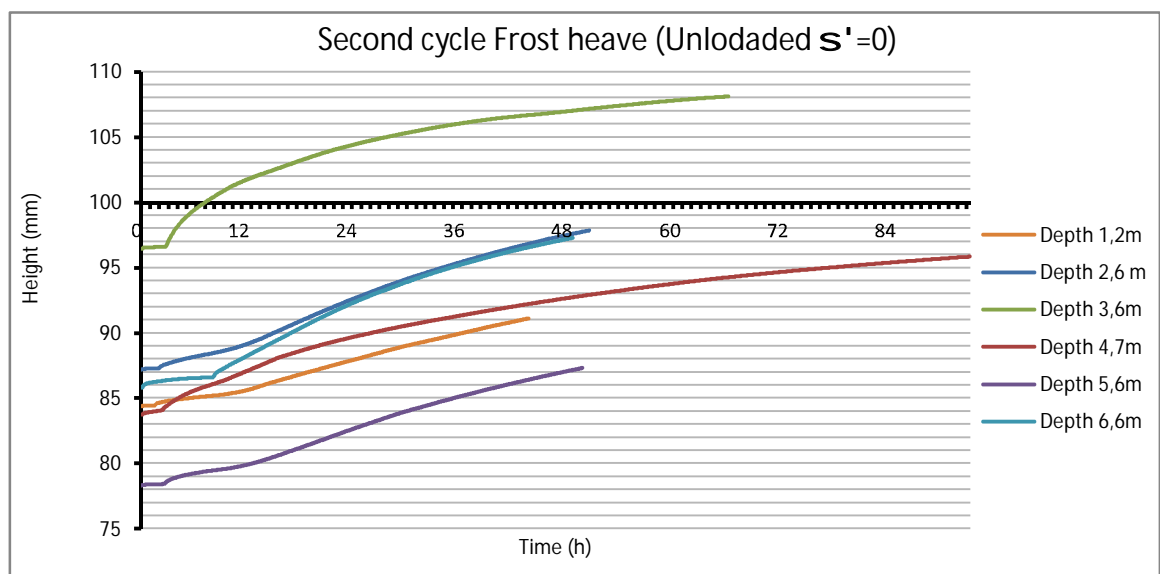
Figure 6-27. Comparison of the second cycle frost heave (unloaded) by time
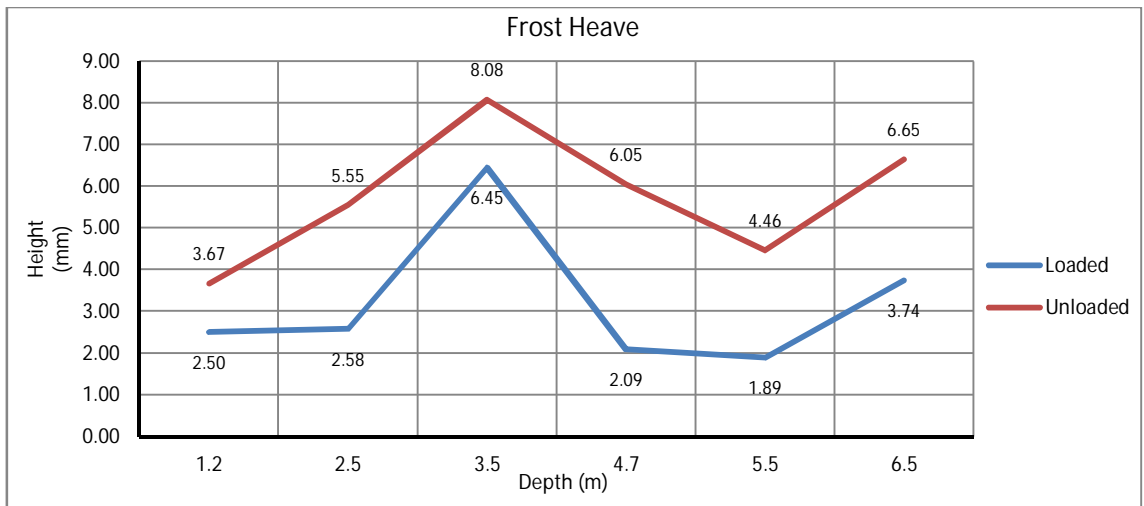
Figure 6-28. Comparison of the loaded and unloaded frost heave by depth after 24 hours
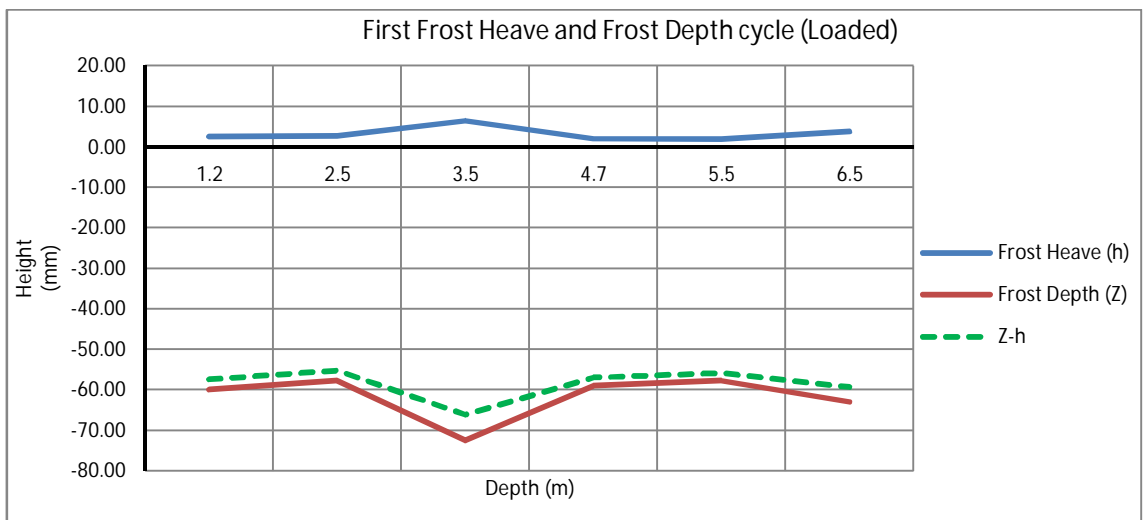
Figure 6-29. Loaded frost heave and frost depth by depth after 24 hours
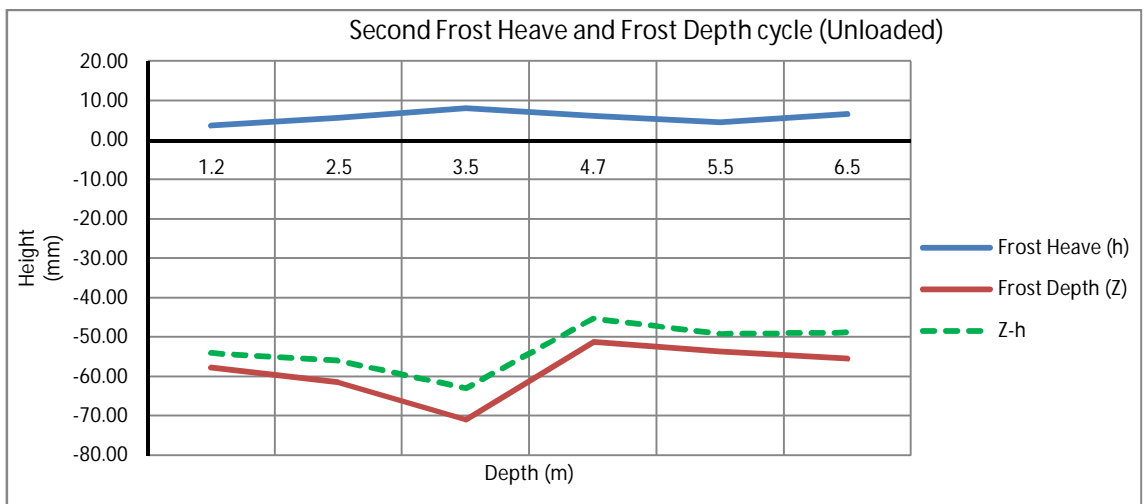
Figure 6-30.Unloaded frost heave and frost depth by depth after 24 hours

6.5.3 Frost Heave Estimation with SSR Model:

The SSR model (Saarelainen, 1992) is a program used to calculate the depth of the frost penetration (z_f) and the frost heave (h) in soils by using equations [6.1] & [6.2]. It estimates the frost heave and frost penetration in an uniaxial multilayer structure but cannot be applied for the thaw settlement estimation.

$$z_f = k \sqrt{F} \qquad\qquad [6.1]$$

$$h = \frac{2\,SP\,\sqrt{F}}{k} \qquad\qquad [6.2]$$

In these equations k is a coefficient proportional to the thermal conductivity (λ) and the volumetric heat capacity in square roots (Saarelainen, 1992). The freezing index (F) was calculated for 30 years with an average temperature (T_{av}) of the ice rink of -6°C [6.3].

$$F = \sum T_{av}t = \mathbf{30}_{years} * \mathbf{12}_{months} * \mathbf{30}_{days} * \mathbf{24}_{hours} * T_{av} \qquad [6.3]$$

The accuracy of the model is related with the accuracy of the thermal properties, segregation potential and stratification of the site. With it, the coefficient of variation of the observed and calculated frost heave and frost penetration is about 10-15% (Saarelainen, 1992). In this thesis the SSR model was used to estimate the total frost depth and frost heave in Myllypuro ice rink after 30 years of operation. In addition the results were used to validate the initial conditions applied in the models explained later (Point 6.6).

The values of the segregation potential (SP) were obtained with the results of the frost heave test. With these values, it is possible to estimate the total value of the frost heave in Myllypuro ice rink using the SSR model. Table 22 shows the values of the segregation potentials obtained in the frost cell.

Table 22. Values of the segregation potential when the net frost depth remains constant

Segregation Potential (mm^2/Kh)	Depth (m)					
	1,2	2,5	3,6	4,8	5,8	6,8
First cycle (loaded)	1.6-1.7	2.4-2.6	3-3.5	0.6-0.7	0.7-0.9	2.7-3.0
Second cycle (unloaded)	3.2-3.5	5.0-5.3	3.5-3.8	2.2-2.3	3.8-4.0	4.2-4.4

The results of the SSR model are shown in the following figure (Figure 6-31). For the model, the ground was divided into 6 different layers using the values of the thermal properties (see point 6.4) and the values of the segregation potential of the first frost heave test cycle (loaded). A thin layer of insulation (100 mm of EPS) was also modelled.

Figure 6-31 shows that the maximum frost depth (6.39m) and frost heave (622mm) obtained with SSR model after 30 years is really similar to the observations done before the renovation process started. The values of frost depth and frost heave correspond to the ground below the middle point of the ice rink where the frost depth and frost heave have their maximum values. In other points closer to the ice rink borders these values are lower. These results obtained with the SSR model were used for the validation of the initial conditions of the models explained above.
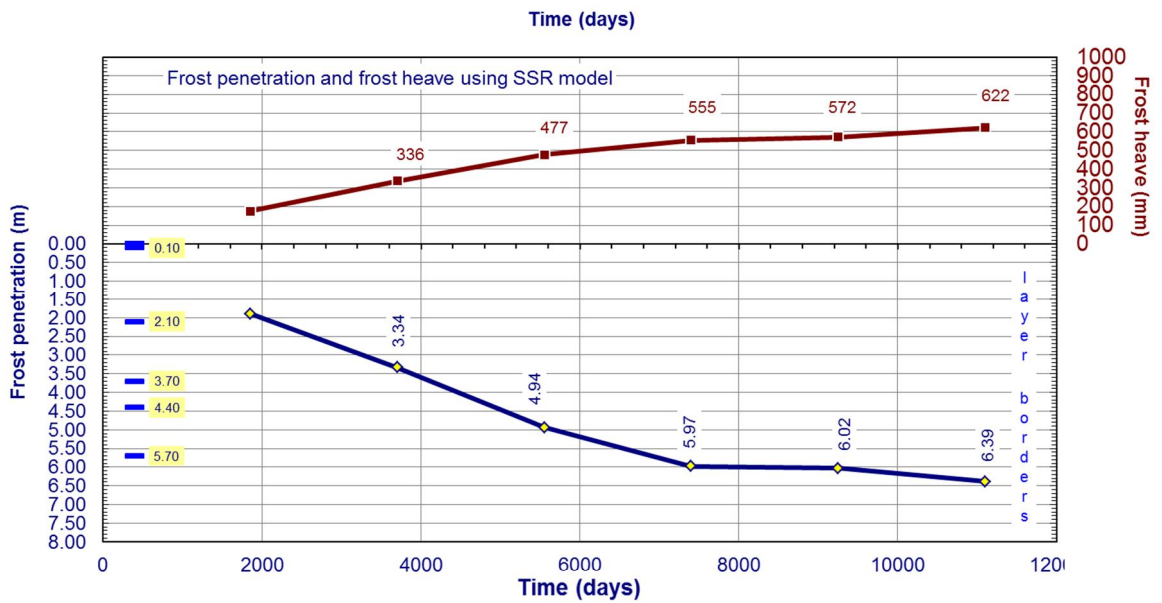
Figure 6-31. SSR model results of frost depth and frost heave in Myllypuro ice rink after 30 years

6.5.4 Manual Estimations of the Thawing Process

To estimate the energy required to melt all the frozen ground below Myllypuro ice rink some manual calculations were also done. Taken five meters depth of frozen soil as average, the total frozen volume is around 18.000m^3. For melting the frozen ground, first is needed to raise the temperature of the ground up to 0°C. If the average temperature of the frozen ground is -3°C and its heat capacity is 2000 kJ/m^{3}K, the total energy required is 108 GJ (30MWh). The second step was to calculate the energy required for the phase change. Taken the average volumetric water content as 60%, the total amount of water is 10800m^3. The latent heat of the water is 334kJ/kg, thus the energy required for the phase change is 3607.2 GJ (1002MWh). Finally, the total amount of energy required for melting the frozen ground was calculated to be 1032MWh.

The energy pumped by the energy piles was estimated by the designer of the heat pump system (Tapio Alijoki from Johnson Controls Finland Oy.). In situ temperature and pressure values were measured. The pressure of the system was 1 bar and the inlet and outlet temperature of the piles was between +28°C to +20°C respectively, so the estimated energy pumped by the system is around 112kW. Under these conditions, the energy pumped in one year is 981.2MWh, less than the energy required (1032MWh). Consequently for melting all the frozen ground is needed more than one year pumping heat by the energy piles. Applying the same calculation to the influence area of one energy pile, the result obtained was that is needed more than 750 days to melt the frozen soil completely. It is important to consider that inlet and outlet temperatures were not constant, so the energy pumped could have varied through the year.

6.6 Thermal Modelling

6.6.1 Objectives

The main objective of this modelling was to study the melting process of the frozen ground below Myllypuro ice rink. For this, several transient analysis and models have been carried out to evaluate the thawing process of the ground and to know the time that was needed to melt the frozen ground completely. Avoid the ground surrounding the pile foundation from freezing was other of the objectives of this modelling. Because of this, know the temperature of the liquid inside the thermal pipes that has to be pumped to avoid ground freezing was another target of this study.

6.6.2 Model Geometry, Limitations and Characteristics

Myllypuro Ice Rink was modelled with two different software tools (SoilVision Heat and Geo-Slope Temp/W). There were two different models carried out with SoilVision: one was a 2D transient analysis representing a cross section of Myllypuro Ice Rink and the other one was a 3D transient analysis representing the influence area of one energy pile located below the ice rink. The models do not represent perfectly the real situation and have some limitations such as the piles were modelled as a *well boundary condition* (models done with SoilVision Heat). It means that piles were modelled as empty cylinders which pump heat through its perimeter. In these models the mechanical properties of the piles and the surrounding soil were not taken into account. Otherwise, ground freezing and phase change processes difficult calculation and converge process. Thawing processes of the soil and water phase change are related to the unfrozen water content and its freezing curve. These parameters were not calculated in the laboratory test and its values were estimated from literature.

Both models were divided into three different time periods. The first period was the initial conditions in steady-state analysis that established the ground temperature gradient and the total amount of frozen soil below the ice rink. To determine this steady state analysis previous analysis and models were done. This previous models were validated with the results obtained with the SSR model and the in situ measurements and observations (Appendix 2). The second time period is medium term transient analysis model. The maximum duration of this period was 1000 days, simulating the evolution of the ground thermal behaviour and the thawing process since the facility was opened in November 2012. During this period, is assumed that energy piles are pumping heat at +20ºC or a constant heat flux of 112kWh. Finally, the last step was a long-term transient analysis for 10 years. The main objective of this last step was to determine the temperature of the piles that avoid ground freezing in a long-term analysis. The geometry of the models is shown in the Figure 6-32.

A simplified model was done with Geo-Slope Temp/W with the influence area of one energy pile. This model was carried out to evaluate the radial melting process of Myllypuro ice rink. In it, the pile is modelled as a circular region with two points simulating the simple U-tubes where a constant temperature (+20ºC) boundary condition is applied.
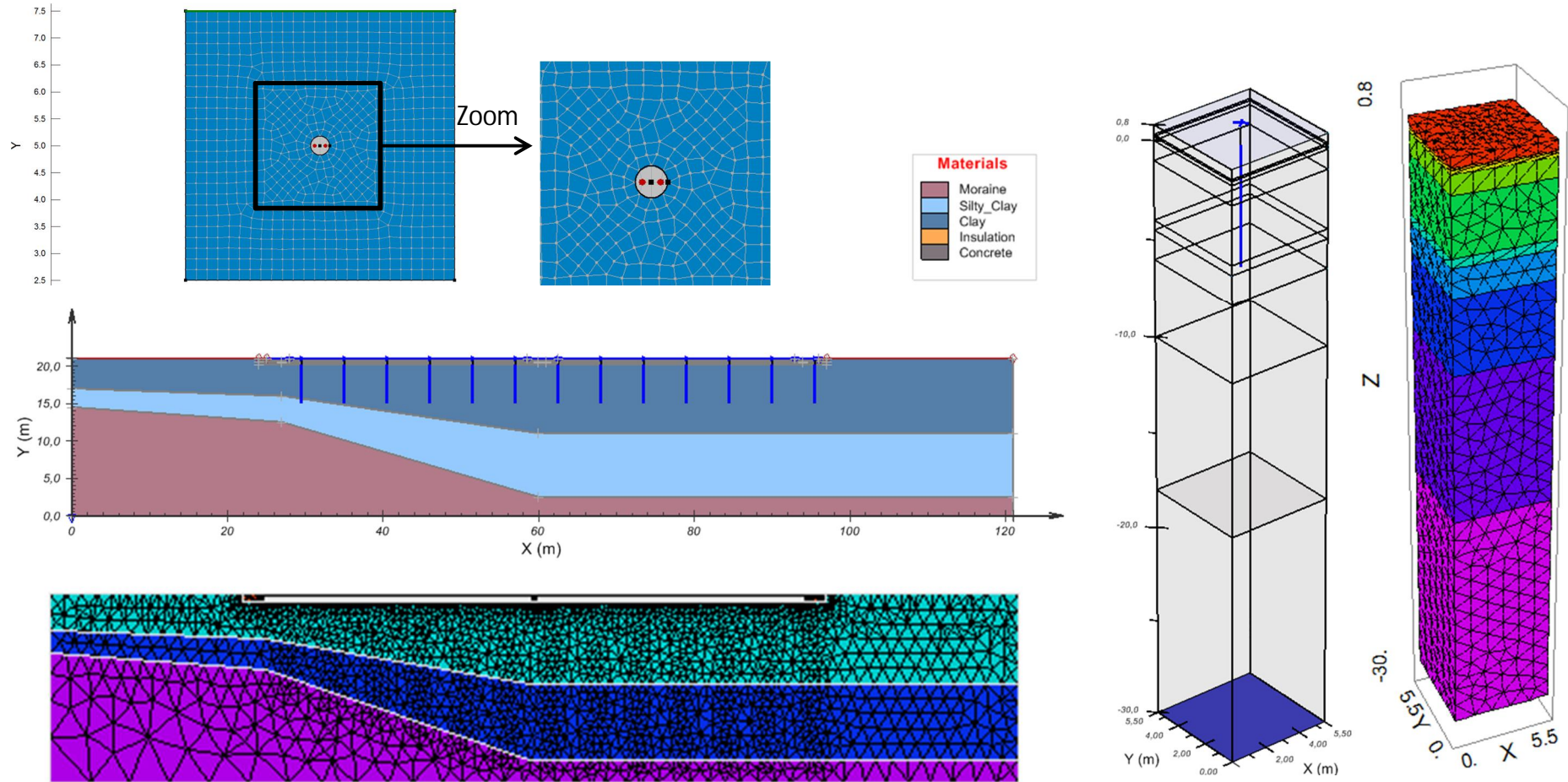
Figure 6-32. Geometry and mesh properties of the 2D (left) and the 3D models (right) carried out with SoilVision Heat and Geo-Slope Temp/W

6.6.3 Materials

The soil profile was divided into three layers and the average material properties are shown in Table 23. The thermal properties of the soils (calculated values in point 6.4) were obtained from the laboratory test explained in Chapter 2.4.3 & 2.4.4 and from common values obtained from different reports and books (Sundberg, 1989; Clauser, 2006; Andersland et al., 1994)

In the 2D models the thermal conductivity used in the clay layer was calculated as the average of the values obtained in the laboratory test in order to simplify the model and reduce time of calculation. Otherwise, in the 3D model, the clay layer was divided into 6 layers with different thermal parameters obtained from the tests in order to get more accurate results (point 6.4).

Table 23. Input values: Ground thermal parameters for 2D models

Soil		Thermal Conductivity	Heat capacity	Vol. Water Content
		W/m K	KJ/m^3K	m^3/m^3
Clay	Unfrozen	1,07	2400	0, 675
	Frozen	2,46	2000	0,675
Silty-Clay	Unfrozen	1,75	3000	0,366
	Frozen	3	2000	0,366
Moraine	Unfrozen	3,01	2700	0,05
	Frozen	3,36	2000	0,05

Other construction materials were used for modelling Myllypuro Ice Rink such as the concrete slab and the insulation (100mm of XPS). Next Table 20 shows the properties of the construction materials used for the models.

Table 24. Thermal parameters of construction materials

Material		Thermal Conductivity	Heat capacity	Vol. Water Content
		W/m K	KJ/m^3K	m^3/m^3
Concrete	Unfrozen	1,63	2300	0,1
	Frozen	2,50	2000	0,1
XPS	Unfrozen	0,035	52,5	0,01
	Frozen	0,035	52,5	0,01

Freezing and thawing processes in fine soils are related to the values of the unfrozen water content. The values of the unfrozen water content were not calculated in this thesis. The estimated freezing curves of the soils and the values of the residual unfrozen water content were obtained from different manuals (SoilVision Verification Manual, 2012) and articles (Liu, B & Li, D., 2012). According to the references, the residual values of the unfrozen water content for the clay layer were between 8-13%. The unfrozen water content for silty soils was between 5-7%. The characteristic curve of unfrozen water content was calculated as an exponential function for the different soil layers according to these values. Following figure 6-33 show an example of the

characteristic curves of the unfrozen water content and its residual values during the ground freezing process used in the models carried out.
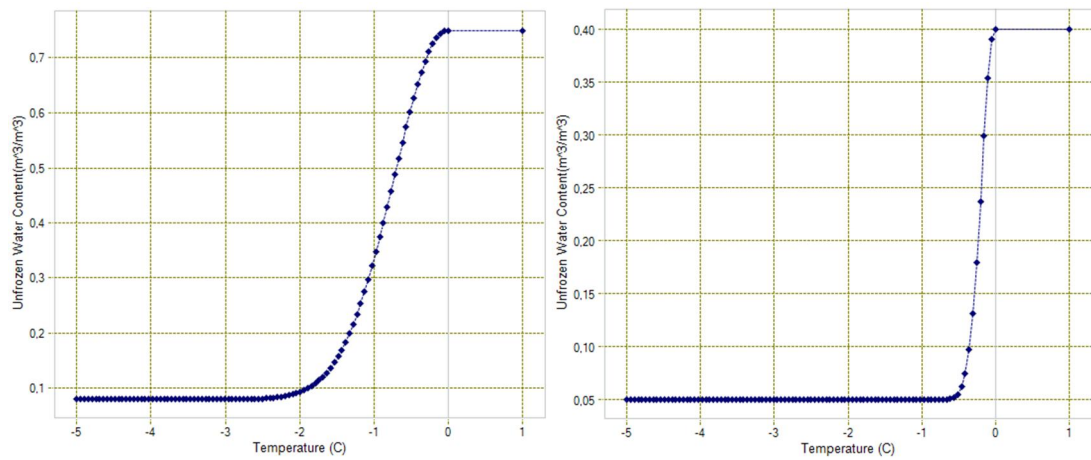
Figure 6-33. Unfrozen water content curve in clay (left) and in silty soils (SoilVision Heat VM,2012)

6.6.4 Boundary Conditions

a.   Initial conditions: Steady-state

The initial steady-state was created with previous models in order to create a similar situation to the real conditions below the ice rink in Myllypuro. The models done with SoilVision Heat and Temp/W showed that the maximum depth of frozen soil was between 6.5-7m. These results were similar to the in situ test done in Myllypuro and the temperature measurements, validating the model and the initial conditions. The figure (Figure 6-34) shows soil profile temperature after 30 years operation in Myllypuro. This soil temperature profile was used as the initial condition for the next transient analysis.
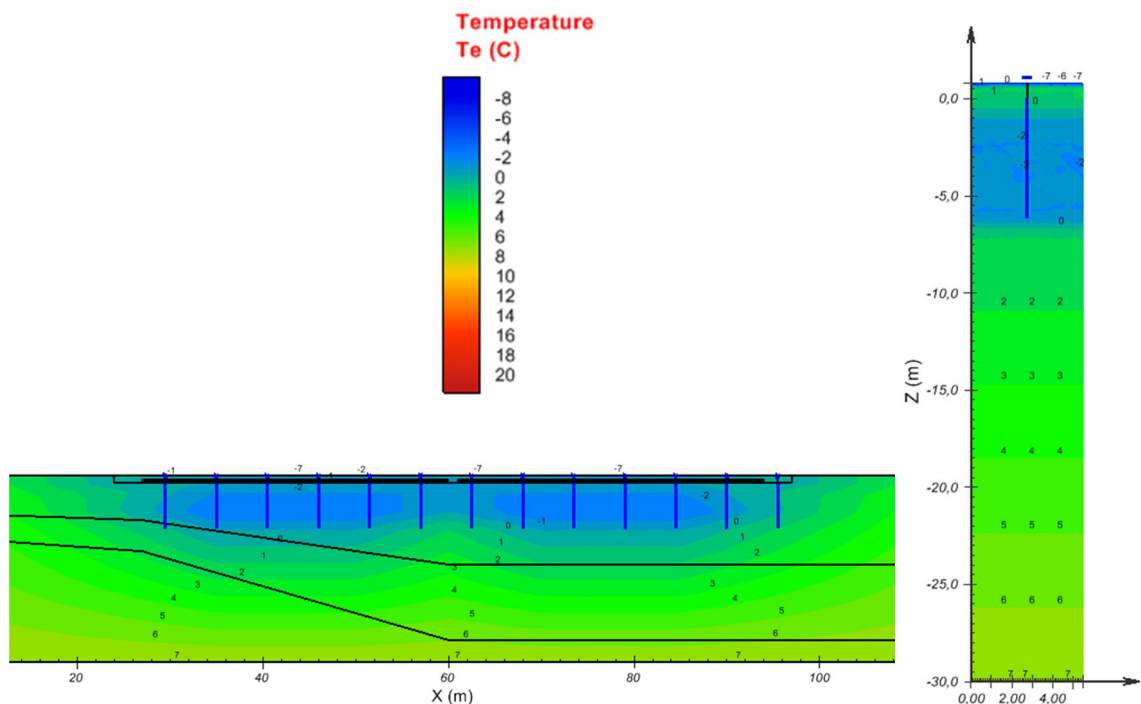
Figure 6-34. Ground Initial conditions in Myllypuro ice rink

b. Constant boundary conditions

For the different transient analysis done in the model some constant boundary conditions were applied:

- Building: This constant boundary condition was applied only in the 2D model that represents the cross section of Myllypuro ice rink. The inner building temperature was between +2°C (in the bottom) and +5°C (in the top). It was represented in the model as a constant temperature boundary condition (Temperature +2°C) and it was applied in the concrete slab which was not in contact with the ice rink.
- Temperature 20-30 m below ground surface: It has been demonstrated that in the depth of 20m below the ground surface the ground temperature remains almost constant during the whole year. In this analysis a boundary condition represents the temperature of the ground at this depth. This temperature boundary condition was assumed to be constant and its value was +7°C during the whole analysis. It was applied in the 2D and 3D models carried out with SoilVision.
- Ice hockey rink: The cooling system for the ice rink pumps cold liquid at temperatures between -6°C and -7°C. In the models, there was a constant boundary condition representing the ice rink with a constant temperature of -7°C. This boundary condition was applied in the 2D and 3D models carried out with SoilVision Heat.
- Energy piles: In the models done with SoilVision Heat the piles were represented in the model as a *well boundary conditions* pumping heat through its perimeter with different constant temperatures or heat flux values. As it was said previously, its physical and mechanical properties were not considered. The length of the piles was between 15-20m but the embedded pipes did not reach the bottom of the piles. The pipes were built until 6-7 meters depth and because of this, the piles were modelled up to this depth.

c. Water table temperature function

The water table in Myllypuro ice rink was at 1.3m below the surface. The water is heated due to the heat pumped by the energy piles. A boundary condition represented the values of the water table temperature (Figure 6-35). The function of the water table temperature was based on the temperature measurements done in Myllypuro ice rink (Appendix 2). The temperature applied in this boundary condition was calculated as the average of the temperature readings at the level of the water table. The water flow could explain the difference between the temperature readings in the different points. Last temperature measurement was +5.54°C on date 30.9.2013 (on average). This temperature remains constant in the transient analysis after the day of the last temperature reading. This boundary condition was applied between the bottom of the concrete slab and the top of the clay layer in the models carried out with SoilVision.
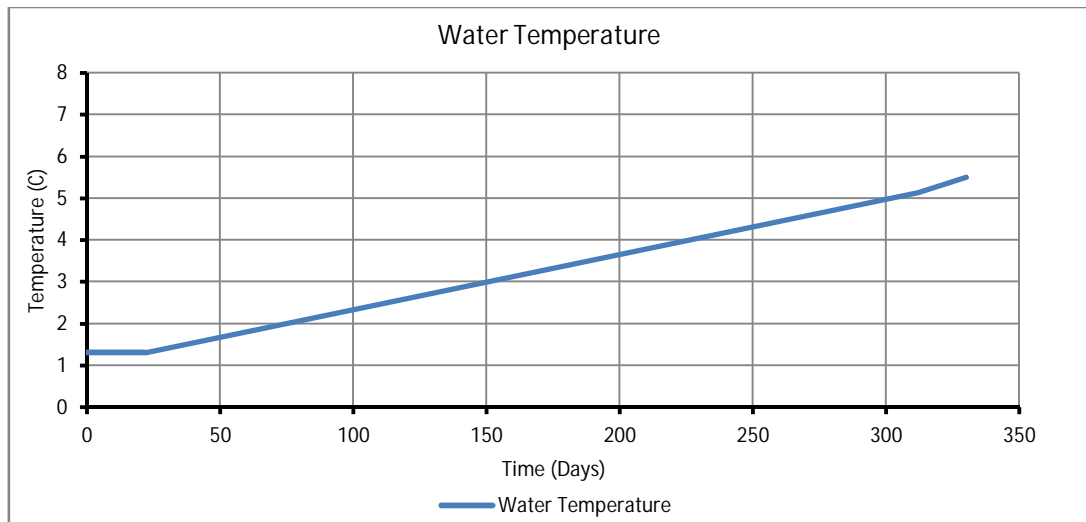
Figure 6-35. Function of the water table temperature. Boundary condition applied in models done with SoilVIsion

d. Climate function

In order to know the outer temperature effect in ground freezing process in long and short term transient analysis a climate function has been designed (Figure 6-36). This climate function is a cyclic boundary condition and is repeated every year during transient analysis using monthly averages temperatures for the last 30 years. Several long term transient analyses were carried out and annual climate variations were not considered in the analysis. The climate function was only applied in the ground surface which is not in contact with the building in the 2D model done with SoilVision.
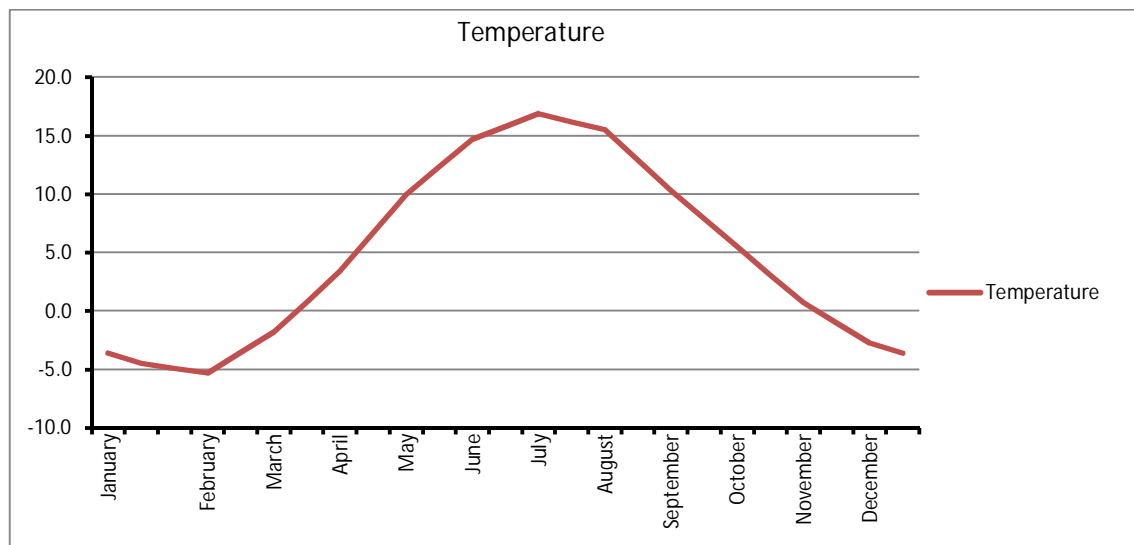
Figure 6-36. Helsinki cyclic climate function

Following tables (Table 25, Table 26 and Table 27) summarize the boundary conditions applied in the different models carried out with SoilVision Heat and Geo-Slope Temp/W and where they are applied.

2D Models

Table 25. Summary of the boundary conditions applied in the 2D model carried out with Temp/W

Boundary condition	Applied
Climate	-
Energy Piles Constant Temperature	Border of the pile & Points inside piles
Energy Piles Heat Flux	-
Water Table Temperature Function	-
Building	-
Constant 20m Below Ground Surface	-
Ice Rink	-

Table 26. Summary of the boundary conditions applied in the 2D model carried out with SoilVision Heat

Boundary condition	Applied
Climate	Ground surface outside the building
Energy Piles Constant Temperature	Border of the pile (Well BC)
Energy Piles Heat Flux	Border of the pile (Well BC)
Water Table Temperature Function	Between concrete slab and the clay layer
Building	Ground surface inside the building
Constant 20m Below Ground Surface	20m Below ground surface
Ice Rink	Ice rink inside the building

3D Model

Table 27. Summary of the boundary conditions applied in the 3D model carried out with SoilVision Heat

Boundary condition	Applied
Climate	-
Energy Piles Constant Temperature	Border of the pile (Well BC)
Energy Piles Heat Flux	Border of the pile (Well BC)
Water Table Temperature Function	Between concrete slab and the clay layer
Building	-
Constant 30m Below Ground Surface	30m Below ground surface
Ice Rink	Top layer of the model representing the Ice rink

6.6.5 Models and Characteristics

Next Table 28 summarizes the models carried out with the different software tools and their main characteristics of each.

Table 28. Summary of the different models carried out and their characteristics

Software	Name	2D or 3D	Description
SoilVision Heat	SV-CTBC	3D	3D model simulating the influence area of an energy pile. Constant temperature BC applied
SoilVision Heat	SV-CHFBC	3D	3D model simulating the influence area of an energy pile. Constant heat flux BC applied
SoilVision Heat	SV-CHFBC	2D	2D model simulating the pile foundation. Constant heat flux BC applied
Temp/W	TW-CTBC-2P	2D	2D model simulating the radial melting process. Constant temperature BC applied in two points inside the pile simulating the exchanger pipes
Temp/W	TW-CTBC-BC	2D	2D model simulating the radial melting process. Constant temperature BC applied in the border of the pile

6.7 Modelling Results: Melting Process

6.7.1 Constant Temperature Boundary Condition

3D Model: SoilVision Heat [SV-CTBC]

The first time step of the model was to establish the initial conditions based on the data (Appendix 2). After that, the second step of the model represented a transient analysis starting the day when the facility was re-opened in November 2012. In this analysis it was assumed that energy piles were pumping heat to the ground at +20°C.

Next figure (Figure 6-37) shows temperature evolution of the ground under the second step conditions at different depths represented by the "Z" coordinate. In the model, Z=0 coordinate represents the border between the concrete slab and the top of the clay layer. The figure 6-37 shows that it is needed 400-450 days to melt completely the frozen ground below Myllypuro ice rink.
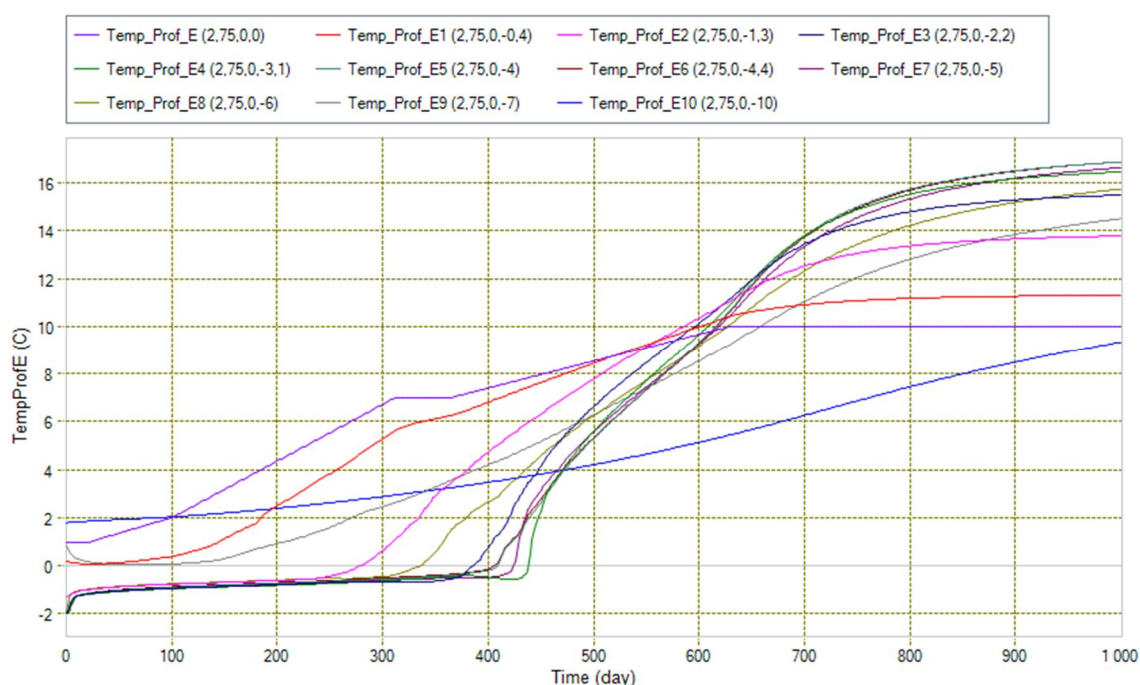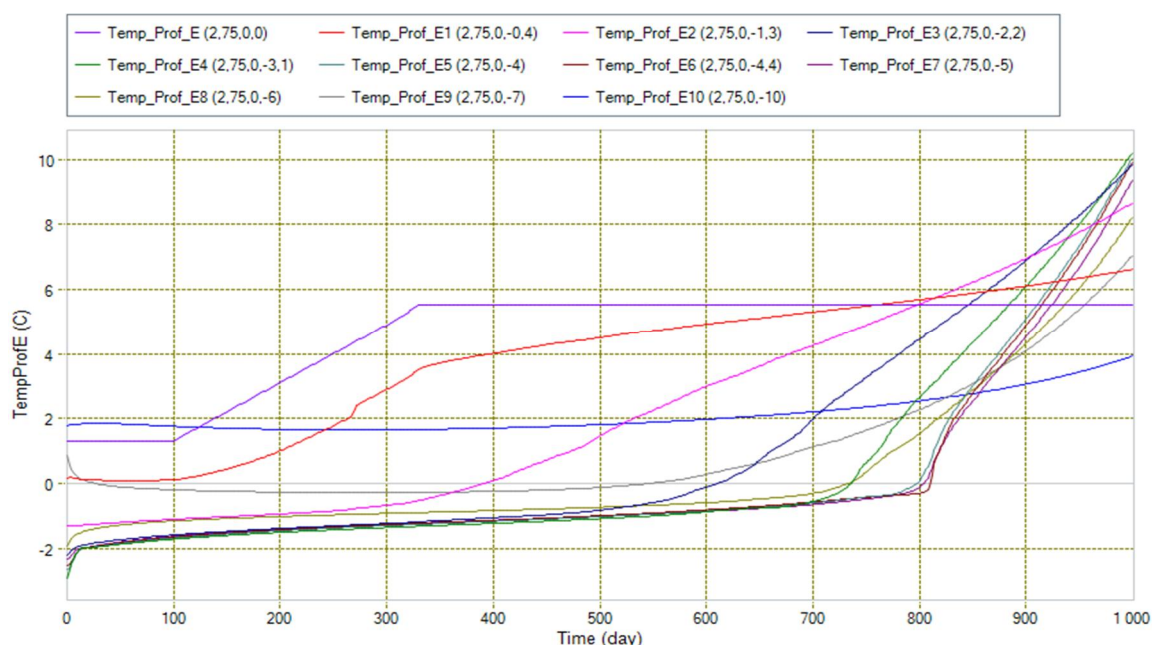

Figure 6-37. Temperature profile evolution in the middle of two piles (2.75m from the piles) after 1000 days pumping heat at 20°C. Results obtained in 3D model done with SoilVision Heat

Following figure (Figure 6-38) shows the ground temperature profile after different time steps. The figure shows the ground temperature of points located in the middle point between piles. The results obtained with the 3D model carried out with SoilVision Heat and the temperature measurements done in situ in Myllypuro (Appendix 2) are really similar. To compare the model results with the real readings, it has to be considered that in the 3D model, the Z=0 coordinate is in the border between the concrete slab and the clay layer. Whereas, in the in situ temperature measurements, the Z=0 coordinate is in the surface of the concrete slab.

The results obtained validate the results of the preliminary manual calculations where it was necessary to pump heat during more than one year to melt completely the frozen ground bellow Myllypuro ice rink. Even though, the results show that the time

needed to melt the frozen ground applying the temperature boundary condition was less than in the manual calculations.
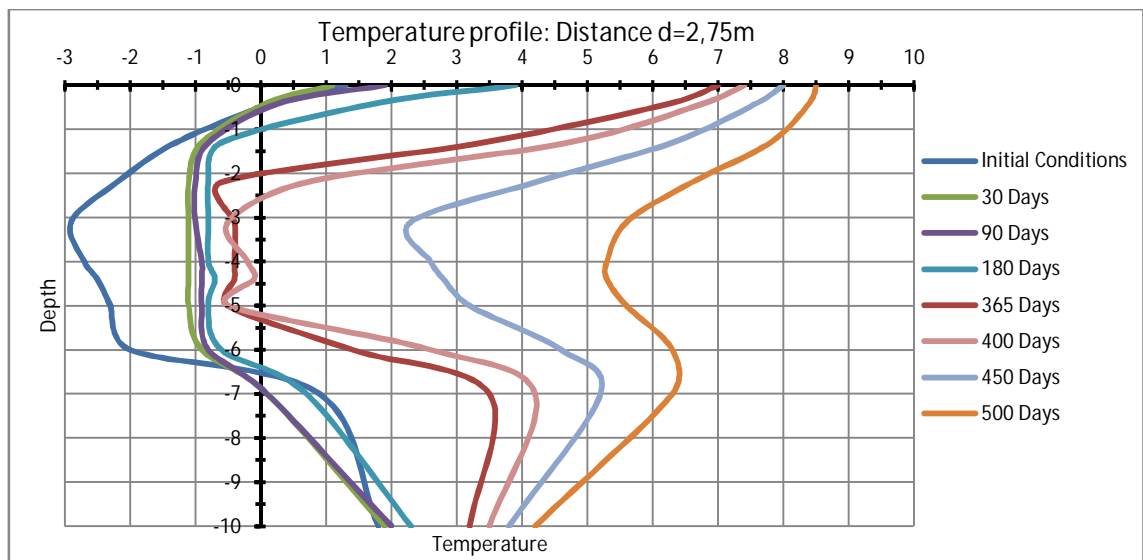
Figure 6-38. Ground temperature profile after different time steps in points located between piles (D=2,75m). Model carried out with SoilVision Heat

The figure 6-38 shows that the temperature in the frozen soil below the ice rink rises rapidly if the piles pump heat at +20°C temperature. After that, the energy required to melt the frozen ground is bigger and it takes more than 400 days to melt it completely. This is due to the phase change and the unfrozen water content curve of the soil. Next picture (Figure 6-39) shows the temperature evolution of the ground surrounding the pile at different time steps:
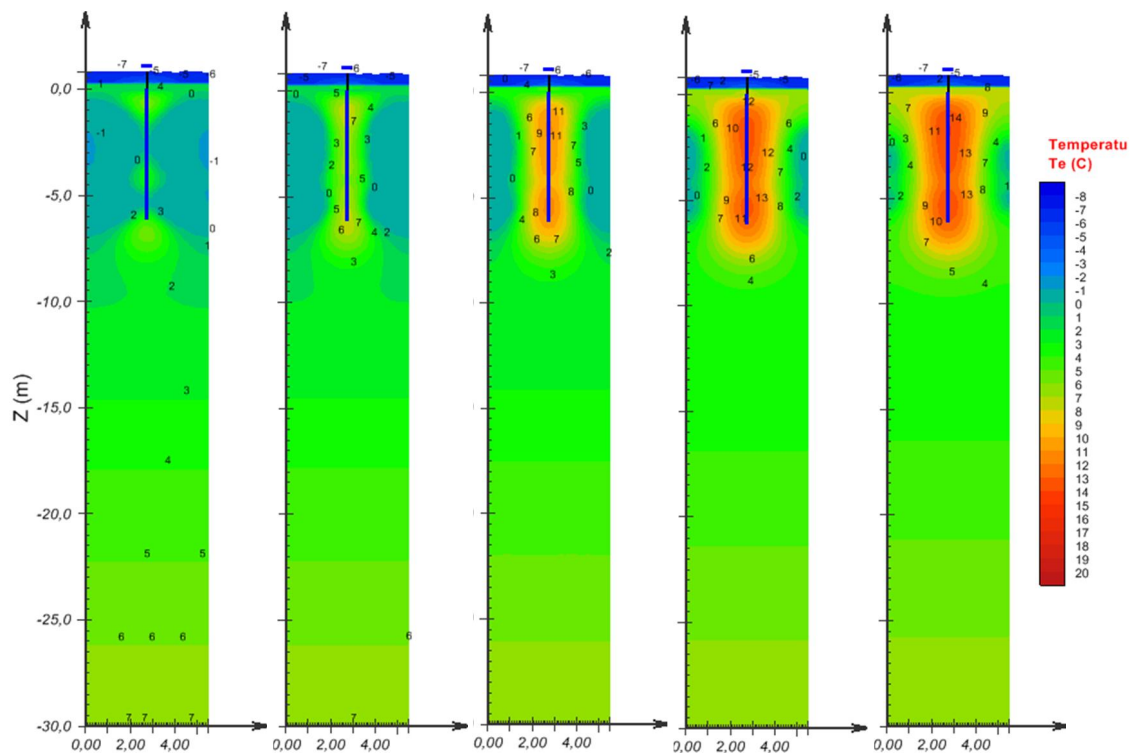
Figure 6-39. Ground temperature evolution after 30, 90, 180, 365 and 420 days (from left to right). Model carried out with SoilVision Heat

2D Model: Geo-Slope Tempe/W [TW-CTBC-2P]

The 2D model carried out with Geo-Slope Temp/W shows the results of the radial melting process in a transient analysis (Figure 6-40).
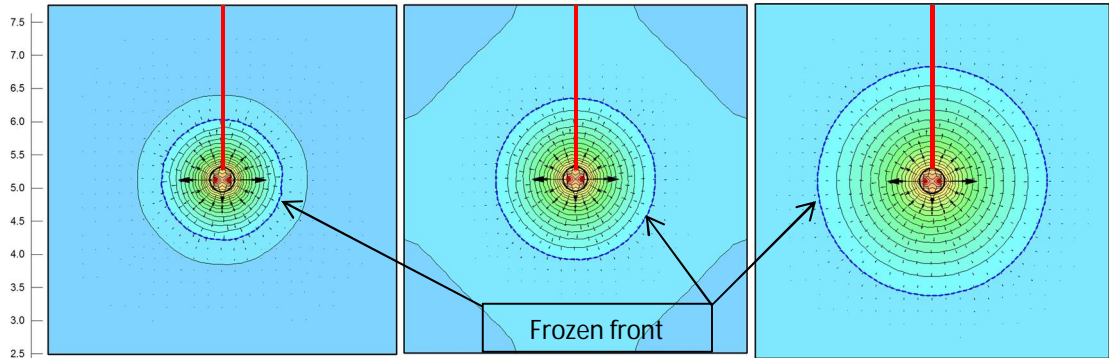
Figure 6-40. Radial melting evolution after 150 days (left), 300 days (centre) and 2 year (right) pumping heat at +20ºC by the energy piles. Model carried out with Geo-Slope Temp/W

In the figure 6-40 each line represents an iso-temperature line with difference of $1^{o}C$ and the frozen front is represented by the blue discontinuous line. The model shows that after two years pumping heat by the pile still remains frozen ground surrounding it.

Figure 6-41 is a plot where ground temperature evolution of the radial melting process in different time steps is represented. This figure shows the temperature of the ground in points located from the border of the pile to the end of its influence area (red line in figure 6-40). As in the previous calculations, Figure 6-41 shows that the time needed to melt all the frozen ground is more than 750 days.
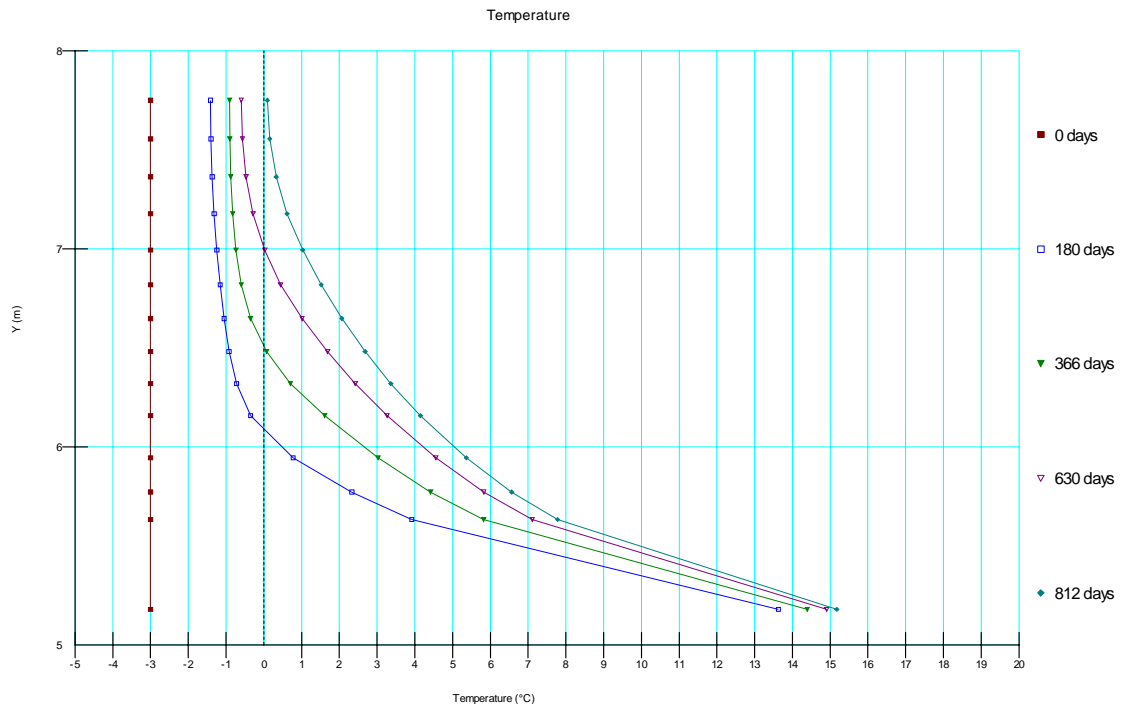
Figure 6-41. Ground temperature evolution of the radial melting process from the border of the pile (Y=5.1) to the end of its influence area (Y=7.75)

Comparison of the results with SoilVision Heat and Temp/W

The comparison of the results obtained with Temp/W and SoilVision show that in both cases it was needed more than 400 days to melt the frozen ground. The calculations carried out with Temp/W showed that it was needed more than 800 days to melt the ground completely. This can be explained because the in the Temp/W model, the temperature boundary condition was applied in two points inside the pile (considering the thermal properties of the concrete) instead of in its perimeter. In order to compare better the results, the same model was carried out with Temp/W applying the boundary condition in the perimeter of the pile [TW-CTBC-BP] (See Appendix 3). The result was that it is needed between 450-500 days to melt the frozen soil completely.

6.7.2 Heat Flux Boundary Condition with SoilVision Heat

The results obtained in the models carried out with temperature boundary condition show that less time is needed to melt the frozen ground compared to the previous calculations [SV-CHFBC 2D and 3D]. The difference between both calculations is around 200 to 300 days. Because of this, new calculations were carried out applying a heat flux boundary condition. The heat flux pumped by the energy pile system was calculated with the formula [2.1]. According to the data obtained in situ and the characteristics of the system the total amount of energy pumped was assumed to be 112kW (40320kJ/day-pile). Next figures shows the results obtained with the new boundary conditions.

Figure 6-42. Temperature profile evolution in the middle of two piles (2.75m from the piles) after 1000 days pumping 112kW. Results obtained in 3D model done with SoilVision Heat

Figure 6-42 and Figure 6-43 show that more than 800 days is needed to pump enough heat to melt the frozen ground inside the influence area of one pile. The result obtained with the heat flux boundary condition is closer to the previous calculations and to the results obtained with Temp/W than the previous model carried out with the temperature boundary condition. The time needed to reach the steady-state in the

model with the temperature boundary condition and the energy losses through the pile materials (which were not considered in the models) can explain the differences between the models.

Figure 6-43 illustrates the temperature profile by depth in a point located between piles (d=2,75m) after different time steps pumping 112kW by the energy pile system. The results can be compared with the Figure 6.44, which ilustrates the real temperature measurements at point 5. As it was said before, the zero level in both cases was different. In the models (Figure 6-43), Z=0 was between the concrete slab and the top of the clay layer. Meanwhile, in the real measurements done in situ Z=0 was in the top of the concrete slab (Figure 6-44). See Appendix 2 to compare the results with the complete real temperature measurements at the different points.
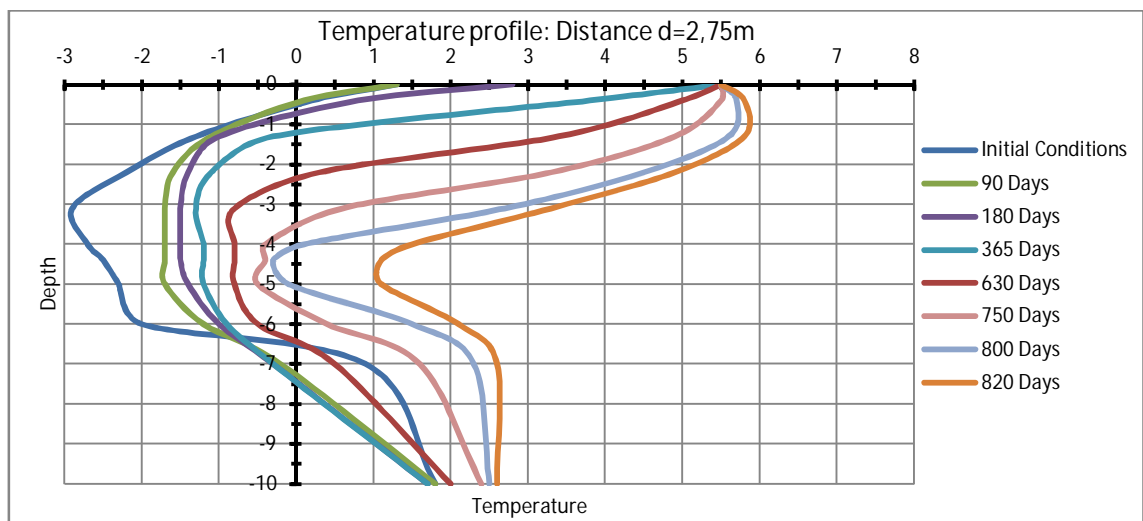
Figure 6-43. Ground temperature profile after different time steps in points located between piles (D=2,75m). Results obtained in 3D model done with SoilVision Heat
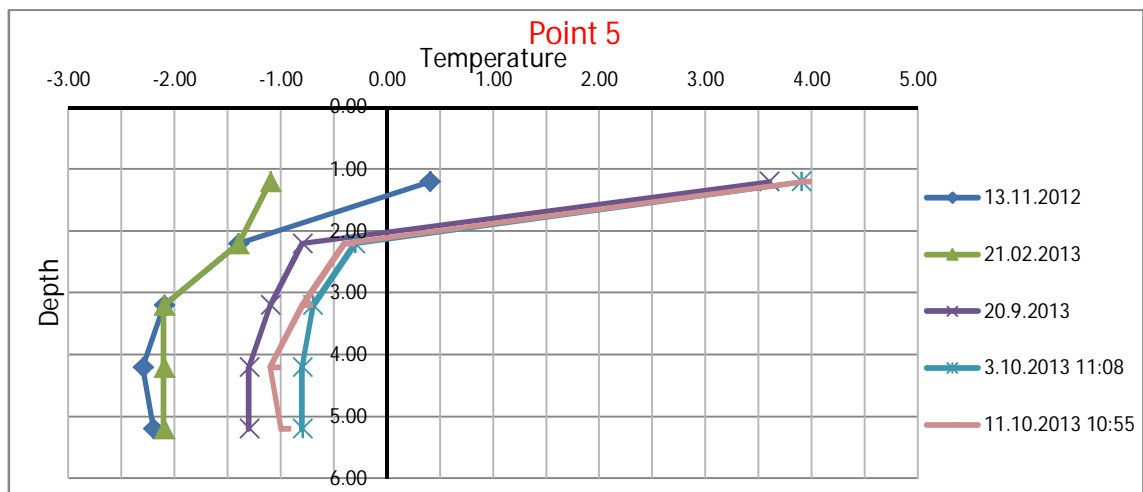
Figure 6-44. Ground temperature profile after different time steps in point number 5

The same result in a bigger scale was achieved in the 2D model carried out with SoilVision (Figure 6-45). In the 2D model, the total heat flux pumped by the piles was divided by the distance between piles (5.5m) in order to get the energy pumped per

meter. The next figure 6-45 shows the ground temperature evolution in the 2D model after different time steps.
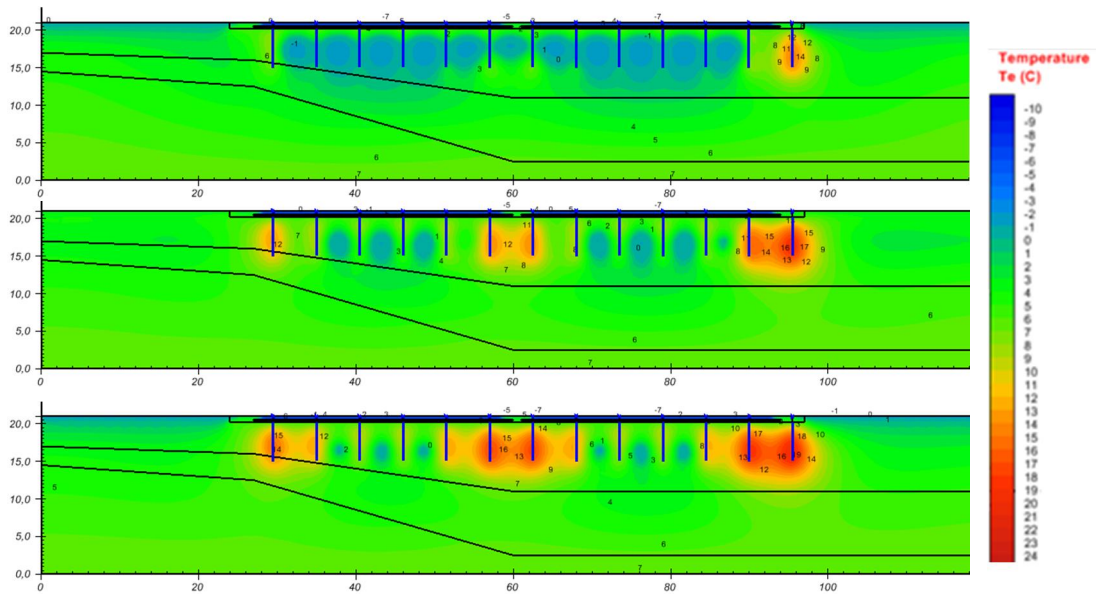
Figure 6-45. Ground temperature evolution after one year (top), 2 years (centre) and 750 days (down) pumping 112kW by the energy piles system

6.8 Modelling Results: Target Temperature

Last step of the analysis consisted in establishing a constant temperature pumped by the piles that avoid the ground surrounding them from freezing. Another objective was that the temperature pumped by the piles has to be as low as possible in order to minimize energy consumption.

To define the target temperature which prevents the ground from freezing, many models were done with different range of temperatures. The initial conditions (Figure 6-46) for these models were the soil temperature profile obtained in the previous step after 1000 days pumping 112kW.
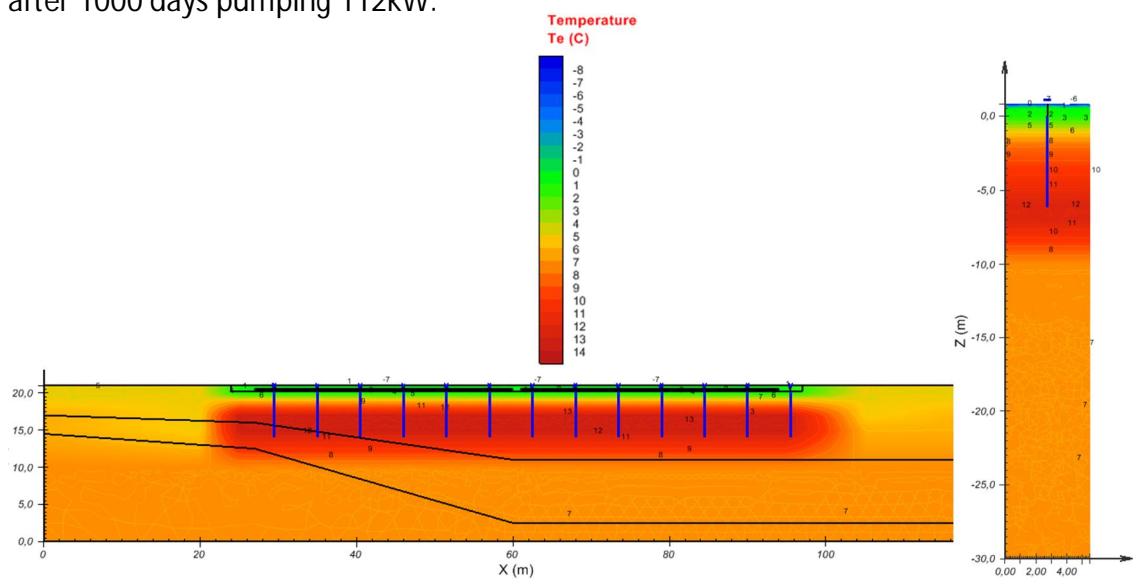
Figure 6-46. Initial condition in the 2D and 3D models for the last transient analysis

Once the new initial conditions for the new transient analysis were established, different ranges of temperatures were studied in order to get the target temperature that avoid ground freezing. The easiest way to calculate the target temperature was to start with high temperatures and go further by reducing the temperature pumped by the piles. In this way, the next temperatures were studied:

- Piles pumping heat at +20°C
- Piles pumping heat at +15°C
- Piles pumping heat at +10°C
- Piles pumping heat at +7°C

The different analysis done showed that once all the ice below the ice rink was melted, it was enough to pump heat at +7°C to avoid the ground from freezing. It is important to remind that in the models, the piles were modelled as a *well boundary condition*. It means that piles were modelled as an empty cylinder and their physical and mechanical properties were not considered. Considering this, temperature has to be at least +7°C in the border of the pile. The temperature of the liquid circulating inside the piles may be different because thermal losses through the materials of the piles were not considered in the model.

Next figure (Figure 6-47) shows temperature evolution between piles at different depths in a transient analysis pumping heat at +7°C during five years. As can be seen from the figure the steady state situation is reached after three years. If the piles pump heat at +7°C, only the ground below the concrete slab has negative temperatures.
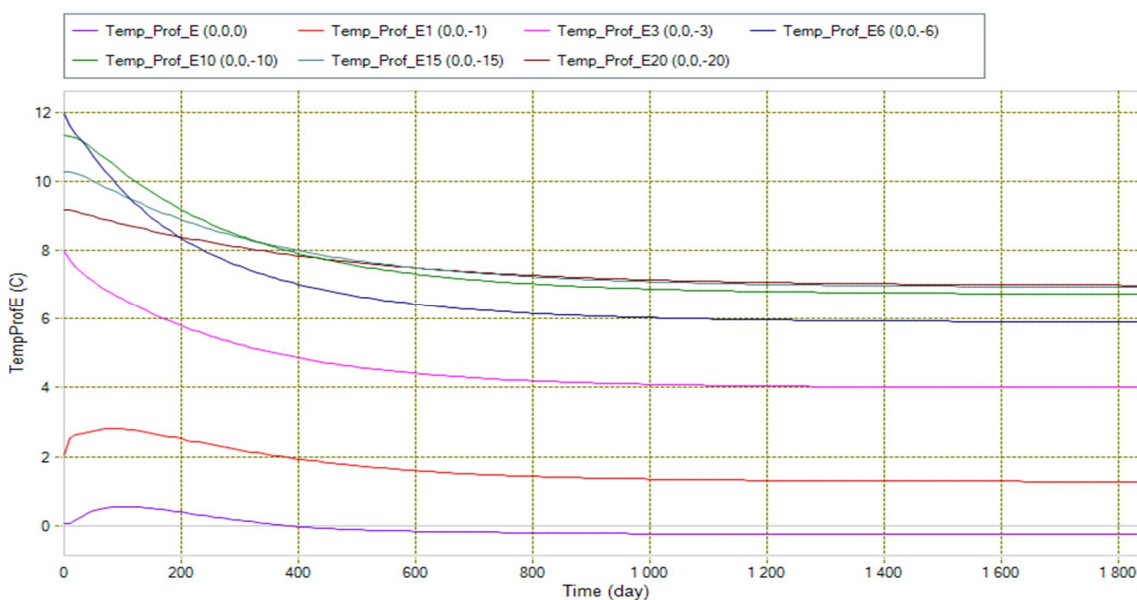
Figure 6-47. Temperature evolution between piles at different depths after five years

Comparing this situation with a point located ten centimetres from the pile border, the temperature profile evolution changes. As it is show in the next figure (Figure 6-48) if the piles pump heat at +7°C all the ground surrounding the pile has positive temperatures.
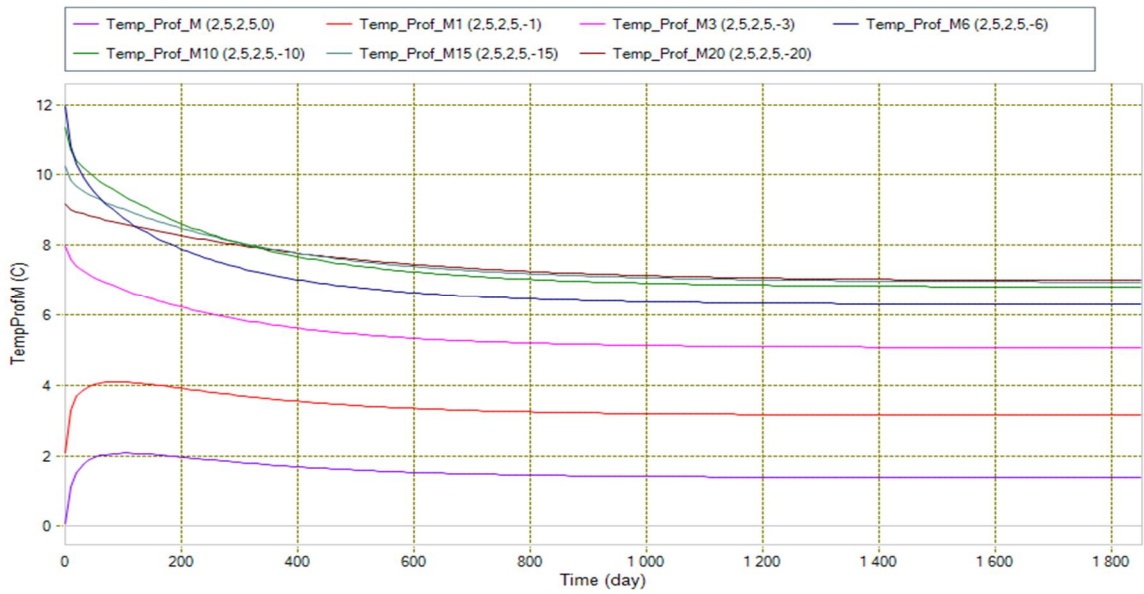
Figure 6-48. Temperature evolution in points located next to a pile at different depths after five years

Following figures show temperature profile of the ground after one year pumping heat by the energy piles at +7°C:
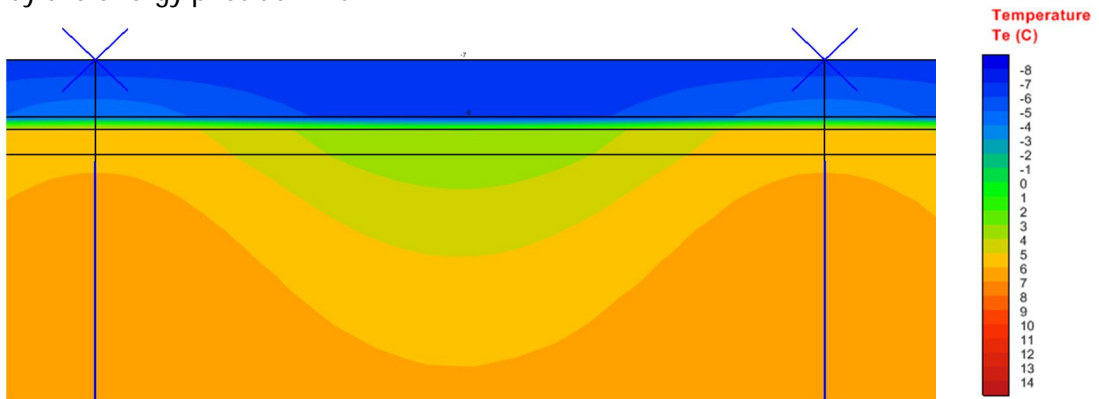
Figure 6-49. Ground temperature between piles after 1 year pumping heat at 7°C
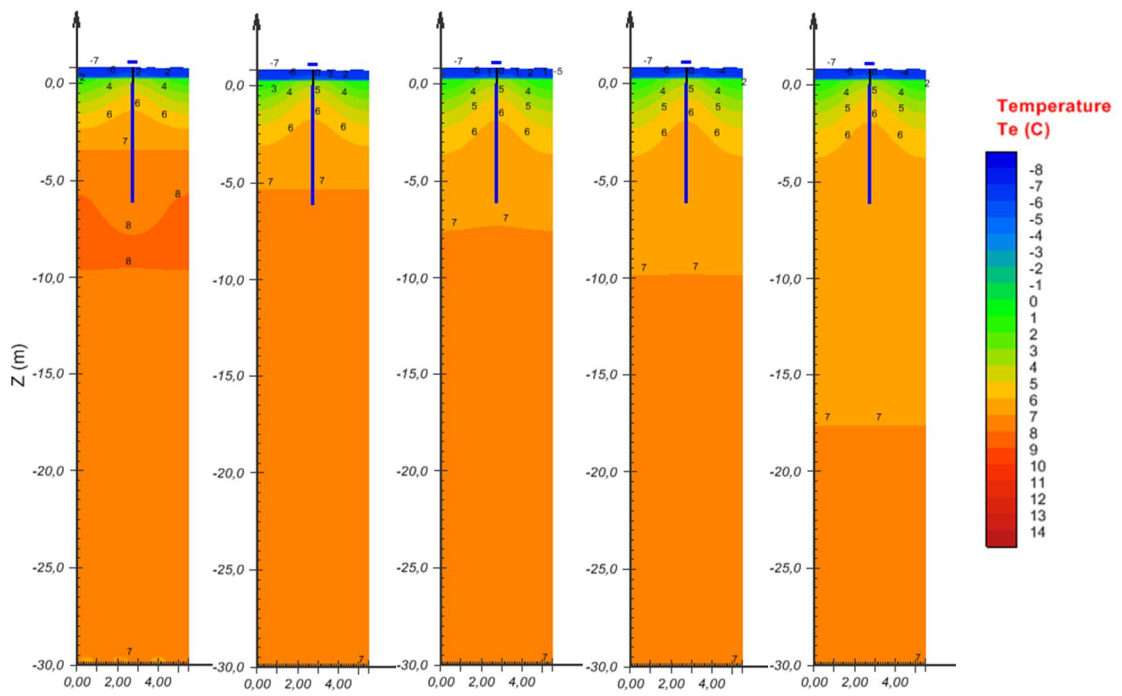
Figure 6-50. Ground temperature evolution surrounding the pile after 150 days, 300 days, 600 days, 1000 days five years
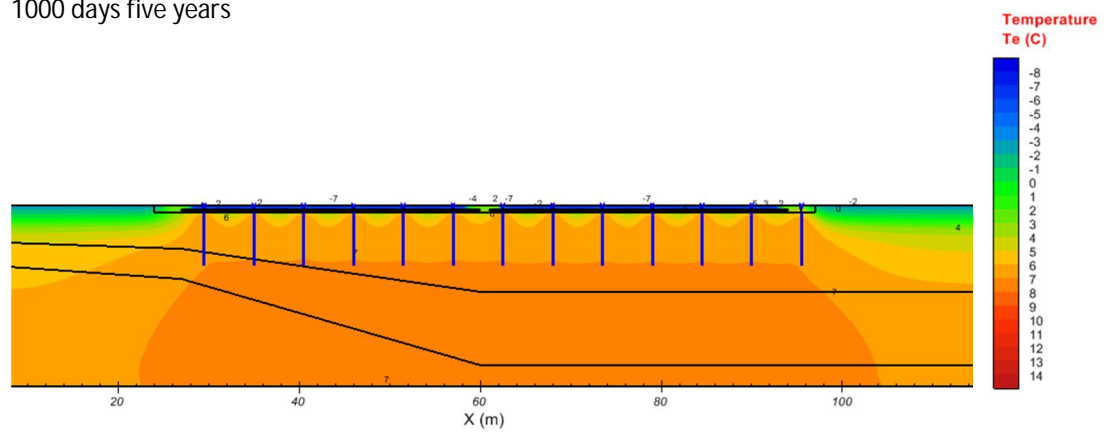
Figure 6-51. Soil profile temperature after one year pumping heat at $7^{o}C$

7 Conclusions

Numerical modelling represents and powerful tool in engineering design saving time and sources. The main purpose of this thesis was to study numerically ground thermal response to energy pile foundations and contribute to the improvement of the knowledge of ground thermal behaviour. In the cases studied, mechanical properties of the piles as well as the hydrological ground conditions were not considered. Both can affect the reliability of the results obtained. Further analysis and modelling should be done in order to determine the effect of hydrological and mechanical conditions to energy pile foundations. Multi-physical finite element modelling must be done to evaluate the structural consequences and geotechnical risks related to energy foundations under cyclic thermal loading especially if it produces any change in the effective stresses in the soil.

7.1 Kupittaa case in Turku

For energy piles foundations exists some guidance that suggests typically values for the amount of energy that can be extracted from the soil. However, these typically values are related to soil properties and ground temperatures. In Finland, due to the climatic conditions, ground temperatures are relatively low and it means that the capacity of extracting heat from the soil is lower than in other warmer countries where ground temperatures are higher.

The energy function created for the evaluation of the ground thermal behaviour was adapted to the ground conditions in Finland and it is repeated cyclically every year. Compared with Ruukki pile testing site, the energy function has high values of energy pumped during the summer time. Each pile (40 meters pile) extract every winter a total amount of energy of 3.94 MWh (Maximum heat extraction 23 W/m-pile) and pumped into the soil 2.88MWh during summer (Maximum heat pumped 32 W/m-pile). That means that exist an annual deficit of 1.047 MWh per pile that does not keep the ground thermal balance and needs to be compensated.

Short piles were planned to pump heat to the ground collected by solar panels in order to keep the thermal balance. The total estimated amount of energy pumped during the summer time by the short piles is 2.216MWh, more than the double that the energy needed to keep ground thermal balance. Moreover, the energy pumped during the summer time is heating the area few meters below the building because of the short length of the piles. This situation means that high temperatures are reached on the ground (more than +30°C) between the building and 20m below it. Meanwhile, between 35 to 40m depth, ground temperature is lower and remains almost constant with values around +5 to +7°C yearly. This high temperature differences between the top and the bottom of the piles may produce differences in the behaviour of the pile due to thermal stresses. In addition, the heat carrier fluid inside the piles, which was not modelled, can be affected by the different temperatures and modify the total amount of heat extracted. According to the results it would be better to distribute the collected solar energy between the short and long piles in order to solve this high temperature difference between the top and the bottom of the energy pile foundation.

Concerning the efficiency of the vertical insulation barrier surrounding the pile foundations, the insulation improves thermal balance in the first meters below the ground surface reducing thermal losses through the building. Ground temperature differences between with or without insulation barrier is between 1.5-3.5^{o}C depending on the depth. With the insulation barrier, temperature differences between the inner and outer part of the insulation barrier decrease with depth. The temperature difference between the insulation is around 5-10°C, having maximum values in points close to the surface. Otherwise, the effect of the insulation barrier decreases with the distance and it only affects the piles located close to building borders. Ground temperature effects of the underground insulation barrier reduce with higher distances from barrier. The effects are practically negligible in points located more than 10-15 from the insulation. In this preliminary modelling no insulation was used below the floor slab, which also could affect the thermal behaviour and the reliability of the modelling results.

7.2 Myllypuro Ice Rink in Helsinki

The study carried out had two different main objectives that have been evaluated. In first place, one of the objectives was to estimate the thaw settlement produced due to the thawing process of the frozen ground below Myllypuro ice rink. This thawing process was evaluated by the laboratory and frost cell test with undisturbed samples. In the objective of the modelling was to estimate the time needed for thawing and also to establish a needed constant temperature in the energy piles that prevents ground from freezing.

The estimations done with empirical formulations resulted that the maximum thawing settlement should be around 1,8m within 6.6 meters frost depth (27% of the total depth). Meanwhile, the total settlement estimated with the test done in the frost cell test was 1,84m (28% of the total depth). The results in both cases of the total settlement down to 6.6m depth were similar. Yet there are some points which have to be considered further. The result of the thawing settlement was overestimated compared to the results of the empirical formulations with the tests done in the frost cell at different depths when the water content was higher than 80%. The same conclusion was achieved by comparing the density of the samples, overestimated thawing settlements calculated with the empirical formulations when the density is lower than 1,5T/m^3. Because of this and depending on the depth of the frozen front, the settlement produced in some points may be different than the estimated with the empirical formulations. The frost depth was not constant below the ice rink and because of it, differential thaw settlements will appear depending on the frost depth and the percentage of thawing settlement calculated in the frost cell test.

Concerning the modelling, the first step of the model studied in the evaluation of the melting process. The results of the different models showed:

- SoilVision Constant Temperature BC [SV-CTBC]: The frozen soil below Myllypuro ice rink needs between 400 to 500 days to melt completely if a constant temperature boundary condition was applied in the border of the

piles. This approximation did not consider the effect of the pile materials, the energy losses through them and the time needed to reach the steady state condition.

- SoilVision Constant Heat Flux BC [SV-CHFBC]: If a constant heat flux boundary condition was applied, the time needed for the complete melting of frozen ground increases up to 750-800 days. This result is closer to the preliminary calculations done.
- Temp/W Constant Temperature BC applied in two points inside the pile [TW-CTBC-2P]: This model studied the radial melting process. The expected time that is needed to melt completely the frozen ground in Myllypuro was around 800 days, closer to the preliminary calculations.
- Temp/W Constant Temperature BC applied in the border of the pile [TW-CTBC-BP]: The expected time that is needed to melt completely the frozen ground in Myllypuro was around 500 days, closer to the results obtained in the model [SV-CTBC].

Compared with the real temperature measurements, the models carried out represent a good approximation of the real situation, even though the accuracy of the in situ temperature measurements was not very reliable. The modelling results obtained could be affected by the existence of water flow, the water table level and possibly by the presence of air between the concrete slab and the soil due to the thawing settlement. In addition, some parameters that have not been calculated, such as the unfrozen water content curves, could affect the final results obtained in the modelling. Because of this, it is important to monitor the melting process of the frozen ground below the ice rink by checking the in situ temperature measuring points occasionally in order to have real data of the melting process.

Once the ground below Myllypuro ice rink have melted, the models showed that pumping heat of $+7^{\circ}$C is enough to prevent ground from freezing again. The temperature boundary condition was applied in the border of the energy pile, so thermal losses through the pile or the hydraulic circuit were not taken into account. Preventing the ground surrounding the piles from freezing was another of the main objectives in this studied case. Because of this, in the future it would be important to monitor ground temperatures with the measuring points located below the ice rink in order to check if the ground temperature remains above 0°C. A monitoring program establishment of the ground temperatures is recommended.

References

Amatya, B.L., Soga, K., Bourne-Webb, P.J., Amis, T., Lalui,L. (2011) Thermo-mechanical behavior of energy piles. *Géotechnique* 62, No. 6, 503-519.

Andersland, Orlando B. & Ladanyi, B. (1994) *An introduction to Frozen Ground Engineering.* New York, Chapman & Hall.

Bhalchandra V.K. & Robert M.D. (1982). *Heat Transfer.* 2nd Edition. St. Paul, West Publishing Company.

Boënnec, O. (2009). *"Piling on the energy" Geodrilling int.,* (150), 25-28

Brandl, H. (2006). Energy foundations and other thermo-active ground structures. *Géotechnique* 56, No. 2, 81-122.

Brandl, H. (2013). Thermo-Active Ground-Source Structures for Heating and Cooling. *Procedia Engineering* 57, 9-18

Banks, D. (2008). *An introduction to thermo-geology: Ground source heating and cooling.* Blackwell Publishing, Oxford.

Clauser, C. (2006). Geothemal Energy. In: K. Heinloth (ed), *Landolt-Börnstein, Group VIII: advanced Materials and Technologies, Vol. 3: Energy Technologies, Subvol. C: Renewable Energies,* Springer Verlag, Heidelberg-Berlin, 493-604.

Clauser, C. (2009). Heat Transport Processes in Earth's crust. AA(Institute of Applied Geophysics and Geothermal Energy, E.ON Energy Research Center, RWTH Aachen University). *Surveys in Geophysics*, Volume 30, Issue 3: 163-191

De Vries, D. A. (1963) Thermal properties of soils. In Physics of Plant Environment (W.R. Van Wijk, Ed.). Amsterdam: North-Holland Publishing Company.

Farouki, O. T. (1986). *Thermal properties of soils,* Series on Rock and Soil Mechanics, Vol. 11. Clausthal-Zellerfeld: Trans Tech Publications.

GSHPA (2012) Thermal pile design, installation and materials standard, Ground Source Heat Pump Association, Milton Keynes, October 2012.

Geothermal Energy Association (2012). *Geothermal Basics: Q&A.* Geothermal Energy Association

Ghildyal, B.P. & Tripathi R.P. (1987). *Soil Physics.* New Delhi, Wiley Eastern Limited.

Goldstein, B., G. Hiriart, R. Bertani, C. Bromley, L. Gutierrez-Negrin, E. Huenges, H. Muraoka, A. Ragnarsson,J. Tester, V. Zui, (2011). Geothermal Energy. In IPCC Special Report on Renewable Energy Sources and Climate Change Mitigation [O. Edenhofer, R. Pichs-Madruga, Y. Sokona, K. Seyboth, P. Matschoss, S. Kadner, T. Zwickel,P.

Eickemeier, G. Hansen, S. Schlomer, C. von Stechow (eds)], Cambridge University Press, Cambridge, UnitedKingdom and New York, NY, USA.

Google Maps. *Myllypuro ice rink, Helsinki.* [Online] Available from: https://maps.google.es/

Helsingin kaupunki, Kiinteistövirasto, Geotekniikka (2009). Rakennettavuusselvitys Myllypuron Jäähalli. Tarkkailumittauspisteiden sijainti. 1:500. Helsinki

Helsingin kaupunki, Kiinteistövirasto, Geotekniikka (2009). Pohjatutkimuskartta ja leikkaukset. Myllypuron Jäähalli. 1:500. Helsinki

Johansen, O. (1975). Thermal conductivity of soils, Ph.D. thesis, Trondheim, Norway. (CRREL Draft Translation 637, 1977). ADA 044022

John E. Mock, Jefferson W. Tester, and P. Michael Wright (1997) GEOTHERMAL ENERGY FROM THE EARTH: Its Potential Impact as an Environmentally Sustainable Resource. *Annual Reviews Energy Environmental*, 22:305-356

Johnston, I.W., Narsilio, G.A., Colls, S. (2011) Emerging Geothermal Energy Technologies. *KSCE Journal of Civil Engineering*, 15(4), 643-653

Kalandtidou, A., Tang, A.M., Pereira, J.-M. and Hassen, G. (2012) Preliminary study on the mechanical behavior of heat exchanger pile in physical model. *Géotechnique* 62, No. 11, 1047-1051.

Kersten, M. S. (1949). Laboratory research for the determination of the thermal properties of soils. ACFEL Technical Report 23. AD 712516. (Also Thermal properties of soils. University of Minnesota Institute of Technology, Engineering Experiment Station Bulletin No. 28)

Kesti, J., Ruuki. (2012). *Energy pile testing station results.* Zero energy solutions for Multi-functional Steel intensive commercial Buildings. Work Package No WP5.2

Kersten, M.S. (1952) Thermal properties of soils. Highway Research Board Special Report 2, p. 161-166.

Lee, Seung Rae (2009). *Energy Piles - Piles as Heat Exchangers* -. [Presentation] Department of Civil and Environmental Engineering, KAIST, 11th December.

Liu, B & Li, D., (2012). A simple test method to measure unfrozen water content in clay-water systems. *Cold Regions Science and Technology*, 78 (2012), 97-106

Llopis Trillo, G., and Rodrigo Angulo, V., (2010). Guía para la Energía Geotérmica. Fundación de Energía de la Comunidad de Madrid

Loveridge, F. (2012). *The Thermal Performance of Foundation Piles used as Heat Exchangers in Ground Energy Systems.* Doctoral Thesis. University of Southampton.

Loveridge, F. Amis, T. and Powrie W., (2012) Energy pile performance and preventing ground freezing. In, *2012 International Conference on Geomechanics and Engineering (ICGE'12), Seoul, KR,*

Lu, S., Ren, T., Gong, Y., and Horton, R. (2007). An improved model for predicting soil thermal conductivity from water content at room temperature. SSSAJ 71 (1): 8-14

Myllypuro Jäähalli (2012). *Peruskorjaus Kuvagalleria.* [Online] 10.7.2013 Available from: http://www.myllypuronjaahalli.fi/Pages/Peruskorjauskuvagalleria.aspx

Mehto (2010). *Myllypuron Jäähalli Ratasmyllynkuja 1.* 1:10. Helsinki

Mehto (2010). *Nuorisojääkenttä OY / Myllypuron Jäähalli Ratasmyllynkuja 1.* 1:100. Helsinki

Nyholm, V. (2011). Energiapaalujen hyödyntäminen taloteknisissä konsepteissa. Master Thesis, Aalto University.

Nurmikolu, A. (2006). Ratarakenteessa käytettävien kalliomurskeiden hienominen ja routimisherkkyys. Ratahallintokeskuken julkaisuja A 9/2006. Ratahallintokeskus, Helsinki. 170s. 6liites

Onninen, H. (1999). *Frost heave test and Thaw compression test.* Method description TPPT-R07. VTT Communities and Infrastructure. Espoo. 21s.

Paudel, B. and Wang, B. (2010). Freeze-thaw effect on consolidation properties in fine grained soils from the Mackenzie valley, Canada. *In: GEO2010: 63rd Canadian Geotechnical Conference in Calgary, Alberta, GEO2010,12-16 Sep 2010, Calgary, Canada.*

Phukan, A. (1985) *Frozen Ground Engineering.* New Jersey, PRENTICE-HALL, INC ., Englewood Cliffs.

Rees, S. W., Adjali, M. h., Zhou, Z., Davies, M. & Thomas, H. R. (2000). Ground heat transfer effects on thermal performance of earth-contact structures. *Renowable Sustainable Energy Rev.* 4, No. 2, 213-265.

Ruukki (2012). White Paper: Energiapaaluilla energia-tehokkaota rakennuskia.

Saaralainen, S. (1992). *Modelling frost heaving and frost penetration in soils at some observataions sites in Finland. The SSR model.* Doctoral Thesis. Tampere University. VTT Publications 95

Sanner, B. (2005). Examples of GSHP and UTES Systems in Germany. In: Proceedings World Geothermal Congress 2005 Antalya, Turkey, 24-29.

SFS-EN ISO 13793:2001. Thermal performance of buildings. Thermal design of foundations to avoid frost heave

SFS-EN ISO 14688-2:2005. Geotechnical investigation and testing. Identification and classification of soils. Part 2: Principles for a classification

Speer, T. I., G.H. Watson and R.K. Rowley, (1973). Effects of Ground Ice Variability and Resulting Thaw Settlements on Buried Warm Oil Pipelines, North Am. Contrib. Proc. 2nd. Int. Permafrost, Yakutsk, U.S.S.R., National Academy of Science, Washington, pp. 746-751.

Suryatriyastuti, M.E., Mroueh, H., Burlon, S. (2011) Thermo-mechanics behaviour of energy pile subjected by monotonic loading. *Colloque Euro-Méditerranée.* AFM, Maison de la Mécanique, Courbevoie, France.

Sundberg, J. (1988) *Thermal Properties of Soils and Rocks.* Linköping, Swedish Geotechnical Institute, Report No 35

SoilVision Verification manual, (2012). SoilVision Systems Ltd. Saskatoon, Saskatchewan, Canada.

SoilVision Heat theory and tutorial manual, (2012). SoilVision Systems Ltd. Saskatoon, Saskatchewan, Canada.

Tang, A. Cui, Y., and Lee, T. (2008). A study on the thermal conductivity of compacted bentonites. Applied clay science, 41: 181-189

Uotinen, V-M. (2012). Geothermal – Geotechnical coupled structures – Situation in Finland. Shallow Geothermal Energy application in Civil Engineering IV YELGIP Workshop, 5-6th July, Darmstadt, Germany.

Uotinen, V-M., Repo, T. & Vesamaki, H., (2012). Energy piles – ground energy systems integrated to steel foundations piles. In: NGM 2012 Proceedings of the 16th Nordic Geotechnical Meeting, Tivoli Congress Center, Copenhagen, Denmark, 837-844.

Vähäaho, Ilkka (1989). *The Effects of thaw consolidation on geotechnical properties of clay.* Geotechnical Department, City of Helsinki. Report number: 51.

Vähäaho, I., V. Lappalainen and H. Ryhäanen, (1989a). Thaw consolidation of frozen clays of post-glacial origin in Helsinki. Proc.INt.Symp.Frost in Geotechnical Engineering, Saariselkä, Finland, Vol.2 (ed. H. Rathmayer, Technical Research Center of Finland VTT), Espoo. pp.583-600

Vähäaho, I., Koskinen, M. and Uotinen, V-M. (2012). Suomen Paksuin ikirouta. *GeoFoor* 38, 17-21.
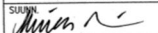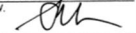
Wendell A., Duffield and John H. Sass (2003) *Geothermal Energy-Clean Power From the Earth's Heat.* U.S. Department of the Interior. U.S. Geological Survey. Circular: C1249

Watson, G.H., W. A. Slusarchuk, and R.K. Rowley, (1973). Determination of some Frozen and Thawed Properties of Permafrost Soils, Can. Geotech. J., 10: 592-606

Appendix 1. Soil profile sections

Section C-C′

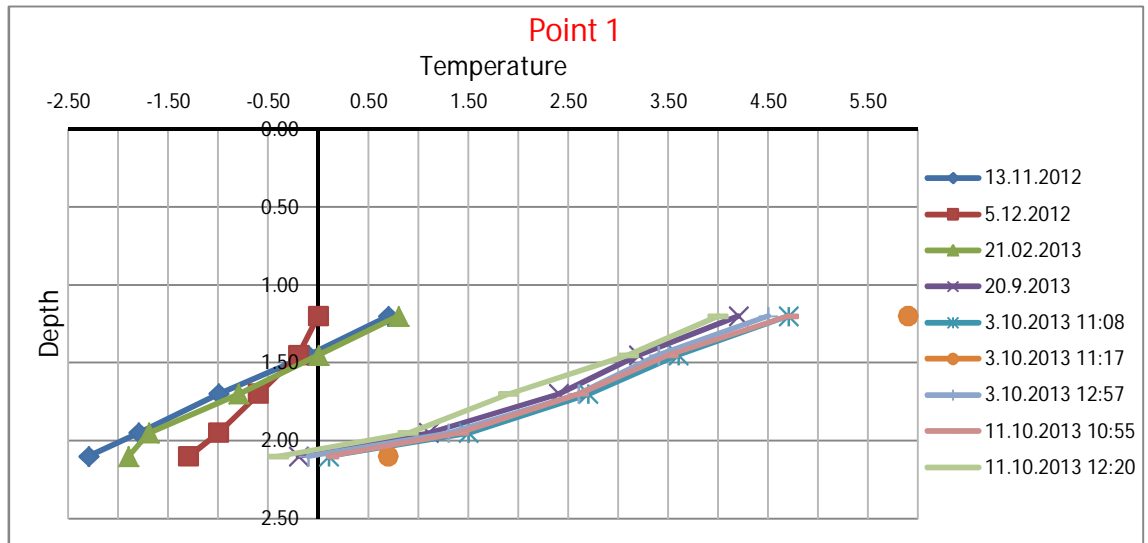Section A-A'

Appendix 2. Weight sounding diagrams

Weight sounding diagram 1 [WSD-1]
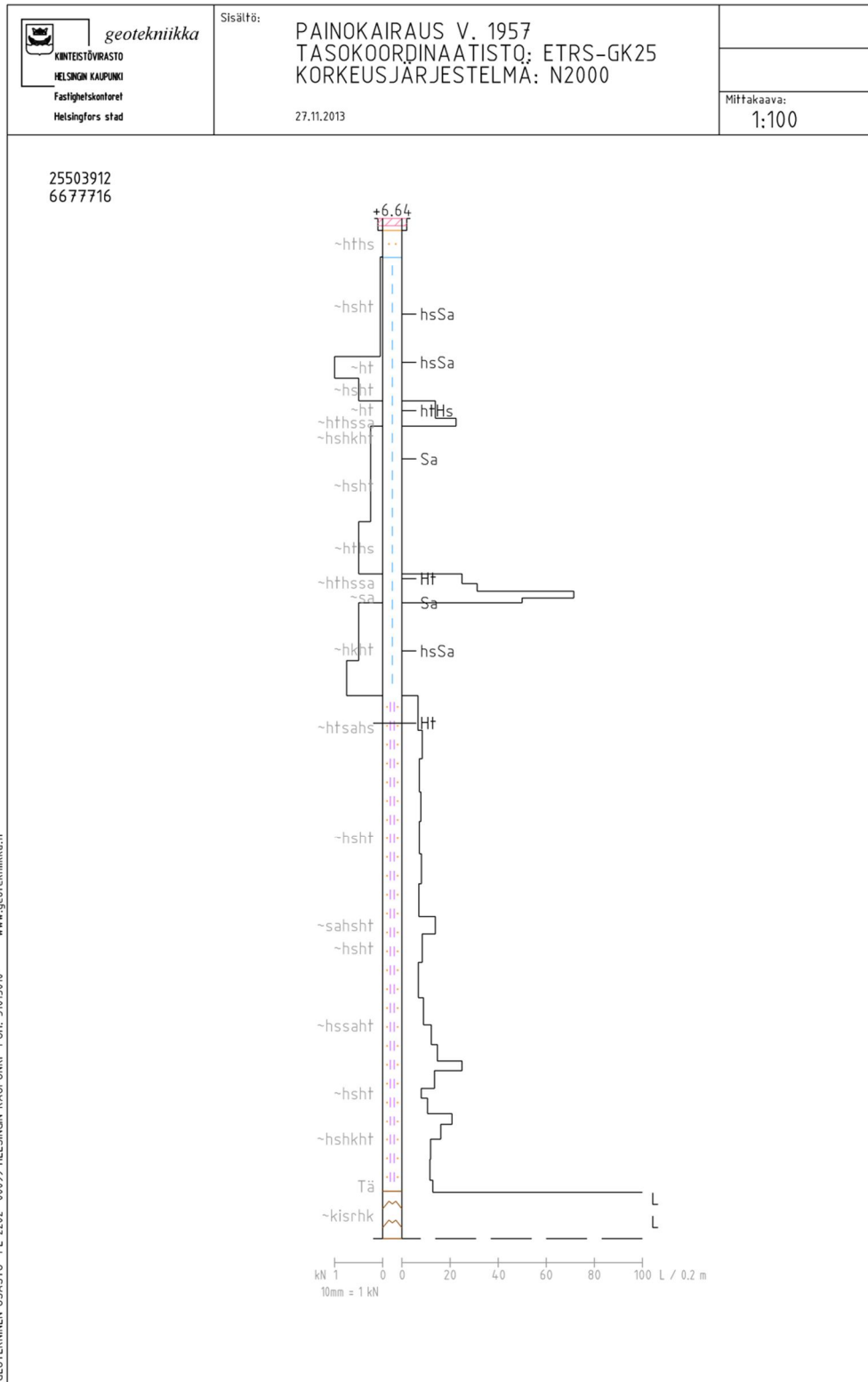
Weight sounding diagram 2 [WSD-2]
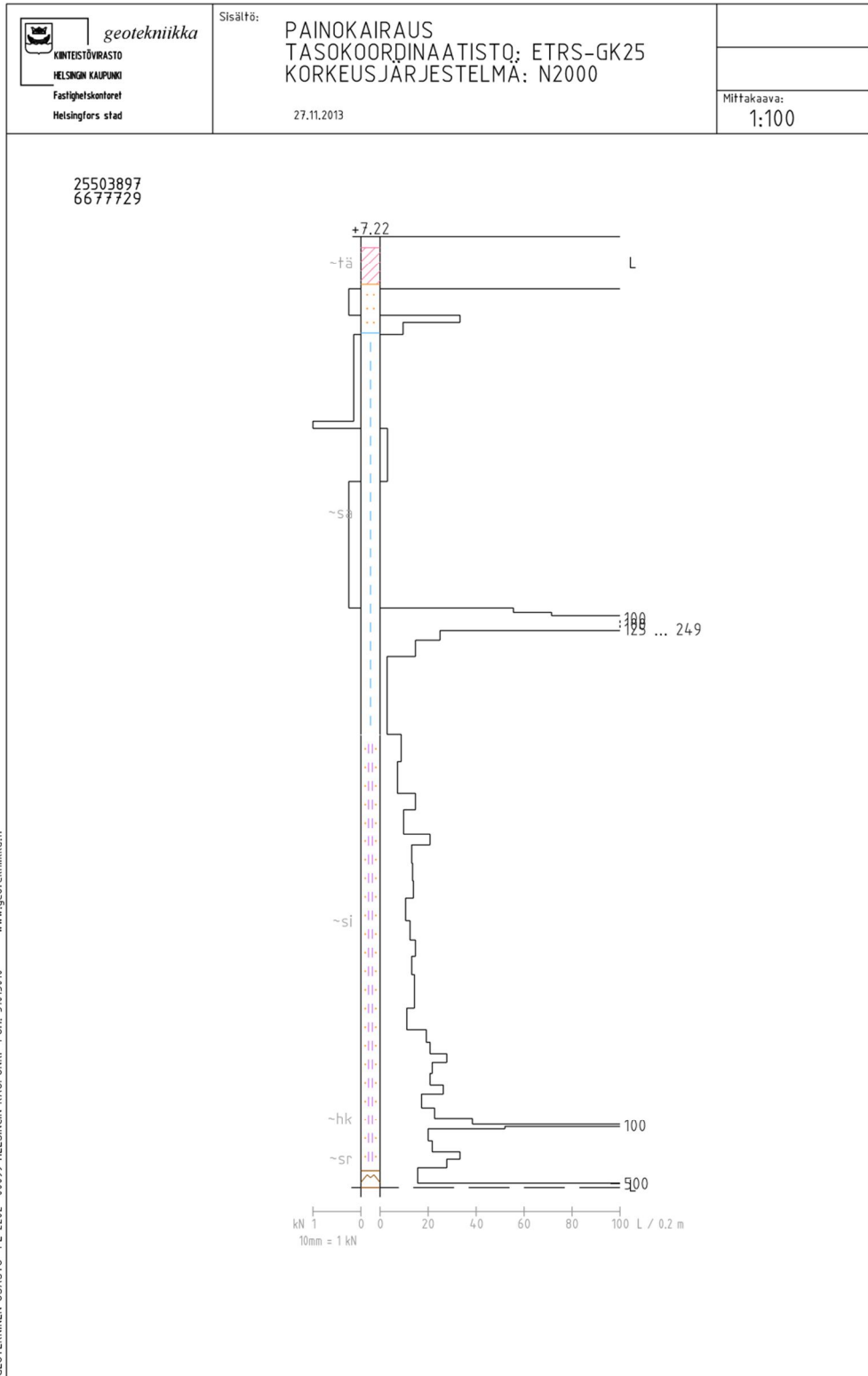
Weight sounding diagram 3 [WSD-3]
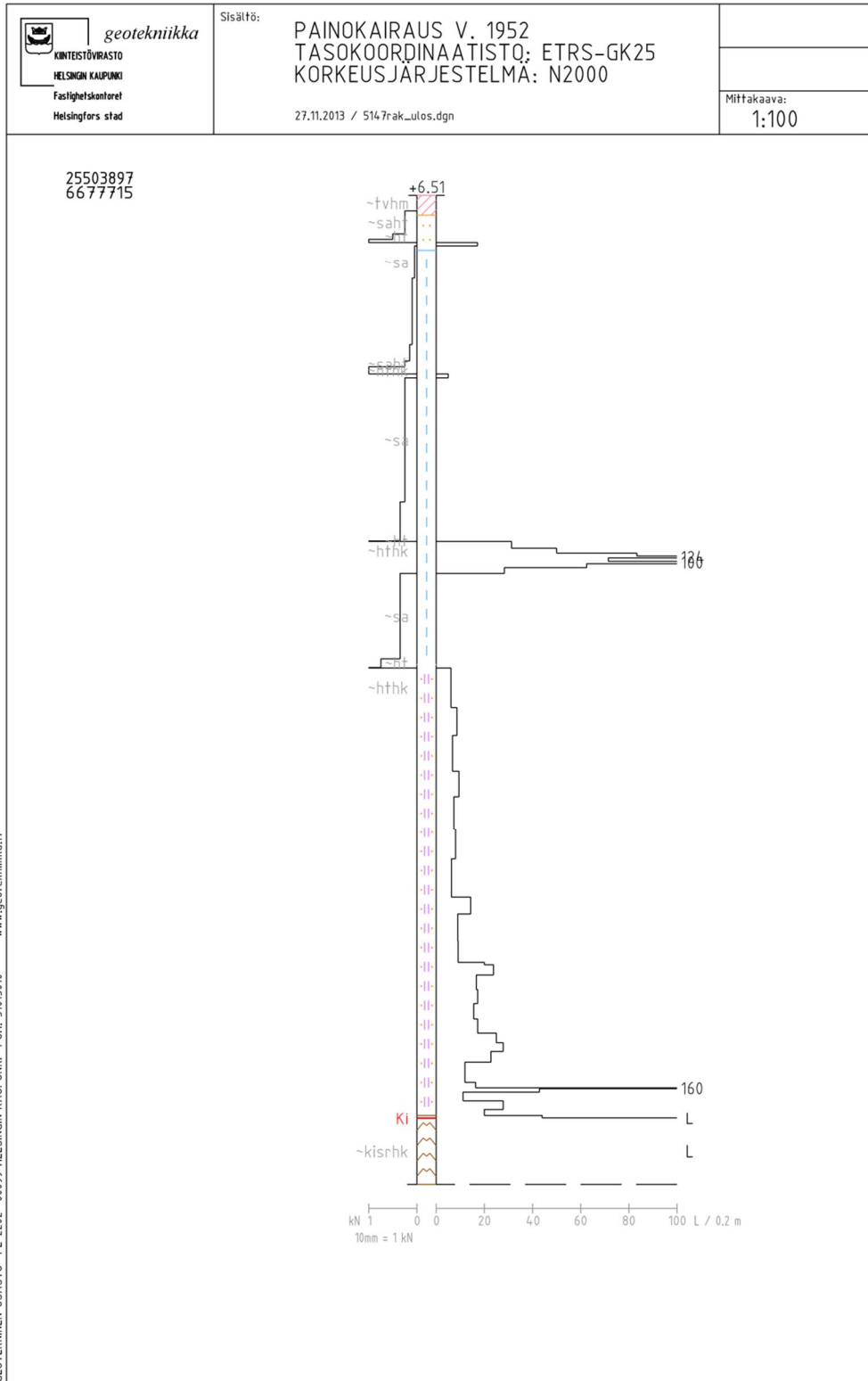
Appendix 3. Temperature readings in Myllypuro ice rink

Point 1

Temperature

Depth

Legend:
- 13.11.2012
- 5.12.2012
- 21.02.2013
- 20.9.2013
- 3.10.2013 11:08
- 3.10.2013 11:17
- 3.10.2013 12:57
- 11.10.2013 10:55
- 11.10.2013 12:20

Point 2

Temperature

Depth

Legend:
- 13.11.2012
- 5.12.2012
- 21.02.2013
- 20.9.2013
- 3.10.2013 11:08
- 3.10.2013 11:17
- 3.10.2013 12:17
- 11.10.2013 10:55
- 11.10.2013 12:20

Point 3

Temperature

Depth

Legend:
- 13.11.2012
- 5.12.2012
- 21.02.2013
- 20.9.2013
- 3.10.2013 11:08
- 3.10.2013 11:17
- 3.10.2013 12:17
- 11.10.2013 10:55
- 11.10.2013 12:20

Point 4

Point 5

Point 6

Appendix 4. Frost cell test results: Sample height evolution

Sample 2 (Depth 1,2 m)

Sample 3 (Depth 2,6 m)

Sample 4 (Depth 3,6 m)

Sample 1 (Depth 4,7 m)

Sample 5 (Depth 5,6 m)

Sample 6 (Depth 6,6 m)
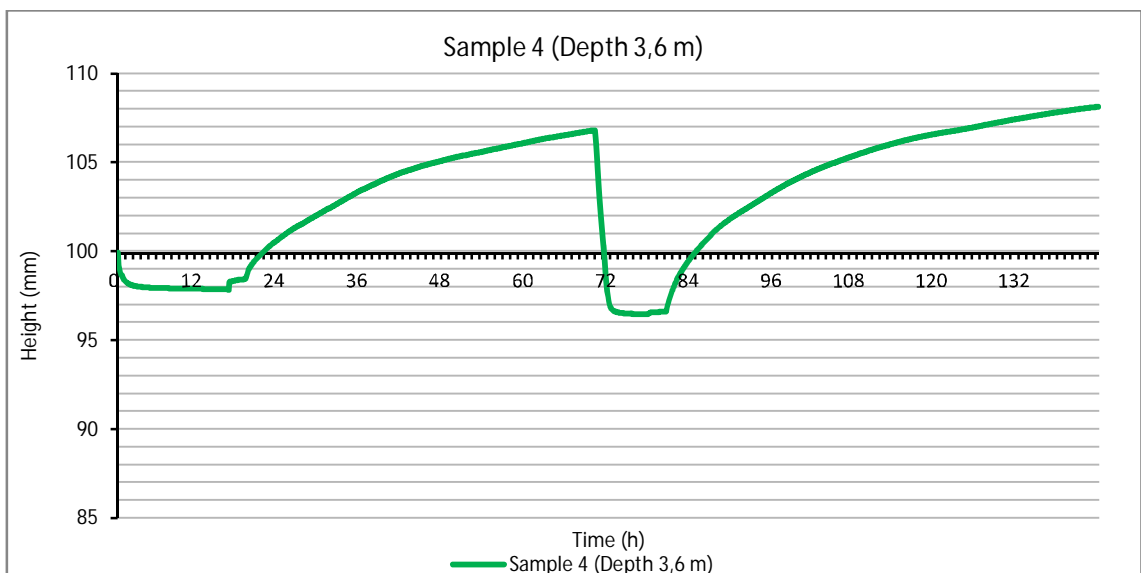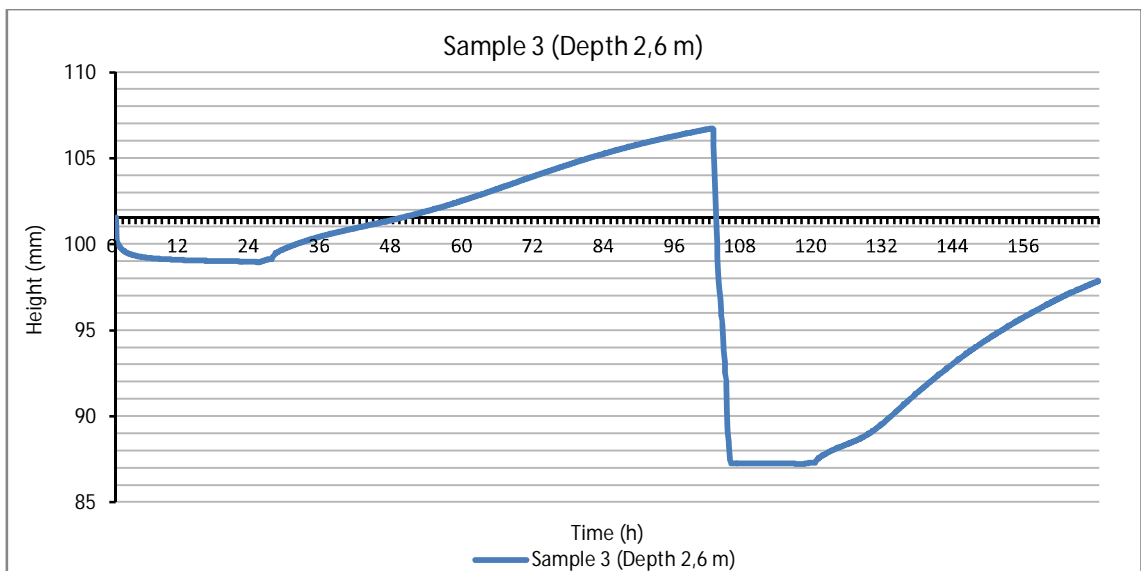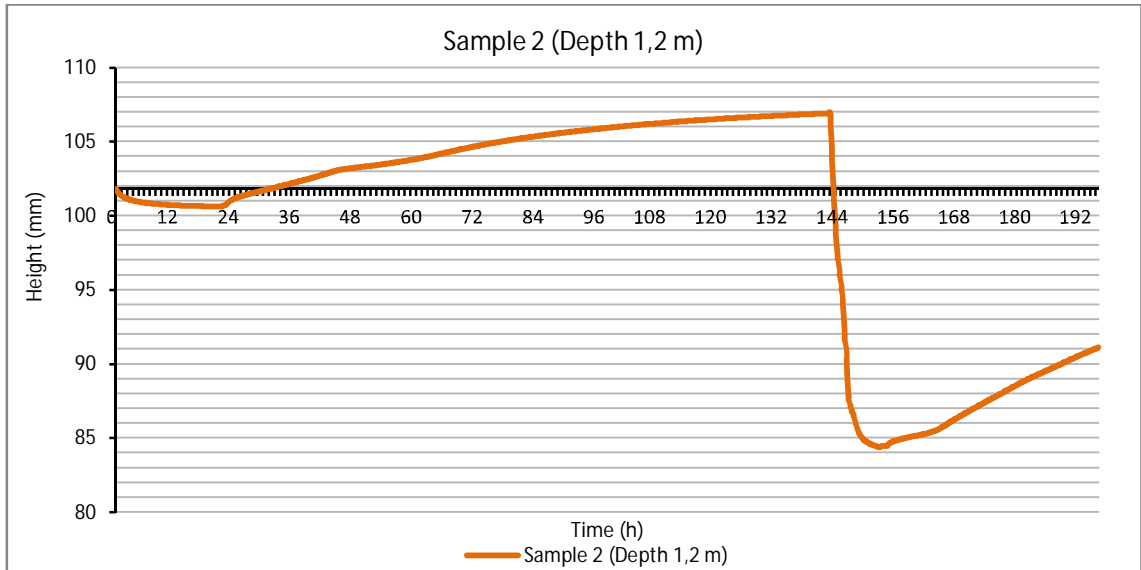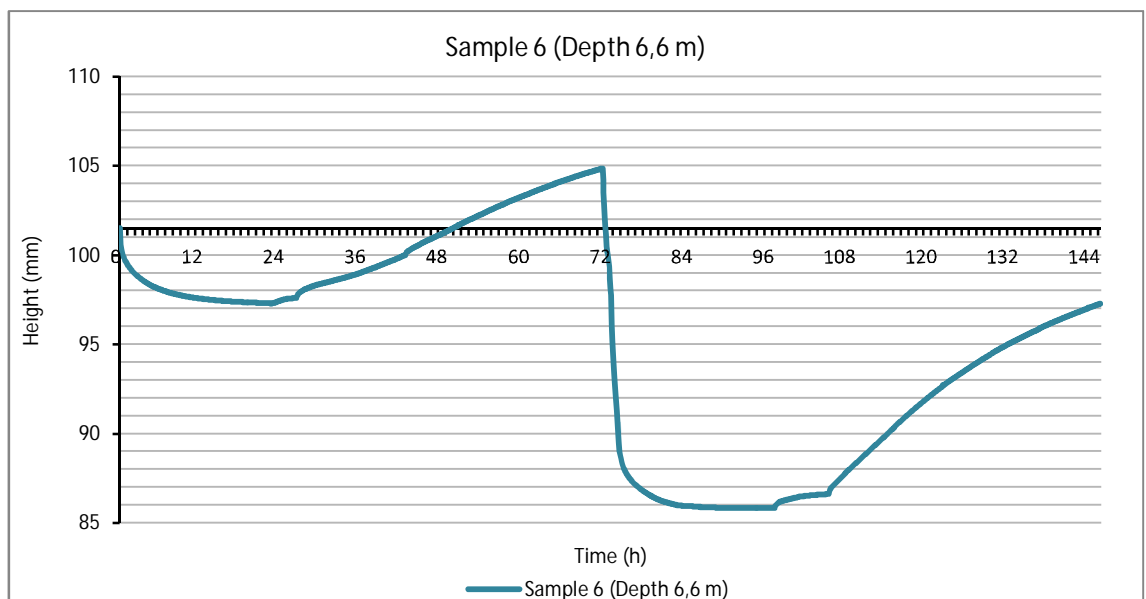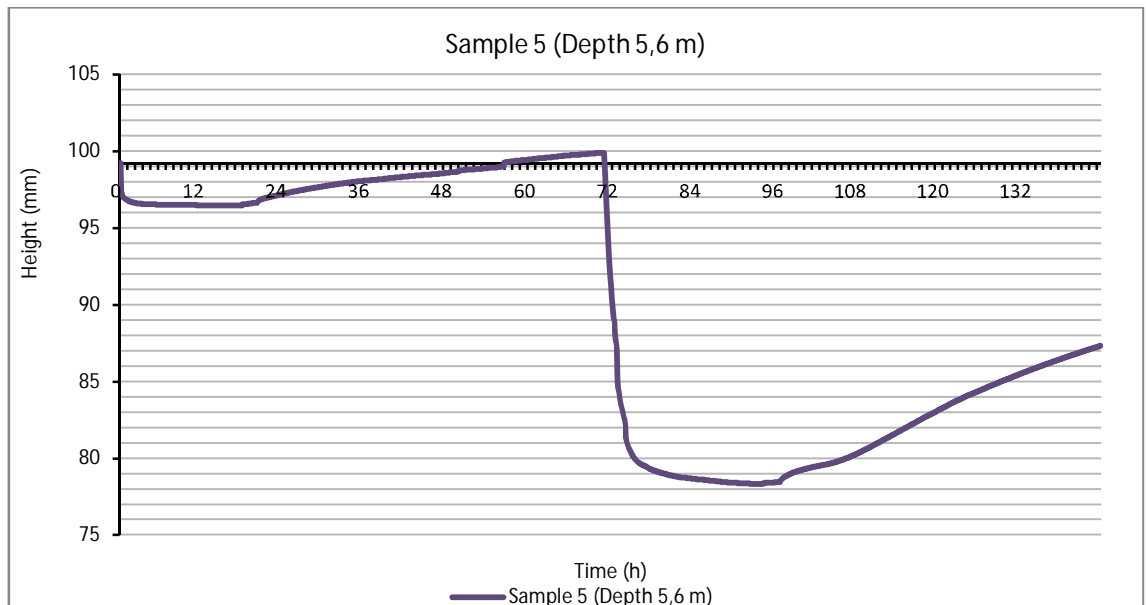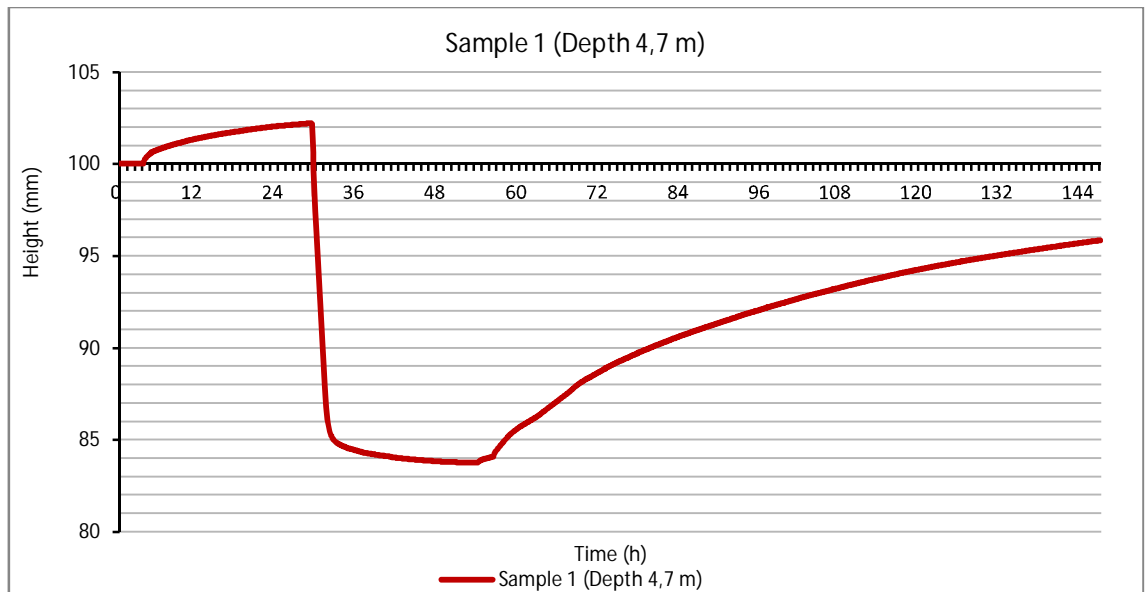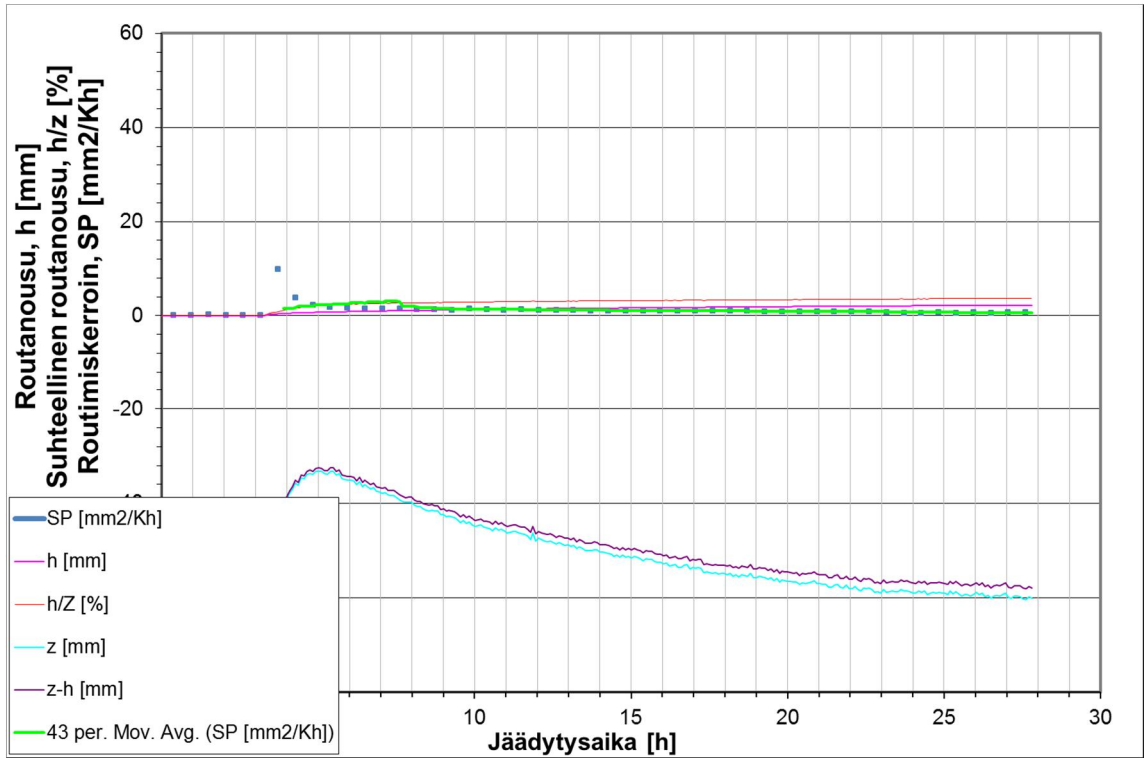
Test 1, loaded (s = 35kPa), 4,7m depth.
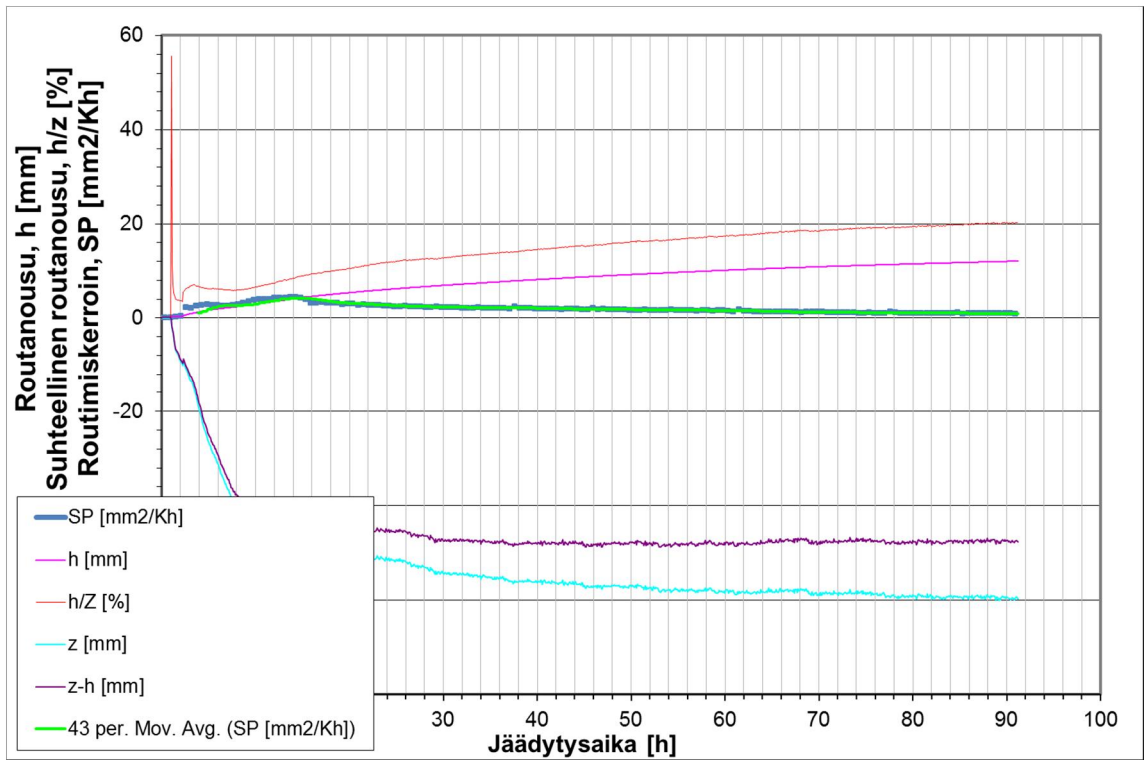
Test 1, unloaded (s = 0kPa), 4,7m depth.
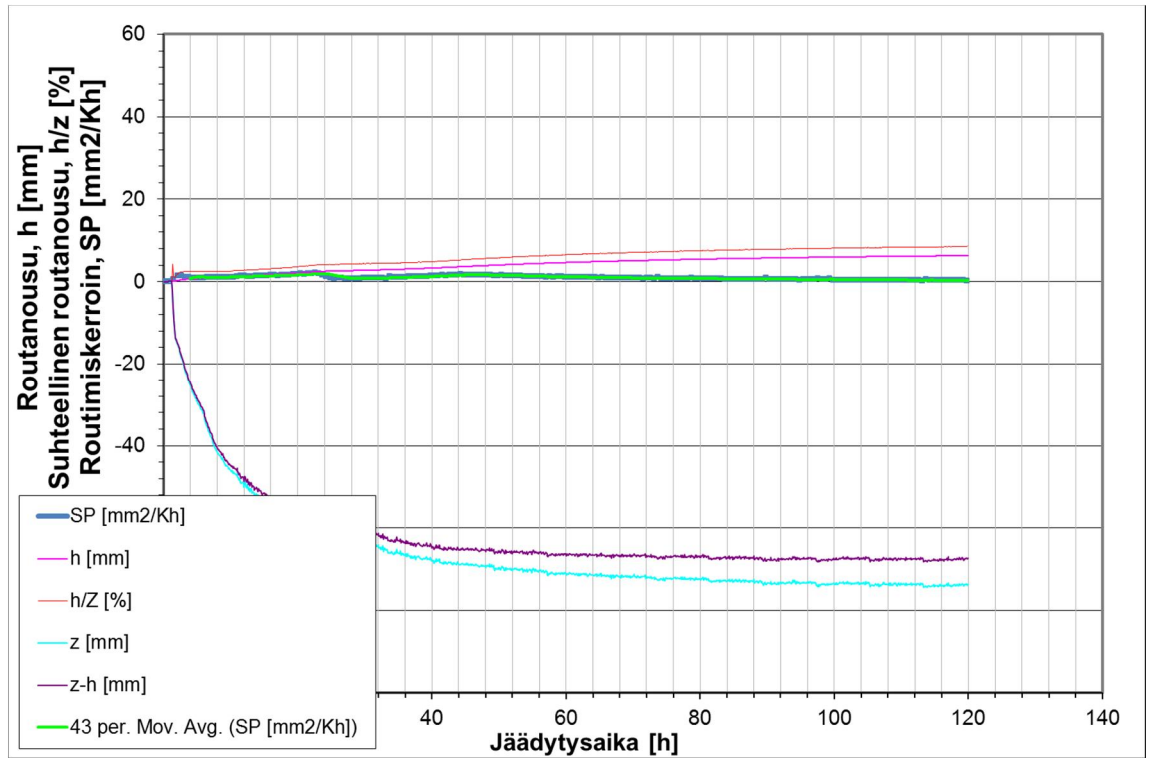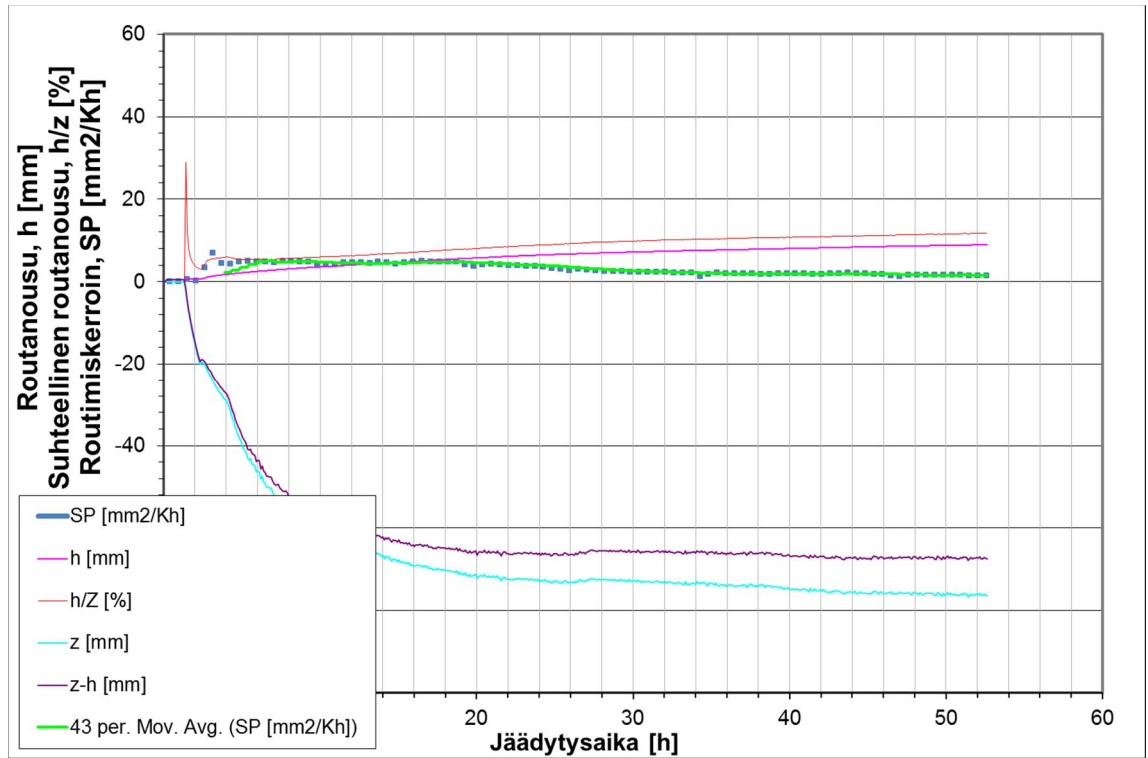
Test 2, loaded (s= 20kPa), 1,2m depth.
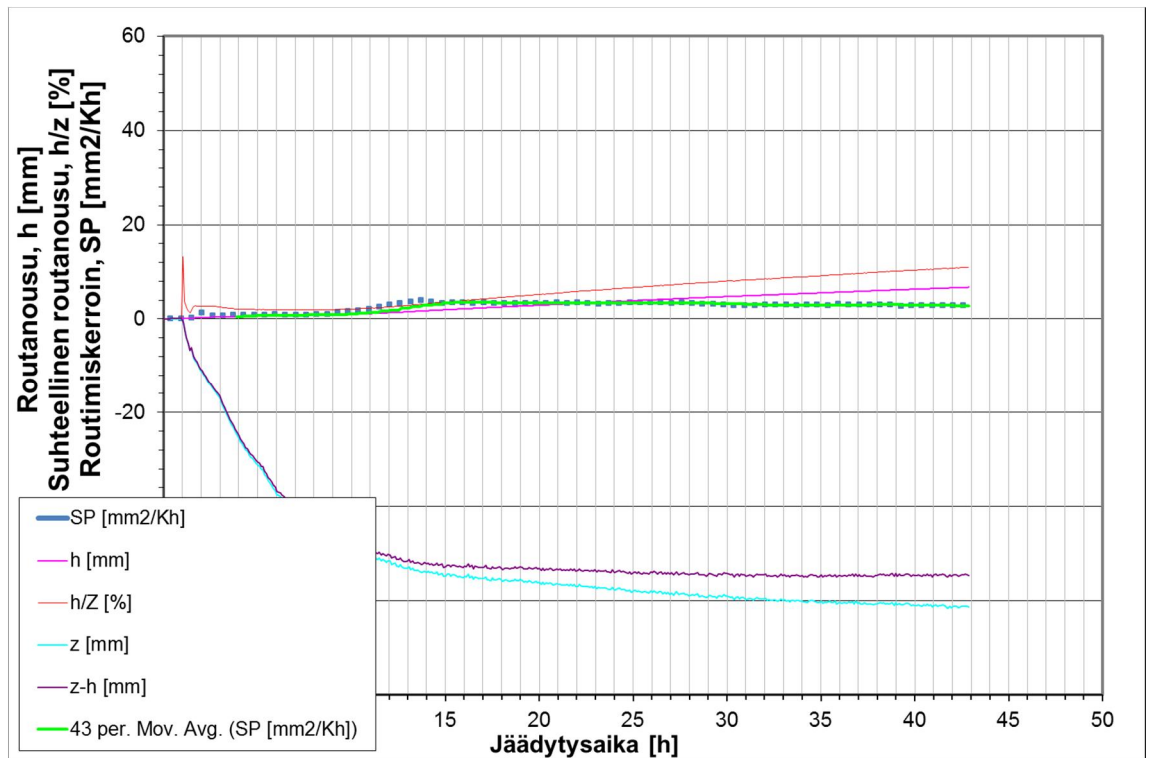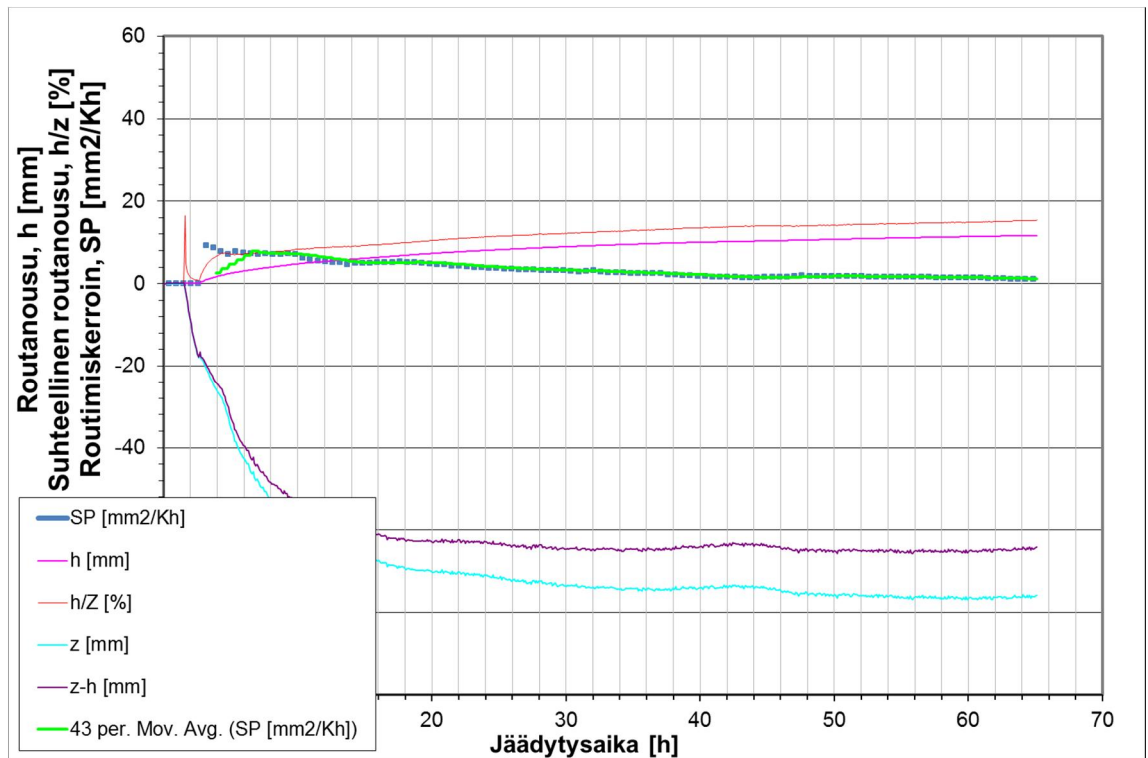

Test 2, unloaded (s= 0kPa), 1,2m depth.
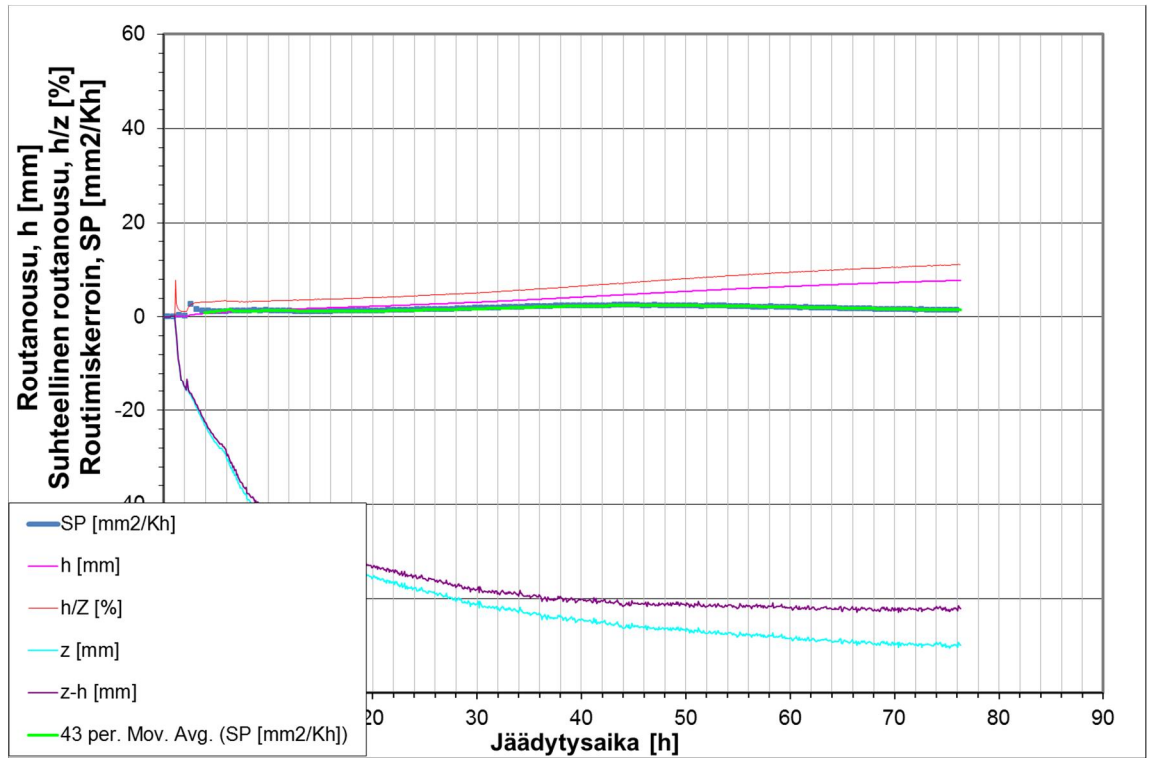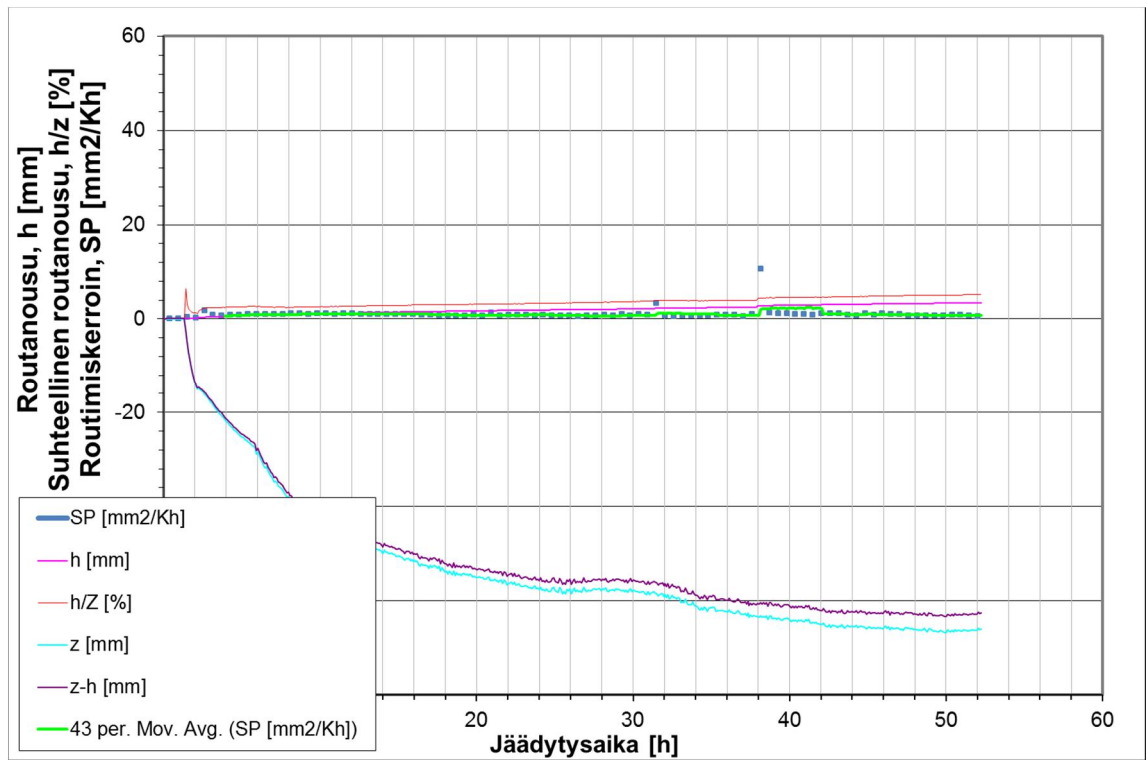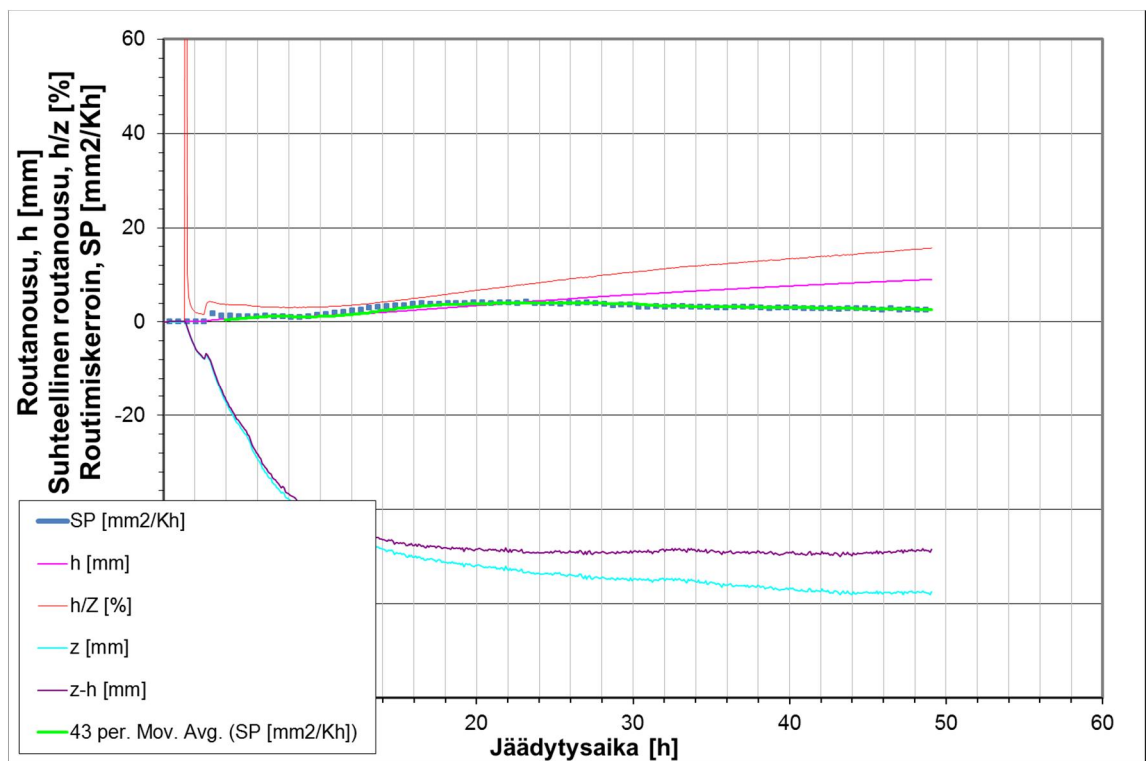
Test 3, loaded (s= 25kPa), 2,6m depth.
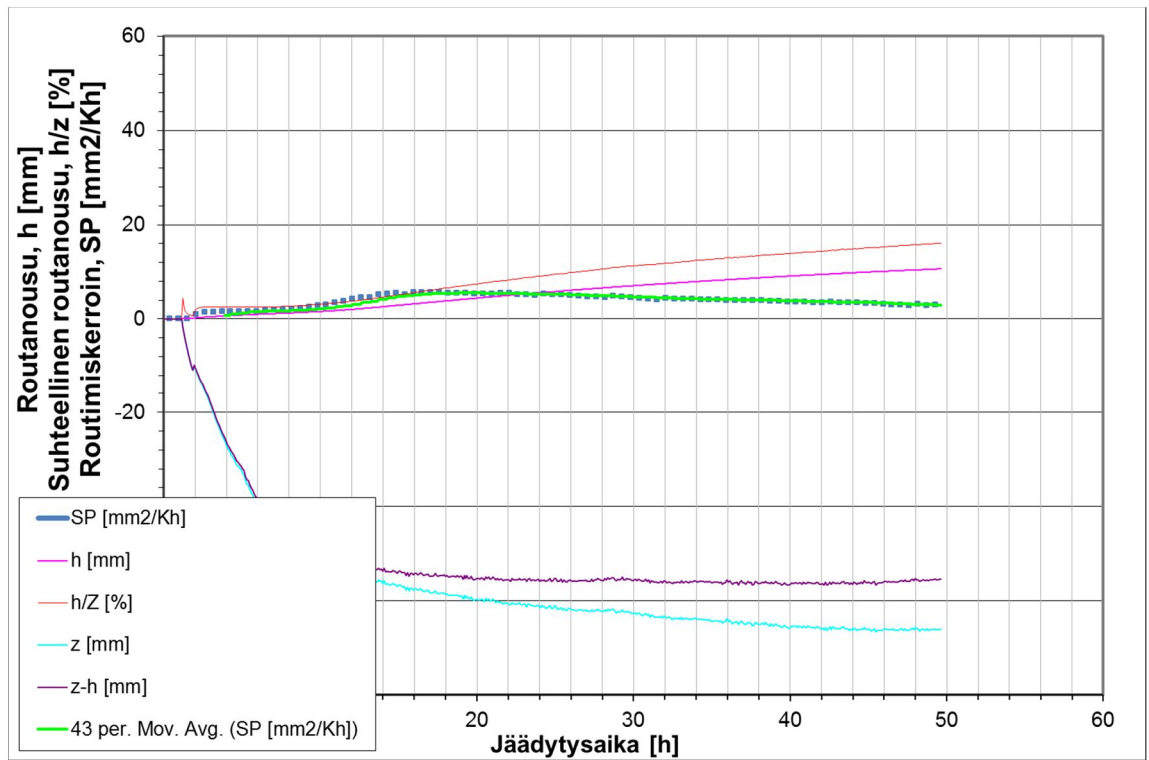
Test 3, unloaded (s= 0kPa), 2,6m depth.

Test 4, loaded (ꜱ= 30kPa), 3,6m depth.

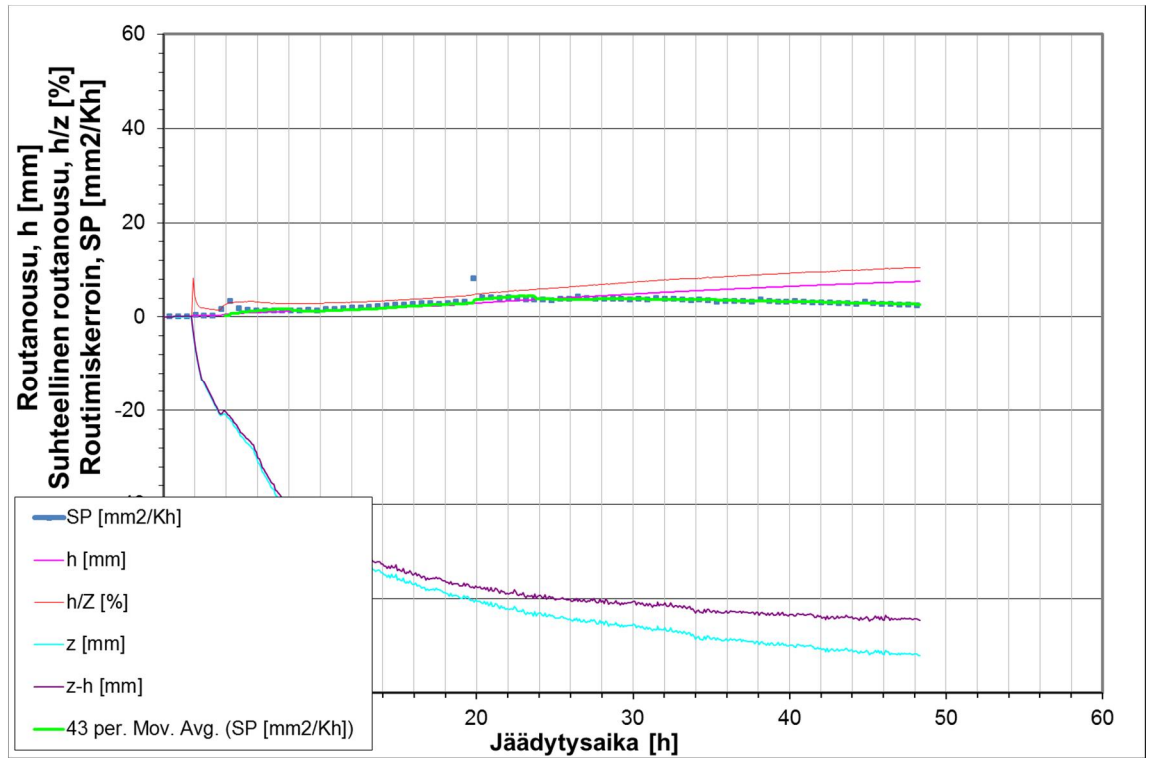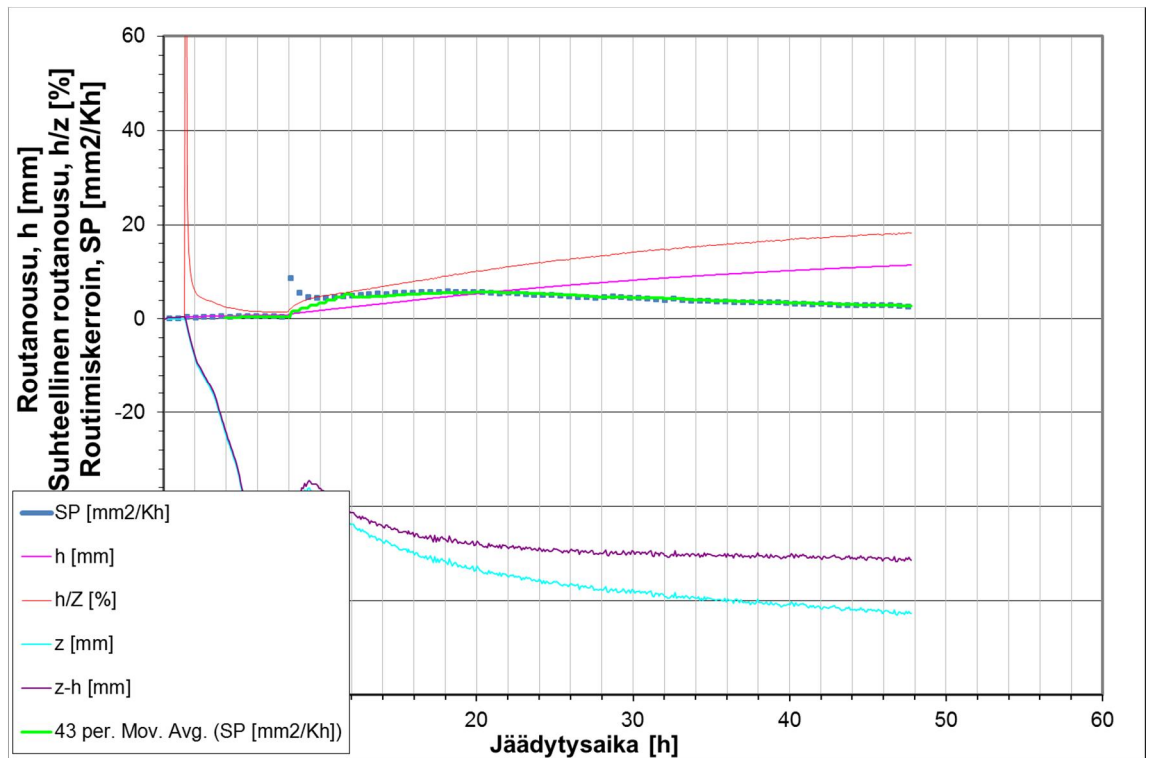

Test 4, unloaded (ꜱ= 0kPa), 3,6m depth.

Test 5, loaded (s= 40kPa), 5,6m depth.

Test 5, unloaded (s= 0kPa), 5,6m depth.

Test 6, loaded (s= 45kPa), 6,6m depth.

Test 6, unloaded (s= 0kPa), 6,6m depth.

Test	Depth (m)	Load (kPa)	Frost heave (mm)	Frost depth (mm)	Difference Z-h (mm)	Percentage (%)	Segregation Potential	Unfrozen sample height (mm)	Frozen sample height (mm)	Total height (mm)	Unfrozen (%)	Frozen (%)
			h	Z	Z-h	h/Z	SP (Tc)	Zs	Zj	Zt	Zs/Zt	Zj/Zt
2	1.2	0	3.67	-57.70	-54.03	6.36	3.35	32.51	57.70	90.21	36.04	63.96
		20	2.50	-59.96	-57.46	4.17	1.65	43.13	59.96	103.09	41.84	58.16
3	2.5	0	5.55	-61.46	-55.91	9.03	5.15	30.63	61.46	92.09	33.26	66.74
		25	2.58	-57.80	-55.21	4.47	2.5	43.13	57.80	100.92	42.73	57.27
4	3.5	0	8.08	-70.98	-62.90	11.38	3.65	33.54	70.98	104.52	32.09	67.91
		30	6.45	-72.49	-66.05	8.89	3.25	31.75	72.49	104.25	30.46	69.54
1	4.7	0	6.05	-51.21	-45.16	11.82	2.25	38.53	51.21	89.74	42.94	57.06
		40	2.09	-58.99	-56.91	3.54	0.65	43.05	58.99	102.05	42.19	57.81
5	5.5	0	4.46	-53.64	-49.18	8.32	3.9	29.13	53.64	82.77	35.19	64.81
		40	1.89	-57.66	-55.77	3.28	0.8	40.68	57.66	98.34	41.36	58.64
6	6.5	0	6.65	-55.46	-48.82	11.99	4.3	37.01	55.46	92.48	40.03	59.97
		45	3.74	-63.01	-59.27	5.94	2.85	38.01	63.01	101.02	37.63	62.37

Frost cell test results after 24 h. The values of the segregation potential were measured when the net frost depth remained constant.
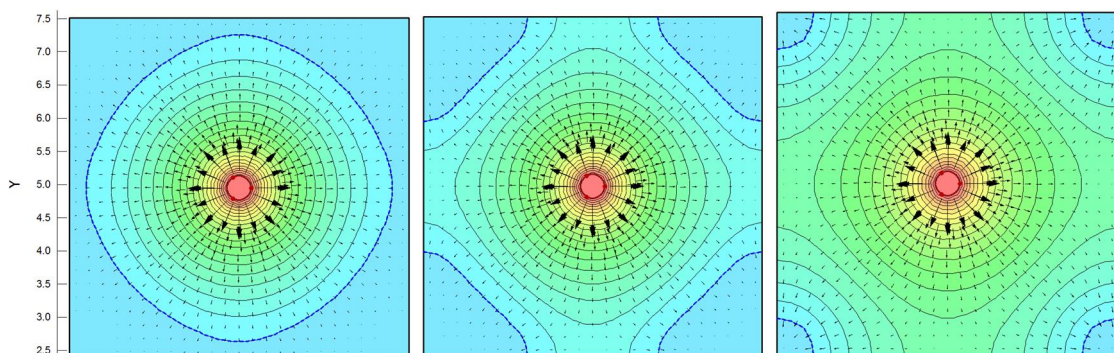
Appendix 5. Geo-Slope Temp/W results with the boundary condition applied in the border of the pile.
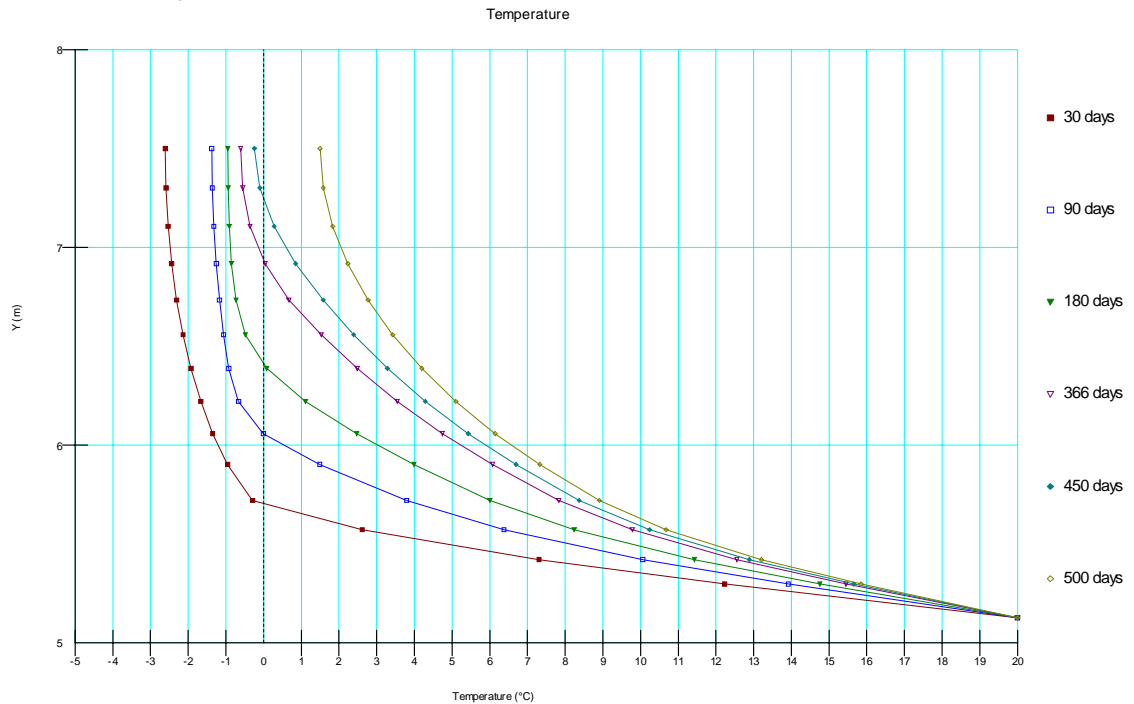
Ground temperature evolution of the radial melting process from the border of the pile (Y=5.1) to the end of its influence area (Y=7.75).
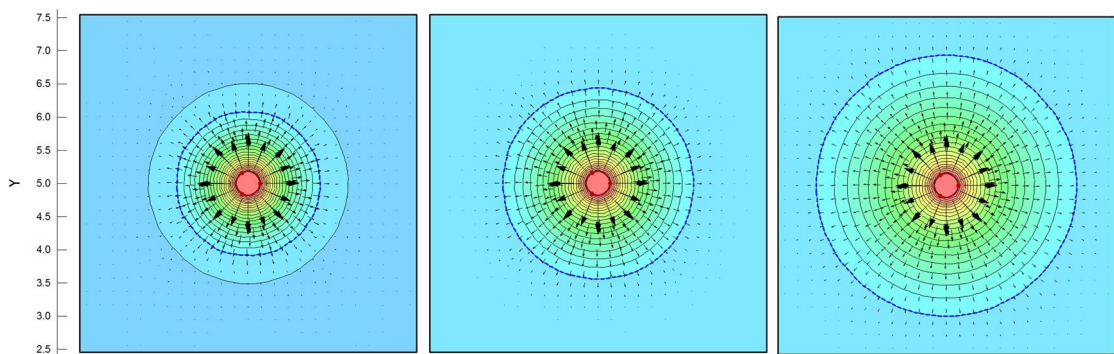
Radial melting evolution after 90 days (left), 180 days (centre) and 1 year (right) pumping heat at 20°C by the energy piles.

Radial melting evolution after 400 days (left), 500 days (centre) and 600 days (right) pumping heat at 20°C by the energy piles.